LUNAR SURFACE COSMIC RAY EXPERIMENT

S-152, APOLLO 16

GENERAL ELECTRIC EXPERIMENT

FINAL CONTRACT REPORT

July 25, 1973

R. L. Fleischer, H. R. Hart, Jr., M. Carter, G. M. Comstock,

A. Renshaw, and R. T. Woods

Principal Investigator: R. L. Fleischer

Prepared under Contract No. NAS 9-11468

by

GENERAL ELECTRIC COMPANY

Physics and Electrical Engineering Laboratory
Corporate Research and Development
P.O. Box 8, Schenectady, New York 12301

for

NATIONAL AERONAUTICS AND SPACE ADMINISTRATION

Johnson Space Center
Houston, Texas 77058

TABLE OF CONTENTS

APOLLO 16 LUNAR SURFACE COSMIC RAY EXPERIMENT (S-152)

by

R.L. Fleischer, H.R. Hart, Jr., M. Carter, G.M. Comstock,
A. Renshaw, and R.T. Woods

Physics and Electrical Engineering Laboratory
Corporate Research and Development
General Electric Company
Schenectady, New York

ABSTRACT

This report presents the work done by General Electric as experiment S-152 under contract NAS 9-11468. The investigation was directed at determining the energy spectra and abundances of low energy heavy cosmic rays ($0.03 \leq E \leq 150$ MeV/nucleon). The cosmic rays were detected using plastic and glass particle track detectors. Particles emitted during the 17 April 1972 solar flare dominated the spectra for energies below about 70 MeV/nucleon. Two conclusions emerge from the low energy data: 1) The differential energy spectra for solar particles vary rapidly (roughly E^{-3}) for energies as low as 0.05 MeV/nucleon for iron-group nuclei. 2) The abundance ratio of heavy elements changes with energy at low energies; heavy elements are enhanced relative to higher elements increasingly as the energy decreases. Galactic particle fluxes recorded within the spacecraft are in agreement with those predicted taking into account solar modulation and spacecraft shielding. The composition of the nuclei at energies above 70 MeV/nucleon imply that these particles originate outside the solar system and hence are galactic cosmic rays.

1. PURPOSES OF THE EXPERIMENT

The detector array on the Apollo 16 version of S-152 was designed with multiple purposes in mind. The primary motivation, however, was to learn as much as possible about the lowest energy nuclei in the cosmic rays, i.e. those below ~150 MeV/atomic mass unit, this being an energy range where very little was known and where the solid nuclear track detectors presented the unique possibility of analysis. Two mutually exclusive, alternate purposes were to be served. One was to examine the composition and energy spectra of solar flare particles; the other was to determine whether the lowest energy nuclei were solar or galactic in origin. Since the sun became active during the mission, it was the first objective that was best served, although in the energy range above 70 MeV/nucleon it has been possible to show that the background particles were galactic. In contrast to these studies, which were based on detectors in three of the four panels of the experiment, the fourth panel was primarily aimed at studying the heavy nuclei in the solar wind. The description of the apparatus and the preliminary results for all these experiments are presented in Appendix I by each of the three groups concerned. The General Electric portion of the equipment had as additional purposes to obtain calibration data on various glass detectors that were included, to establish from such data whether it was possible to measure the space exposure of tektites by recognizing cosmic ray tracks, and measure heavy cosmic ray doses to which the astronauts were exposed during the latter half of the mission.

2. OPERATION OF THE EXPERIMENT

The scientific designs for panels 1, 2, and 3 of the experiment came from the two groups at the University of California at Berkeley and General Electric Research and Development Center, Schenectady; that for panel 4 came from Washington University, St. Louis. The mechanical and thermal design, documentation, and construction was done by the General Electric Space Sciences Laboratory at Valley Forge. Useful details

on the experimental aparatus and design are given in Appendix I.

The significant periods of time during the exposure of the experiment are listed in Table I. The solar flare occurred during the trans-lunar portion of the trip and was greater than 90% complete by the time of lunar landing. The landing led to deposition of dust and/or deflected exhaust products on the outboard surface of the detector sheets and caused heating to temperatures that exceeded the design specifications for the plastic detectors. The heating degraded the data somewhat but, as described in the next section, did not prevent significant scientific results from being derived.

Fortunately the heating came after the flare had ended, so that virtually all solar flare tracks in a given area of the detector were given identical heat treatments and hence with internal calibrations could allow particle identification. During the first extra vehicular activity period there was an unnecessary 4 1/2 hour delay in the cooling off of the experiment that was caused by the temperature labels not having been read at the time the red ring was pulled.

Although the ring was designed to allow a shift to be made in some of the experimental materials in panel 4, only a partial shift was attained. Later examination showed that a protruding screw had prevented the desired motion. Since the panel worked successfully in earlier crew tests at Cape Kennedy, the improper screw must have been inserted during the re-assembly that was later required for flight readiness. The wrong screw could have resulted from an interchange of screws or from a new screw being used. The anomaly has yet to be explained.

3. SUMMARY OF SCIENTIFIC RESULTS

The relative abundances and energy spectra of heavy solar flare and cosmic ray nuclei contain a wealth of information about the sun and other particle sources, and about the acceleration and propagation of the particles. At the time of the Apollo 16 experiment the lowest energy range, from a few million electron volts per nuclear mass unit (MeV/nucleon or MeV/amu) down to a few kiloelectron volts per nucleon, was largely unexplored. The

TABLE I

Time Line for the Exposure of the Experiment

Event	Significance	Ground Elapsed Time* (hr:min)
Undocking	detectors exposed to space	3:04
Lunar orbit insertion	detectors face moon part of time	94:27
Lunar landing	dust deposited on detectors, absorbs solar heat	104:31
Red ring pulled	see part 3 of Appendix I	120:50
Experimental package moved to footpad	experiment faces down-sun; cools	125:25
Experimental package folded for storage	terminates most of experiments; begins personel dosimetry experiment	170:21
Entry to Earth's atmosphere	terminates dosimetry experiment	265:31

*Measured from launch at 17:54 G.m.t. on April 16, 1972.

present cosmic ray experiment was designed to examine this energy range using passive, solid, particle-track detectors.

At the time of the Apollo 16 flight, April 1972, the solar activity was approaching the 1975 minimum in its 11 year cycle. There was thus the possibility that the experiment would allow resolution of the question of the source of low energy heavy cosmic ray particles during a period when the sun was quiet.

The experiment was designed with this low particle flux in mind. If, on the other hand, a solar particle event occurred during the exposure, the experiment would yield valuable information about the energy spectra and composition of low energy, heavy solar particles. Because a solar flare occurred during the translunar portion of the flight, our low energy results characterize solar flare particles.

This report describes the results obtained in the General Electric experiment; separate reports describe the results of the Washington University and University of California experiments flown in the same experimental package. The report is based primarily upon five appended publications, the Apollo 16 Preliminary Science Report,[1] a Physical Review Letter,[2] a paper to be published in the forthcoming Proceedings of the 13th International Cosmic Ray Conference,[3] a paper just published in Science,[4] and an abstract for the Fourth Annual Lunar Science Conference.

The results presented in Figure 1 of this report are based on our most recent data and analyses. Two main points emerge: 1) The differential energy spectra for solar particles are rapidly varying functions of energy down to very low energies, well into the new energy range made available by the Apollo 16 experiment. Thus, for the iron group cosmic rays (points labeled "Heavy Cosmic Rays"), the differential fluence varies roughly as E^{-3} between 0.05 MeV/nucleon and 30 MeV/nucleon. 2) At low energies the spectral shape changes. Thus, below 0.05 MeV/nucleon the iron group spectrum flattens. This break, with its characteristic flattening, also occurs for the spectra of other elements, but at energies which depend inversely on atomic number; thus for carbon-and-heavier cosmic rays (labeled

FIGURE 1

CAPTION

Differential energy spectra for heavy cosmic rays during the period 16-23 April 1972 compared to the spectrum derived from various satellite proton counters. Fluence is given in particles/cm^2 MeV per nucleon integrated over a 2π solid angle. See reference 1 for a detailed schedule of exposure solid angle. The dashed line represents P_2O_5 glass data reanalyzed assuming a zero range deficit instead of the 0.85 micron range deficit assumed for the square points. The "Interior Lexan" points were obtained using the methods described in reference 7. The proton results are from preliminary data from satellite proton counters operated by C. Bostrom (IMP), G. Paulikas (ATS), and S. Singer (Vela).

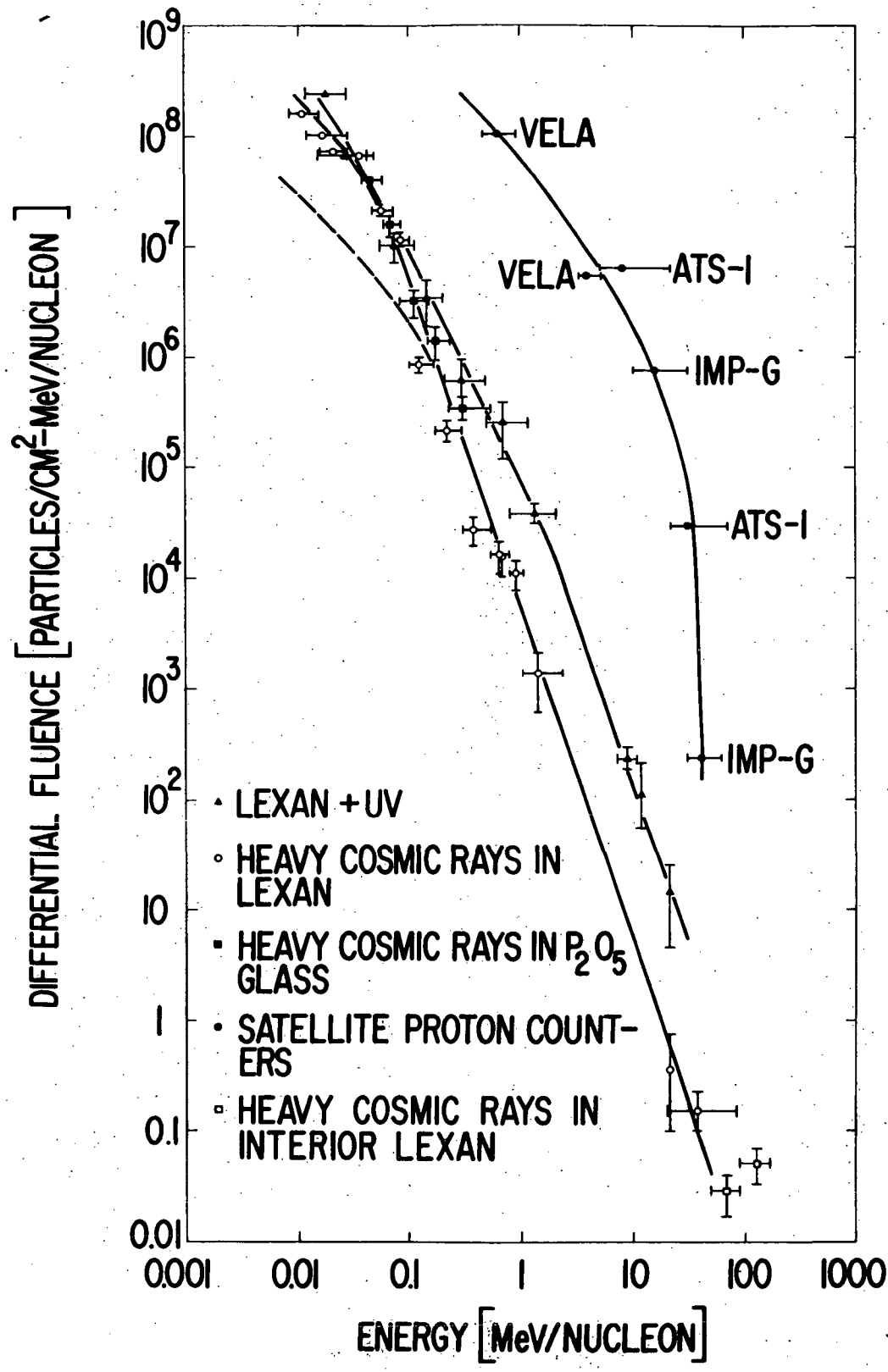
DIFFERENTIAL FLUENCE [PARTICLES/CM²-MeV/NUCLEON]
ENERGY [MeV/NUCLEON]
VELA
VELA
ATS-I
IMP-G
ATS-I
IMP-G
▲ LEXAN + UV
○ HEAVY COSMIC RAYS IN LEXAN
■ HEAVY COSMIC RAYS IN P2O5 GLASS
• SATELLITE PROTON COUNTERS
□ HEAVY COSMIC RAYS IN INTERIOR LEXAN

Fig. 1

"Lexan + UV" in Fig. 1) the break occurs at ~1 MeV/nucleon, and for the satellite proton data the break occurs at ~10 MeV/nucleon. This sequence of changes in spectral shape yields the impressive result displayed in Table II; the elemental abundance ratios for solar cosmic rays change as the energies decrease. At higher energies the ratio of iron group to carbon-and-heavier nuclei is essentially equivalent to that of the solar photosphere, 0.04; at lower energies the heavier elements are enhanced relative to the lighter elements.

The data imply that heavy nuclei in solar cosmic rays are appreciably more abundant than in the solar photosphere. As early as 1958 Korchak and Syrovatskii predicted preferential enhancement, at low energies, of heavier nuclei during the acceleration process. This enhancement of heavier nuclei would occur because of their lower effective change-to-mass ratios.[5] More recent explanations involve not only the acceleration processes but also possible variations in the composition of the solar atmosphere in the vicinity of solar flares.[6]

The heavy cosmic rays above about 70 MeV/amu, where the curve in Figure 1 has again flattened, are galactic, not solar, in origin. These data were obtained from interior Lexan sheets, after UV irradiation, by measuring etching rate as a function of residual range in the manner described by Price and Fleischer.[7]

Other galactic cosmic rays, recorded while the experiment was stowed within the command module in its folded or shifted mode,[1] allow us to determine the effects of solar modulation and spacecraft shielding on the flux of heavy galactic cosmic rays.[4] The results are important to manned space missions because of the lethal damage to biological cells caused by these highly ionizing particles. This experiment, together with earlier experiments using Apollo 8 and 12 helmets[8] and our results[4] from the Apollo 14 electrophoresis experiment,[9] yield two conclusions: 1) Extended space missions (e.g., a two year flight to Mars and back) would be safest during times of peak solar activity, since the solar modulation from an

TABLE II

Abundance Ratios

Energy MeV/Nucleon	Iron/(Carbon + Heavier)	Iron/Proton
10	0.04	2.5×10^{-6}
3	0.03	1.5×10^{-5}
1	0.025	0.8×10^{-4}
0.3	0.11	0.8×10^{-3}
0.1	~0.5	-
0.03	~1	-
Photospheric	0.04	4×10^{-5}

active sun decreases the flux of highly penetrating galactic heavy cosmic rays. (The much higher flux of solar particles is relatively easily shielded against because of their lower energies.) 2) The shielding of galactic cosmic rays due to the mass of the spacecraft and its contents could be considerably enhanced by judicious planning of the distribution of the mass.

Analysis of the glass detectors from S-152 continues. As an illustration of the differences in sensitivity of these glasses, the track densities observed in the GE 1457 phosphate glass, the GE 1484 uranium phosphate glass, and the tektite glass,[1] are in the ratio 50 : 20 : 1 for surface removals of 0.5, 0.3, and 3.7 μm, respectively. For the uranium phosphate glass exposed under the Teflon thermal shield, roughly one in ten of the tracks are multipronged, presumable the result of scattering events in which uranium was the target.

The elemental abundances of the higher energy cosmic rays have just been determined, using interior Lexan sheets. They indicate that the elements of atomic number 21 to 25 are abundant relative to iron, and hence that in the energy range 70-150 MeV/nucleon the observed nuclei are dominantly galactic in origin, just as the higher energy nuclei normally are.

4. FUTURE WORK

The analysis of these valuable detectors continues. Mr. R. T. Woods, a doctoral candidate at the State University of New York at Albany, is analyzing the particle tracks in the glasses for his Ph. D. thesis. This work is being done at General Electric under the guidance of R. L. Fleischer. The different glasses, with their differing sensitivities or thresholds, allow the determination of elemental abundances.

5. DISPOSITION OF FLIGHT MATERIALS

We plan at the present to continue work on glass detectors from the experiment. Shortly the flight parts of the General Electric panels will be returned to J.S.C. along with the plastic detector sheets for refrigerated storage. Finally, the appropriate reports, publications, and data will be forwarded to the National Space Science Data Center for archiving.

Acknowledgments

We are indebted to W.R. Giard, M. McConnell, and G.E. Nichols for experimental assistance, and to C. Bostrom, W.F. Dietrich, G. Paulekas, J.A. Simpson, and S. Singer for permission to quote their preliminary satellite data.

REFERENCES

1. Fleischer, R.L.; and Hart, H.R., Jr.: Cosmic Ray Experiment. Apollo 16 Preliminary Science Report. NASA SP-315, 1972, pp. 15-1--15-11.

2. Fleischer, R.L.; and Hart, H.R., Jr.: Enrichment of Heavy Nuclei in the 17 April 1972 Solar Flare. Phys. Rev. Letters, vol. 30, 1973, pp. 31-34.

3. Fleischer, R.L.; Hart, H.R., Jr.; Renshaw, A.; and Woods, R.T.: Enrichment of Heavy Nuclei in the April 17, 1972 Solar Flare. Proceedings of the 13th International Cosmic Ray Conference, Paper No. 300, 1973, to be published.

4. Fleischer, R.L.; Hart, H.R., Jr.; Comstock, G.M.; Carter, M.; Renshaw, A.; and Hardy, A.: Apollo 14 and 16 Heavy Particle Dosimetry Experiments. Science, vol. 181, 1973, pp. 436-438.

5. Korchak, A.A.; and Syrovatskii, S.I.: On the Possibility of a Preferential Acceleration of Heavy Elements in Cosmic-Ray Sources. Soviet Phys. Dokl., vol. 3, 1958, pp. 983-985.

6. Price, P.B.; Chan, J.H.; Hutcheon, I.D.; Macdougall, D.; Rajan, R.S.; Shirk, E.K.; Sullivan, J.D.: Low-Energy Heavy Ions in the Solar System., Proc. of the Fourth Lunar Sci. Conf., Geochim. Cosmochim. Acta, Suppl. 4, 1973, to be published.

7. Price, P.B.; and Fleischer, R.L.: Identification of Energetic Heavy Nuclei with Solid Dielectric Track Dectectors: Applications to Astrophysical and Planetary Studies. Annu. Rev. Nucl. Sci., vol. 21, 1971, pp. 295-334.

8. Comstock, G.M.; Fleischer, R.L.; Giard, W.R.; Hart, H.R., Jr.; Nichols, G.E.; and Price, P.B.: Cosmic-Ray Tracks in Plastics: The Apollo Helmet Dosimetry Experiment. Science, vol. 172, 1971, pp. 154-157.

9. McKannan, E.C.; Krupnick, A.C.; Griffin, R.N.; and McCreight, L.R.: Electrophoresis Separation in Space--Apollo 14. NASA Tech. Memo X-64611, July, 1971; see also Chem. Eng. News, Jan. 25, 1971, p. 25.

APPENDIX I

15. Cosmic Ray Experiment

INTRODUCTION

The relative abundances and energy spectra of heavy solar and cosmic ray particles convey much information about the Sun and other galactic particle sources and about the acceleration and propagation of the particles. In particular, the lowest energy range, from a few million electron volts per nuclear mass unit (nucleon) to a kiloelectron volt per nucleon (a solar wind energy), is largely unexplored. The cosmic ray experiment contained a variety of detectors designed to examine this energy range.

It is not known whether, in times of solar quiet, the low-energy nuclei are primarily solar or galactic in origin. One objective of this study was to resolve that question by measuring the chemical composition of the particles. Alternatively, if the Sun were active during the mission, it was expected that the flood of solar particles would provide an abundance of detailed compositional information about the Sun and solar acceleration processes. Because a solar flare occurred during the translunar portion of the flight, the latter objective was served.

The cosmic ray experiment equipment consists of a four-panel array of passive particle track detectors to observe cosmic ray and solar wind nuclei and thermal neutrons, and also includes metal foils to trap light solar wind gases. The materials in the panels were chosen for experiments performed by groups at General Electric (GE), the University of California, and Washington University. Preliminary results of the experiments being performed by the GE group are described in part A of this section; the other experiments are described in parts B and C. The experiment equipment is shown mounted on the descent stage of the lunar module (LM) in figure 15-1(a). During the first extravehicular activity (EVA), the equipment was placed on the minus Y footpad of the LM (fig. 15-1(b)).

The detection basis of nearly all of the experiments is that particles passing through solids can form trails of damage, revealable by preferential chemical attack, which allow the particles to be counted and identified. Much of this work is reviewed in references 15-1 to 15-4. An example of an etched track

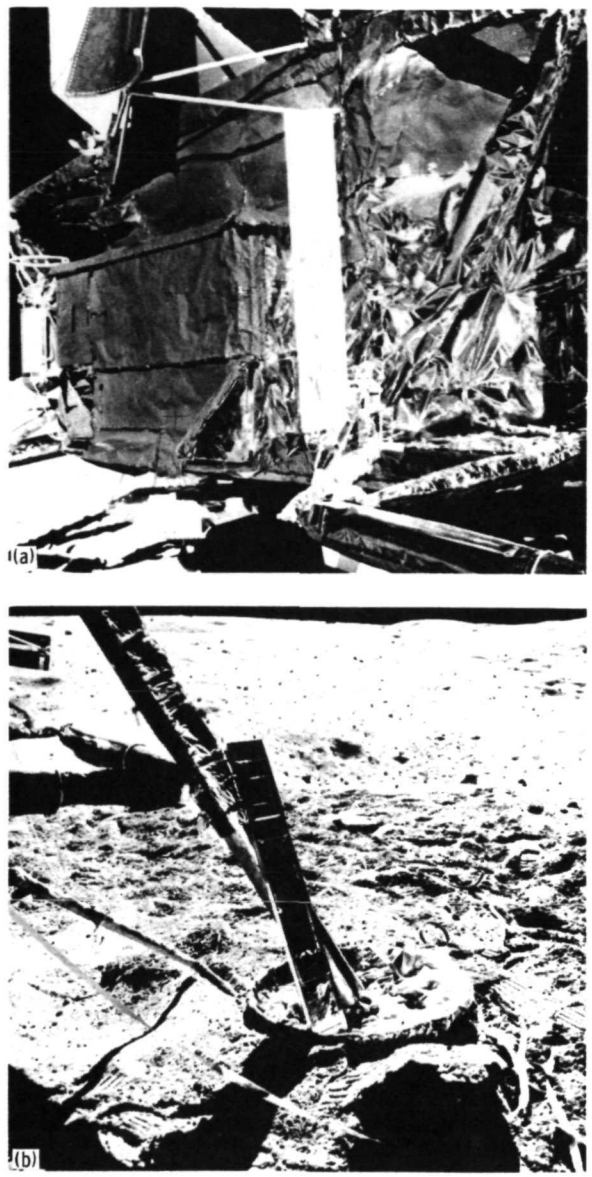

FIGURE 15-1.–The cosmic ray experiment (a) on the descent stage of the lunar module, of Apollo 16, where originally mounted, and (b) on the LM minus Y footpad (on the left footpad, looking down-Sun), where it was placed during EVA 1. Panel 2 and the bottom of panel 3 were used for the GE experiment; panel 1 (the lowermost panel) and panel 4 (the topmost panel) were used for experiments by the University of California and Washington University, respectively. Solar elevation was 35.8°.

that was identified as a zinc ion is shown in figure 15-2 (ref. 15-5).

The detector array was mounted on the LM before launch and was first exposed to space at the time just after translunar injection when the LM was withdrawn from the service module/LM adapter (the panels that, during launch, enclose the LM with aluminum equivalent to 0.3-cm-thick Lexan polycarbonate plastic). Exposure ended just before the termination of the third EVA on the Moon, at which time the four-panel array was pulled out of its frame and folded into a compact 5- by 18.4- by 30-cm package (fig. 15-3) for return to Earth. Because the folding and stowing of the device ended the period of useful exposure of the detectors, provision was made to distinguish particles detected during the useful period from those that subsequently penetrated the spacecraft and entered the detectors.

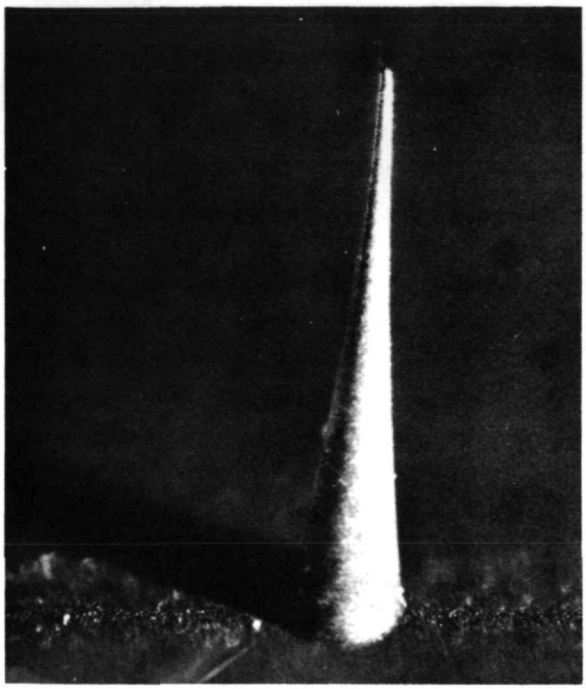

FIGURE 15-2.–Replica of a 0.07-cm etched track in an Apollo space helmet. From the shape, the track can be inferred to have been caused by a zinc ion.

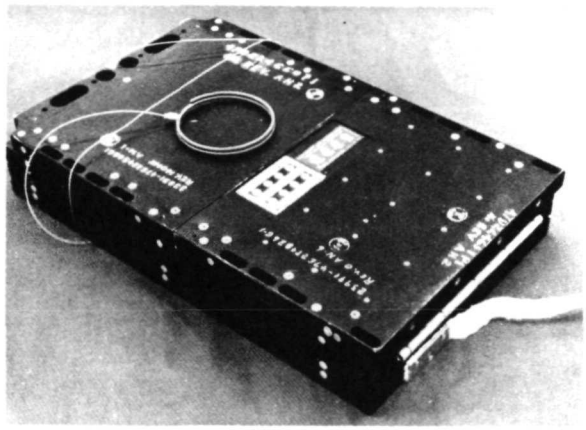

FIGURE 15-3.–Folded detector array. After exposure, the array was folded into the configuration shown to form a convenient package for return to Earth. Temperature labels are visible.

PART A

COMPOSITION AND ENERGY SPECTRA OF SOLAR COSMIC RAY NUCLEI

R. L. Fleischer[a] *and H. R. Hart, Jr.*[a]

The GE experiment consisted of two types of detectors: plastics and glasses located in panel 2 and the lower half of panel 3. In panel 2, the entire exposed detector area of 14.7 by 22.6 cm was composed of 31 sheets of 0.025-cm Lexan polycarbonate plastic 9070-112. In panel 3, 39 sheets of 0.02-cm Eastman Kodacel cellulose triacetate TA-401 with no plasticizer made up the major volume fraction. The lower part of panel 3 contained five types of glass detectors: 2.5- by 1.3- by 0.1-cm GE phosphate-uranium glass 1484 (ref. 15-6), 2.5- by 2.5- by 0.1-cm GE phosphate glass 1457 (ref. 15-7), 2.5- by 2.5- by 0.1-cm Corning alumina-silicate glass 1720, 2.5- by 2.5- by 0.1-cm silicon dioxide (Suprasil 2 silica glass from Amersil, Inc.), and a nearly elliptical tektite slab (Santiago, Philippines, tektite 1, supplied

[a]General Electric Research and Development Center.

by D. Chapman, NASA Ames Research Center) that fit within a 2.5- by 3.8- by 0.1-cm space.

Particles that entered the array after it was folded were recognized, if they crossed from one sheet to another, by means of a 2-mm relative shift of alternate sheets (fig. 15-4). This shift was produced automatically by the folding of the array at the end of EVA 3 just before the array was stowed in the LM. The designed full 2-mm shift occurred in panel 2, and a lesser shift occurred in panel 3.

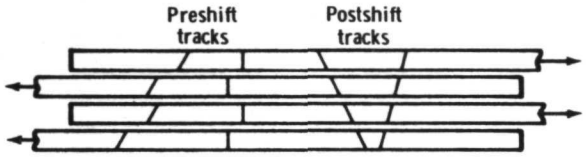

FIGURE 15-4.–Shifting procedure. A 2-mm relative shift of alternate plastic sheets allowed the preshift and postshift tracks to be distinguished. Postshift tracks are interesting only for personnel dosimetry purposes because the tracks represent particles that penetrated the spacecraft before entering the detectors.

Detector temperatures are important because thermal effects can be observed in the plastics and in some of the glasses used in panel 3 after the materials were exposed at temperatures above 328° K. Although tracks are retained to much higher temperatures in all the detectors, the quantitative relation between the ionization rate of the particle and the track etching rate is disturbed. Consequently, for particle identification to be possible, all tracks must have identical thermal histories above 328° K (ideally no exposure above that temperature). To keep temperatures less than 328° K in full sunlight during both translunar flight and the time on the Moon, panels 1, 2, and 3 were covered with a perforated thermal control material, 0.005-cm Teflon backed with thin silver and Inconel coatings (a composite that has a high reflectivity in the visible region of the solar spectrum and a high emissivity at infrared wavelengths). The space-exposed surfaces of the detectors also were coated with a 210-nm aluminum film to avoid ultraviolet (UV) exposure of the plastics, which is known to affect track etching rates (refs. 15-8 and 15-9). Because of the slowing down of cosmic ray nuclei in the silver-backed Teflon, particles of less than 5 to 6 MeV/nucleon are registered in the plastic detectors only through the perforations in the Teflon. There were sixty 0.3-cm-diameter perforations above the Lexan detectors (4.26 cm^2 total area) and 15 above the Kodacel (1.06 cm^2 total). Similarly for the glasses (fig. 15-5), nuclei of less than 10 to 20 MeV/nucleon are registered only beneath the single 0.5-cm-diameter hole that was positioned over the center of each glass plate.

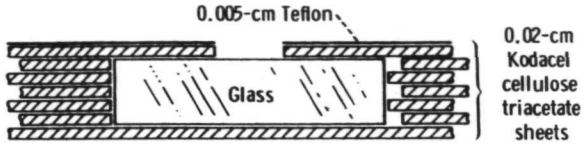

FIGURE 15-5.–Exposure of glass detectors. Glass plates were recessed within the triacetate sheets as sketched. Except for the single 0.5-cm-diameter perforation, the aluminized glass was covered by a 0.005-cm Teflon sheet and a 0.02-cm triacetate sheet. The 0.3-cm-diameter perforations allowed portions of the top Lexan and Kodacel sheets to be directly exposed. The Teflon was backed by a 165 ± 15 nm silver coating covered with an 85 ± 15 nm Inconel layer.

Consequently, for the low-energy nuclei that are of primary interest, the Teflon constitutes a shield, the quantitative effect of which on the observed track density can be calculated. For an isotropic bombardment with φ nuclei/[(area) X (solid angle)], the track density ρ is given by $\int \varphi \cos\theta \, d\Omega$ where θ is the angle of incidence and the integration is over the solid angle Ω permitted by the Teflon shield and the cone angle of the etched tracks. The Teflon is approximated by a straight-edged semi-infinite sheet spaced a distance h from the detector. For this case, the ratio ρ/φ depends only on the track cone angle θ_c and the ratio u of the distance x along the detector under the shield to the spacing h. The result

$$\rho/\varphi = \cos^2\theta_c \cos^{-1}\left(u \tan\theta_c\right) - \left(1 + u^{-2}\right)^{-1/2} \tan^{-1}\left(\left[1 - \left(u \tan\theta_c\right)^2\right]^{1/2} \Big/ \left[\tan\theta_c \left(1 + u^2\right)^{1/2}\right]\right) \quad (15\text{-}1)$$

is plotted in figure 15-6 for various values of θ_c. The figure illustrates how increasing the cone angle decreases the observable track density and increases the abruptness of the transition from maximum to zero track density near the edge of the shield. These same results are useful for computing effective solid angle of detection for particles of all energies in the case of a thick shield such as the Moon was while the experiment was located close to the lunar surface.

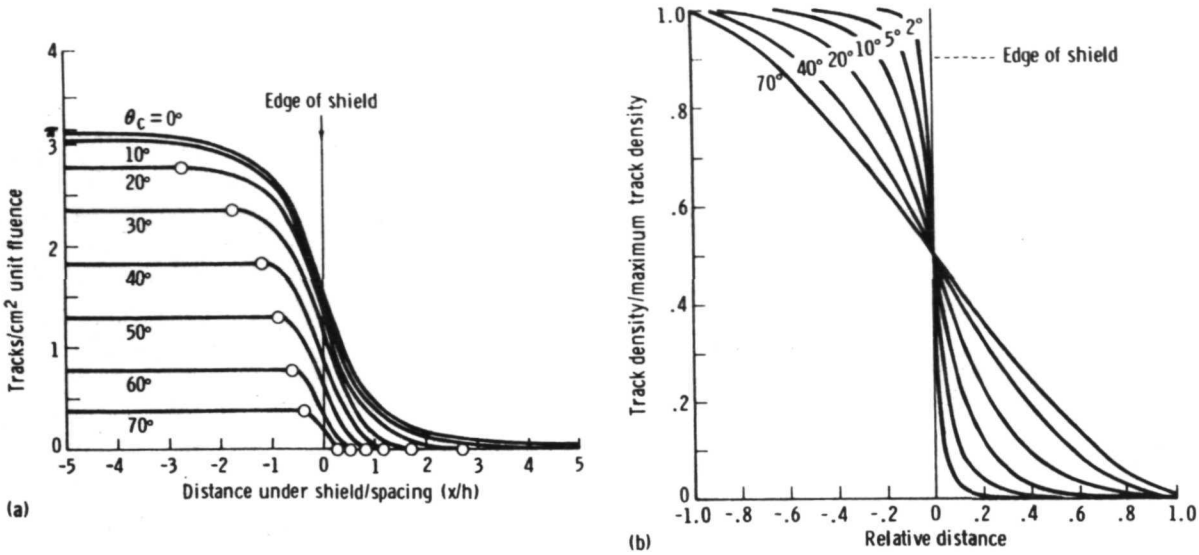

FIGURE 15-6.–Effect of a shield on the etchable tracks per unit fluence as a function of track cone angle. (a) The x is the distance under a parallel, semi-infinite shield a distance h from the detector surface. (b) Normalized data relative to the position where the etched track density goes to zero.

Operation of the Experiment

The experiment was exposed during the mission for nearly 1 week, distributed in time and possible solid angle as listed in table 15-I. The solid angle restrictions listed are merely the shadowing effects of the Moon. The degree of obstruction caused by struts, the scientific equipment bay, and other portions of the spacecraft varies with different positions in the array. For panels 2 and 3, the obstruction is such that the best solid angle factors for $\theta_c < 20°$ are probably those calculated for θ_c = 20°. The LM orientation distribution during lunar orbit prior to landing has been averaged for the appropriate 30.1-hr period. As noted in table 15-I, the last part of the exposure occurred on the LM minus Y footpad with the apparatus leaning against the strut with its face in the down-Sun direction and tilted upward at an angle of 69° to the horizontal, as inferred from a pair of up-Sun and cross-Sun photographs. This shift of the experiment from the LM was a contingency procedure designed to minimize solar heating by exposing to the direct Sun only the multilayer insulation at the back of the experiment.

Although the clean equipment should not have overheated, a deposit of as much as a 10-percent cover of lunar dust or other deposit with similar

TABLE 15-I.–Cosmic Ray Exposure of the Cosmic Ray Experiment

Mission segment	*Time, hr*	*Relative solid angle*	*Tracks per unit flux*		
			$\theta_c = 0°$	$\theta_c = 20°$	$\theta_c = 70°$
En route to Moon	71.4	1.0	3.14	2.76	0.164
In lunar orbit	30.1	0 to [a]1.0	.726	.541	.030
On LM on Moon	20.7	.5	1.57	1.38	.082
On LM footpad (69° to horizontal)	44.9	.64	1.95	1.70	~0
Weighted averages	–	.75	2.19	1.87	.085
Total	167.1	–	–	–	–

[a]Variable with time; 0.5-hr averages used.

optical and infrared properties would have produced excessive heating before the end of EVA 3. Temperature labels designed to sense the approach to the permitted upper limit were located on the outboard face of the frame. Near the end of EVA 1, all these labels were observed by the commander to have been affected, signaling that the polycarbonate temperature had exceeded 318° K; therefore, the contingency procedure was followed at that time. After retrieval, temperature labels within the plastic stacks indicated temperatures of 339° ± 6° K within panel 3 and a part of panel 2, and 350° ± 6° K in another part of panel 2. The temperatures observed in panels 1 to 3 correlate with the dust (or contamination) found on the retrieved panels, the highest temperature (>355° K) occurring in panel 1 and the lowest (<344° K) in panel 3. It is presently not known whether the "dust" cover occurred from rocket exhaust at the time of LM withdrawal from the service module/LM adapter or from ricocheting lunar dust at the time of lunar landing. This is a matter of some consequence because, in the latter case, tracks formed before landing will have had a common thermal history above 328° K.

Solar Flare

During the translunar part of the mission, a medium-size solar flare occurred that contained $\approx 10^8$ protons/cm^2 of energies greater than 5 MeV. Preliminary data, for the flux in various energy intervals, from several satellites are shown in figure 15-7. (The data are from the following satellites: Applied Technology Satellite (ATS), Interplanetary Monitoring Platform (IMP), Pioneer, and Vela.) No extra particles were observed beyond the general steady background at energies greater than 60 MeV. Most of the flare particles arrived before lunar landing; only a few percent greater than 5 MeV arrived after landing, and, even for the slowest particles for which data are available (0.46 to 0.90 MeV), less than 10 percent arrived after landing. If the dust were deposited on the experiment during landing, virtually all the flare tracks recorded will have had the same subsequent thermal history. Even if this were not the case, the highest temperatures to which the detectors were exposed were experienced during the 20.7 hr when the experiment was facing the Sun while on the lunar surface. As a result, most of the thermal effects on solar flare tracks were concentrated in that period and were common to virtually all of the solar particles.

Procedure

Etching and read-out have been performed on Lexan sheets from panel 2 and on glass 1457 from panel 3. For glasses, the final steps in the preflight preparation were annealing (for the tektite and glass 1484, removing preexisting tracks), polishing, etching, inspecting, and coating with an evaporated aluminum reflective coating approximately 210 nm thick. The 210-nm aluminum coating was also present on the top Lexan and Kodacel sheets. After the flight, before the panels were disassembled, the outlines of the 0.5-cm-diameter openings above the glasses and the 0.3-cm-diameter holes above the plastics were scribed into the detector surfaces.

The track etching rates of the detectors can be altered by thermal annealing, the glasses to a lesser extent than the plastics. In figure 15-8, the changes in the track etching rates caused by 1-hr anneals are shown for several glasses. In figure 15-8, V_T is the average track etching rate for californium-252 fission fragments, and V_G is the general etching rate for unirradiated regions. The extreme cases, GE phosphate glass 1457 and Corning glass 1720, are two of the glasses flown on this experiment.

After the panels were disassembled, the glass samples were carefully sectioned by sawing from the underside through most of the thickness and then fracturing the remaining near-upper-surface thickness to avoid the loss of valuable surface material.

One portion of each glass was then etched in room-temperature sodium hydroxide for 1 to 2 min to remove the aluminum coating. The same part was then etched in 50 percent hydrofluoric acid to remove approximately 0.5 μm of glass from each surface to reveal cosmic ray tracks. The etched glasses were scanned at 1000X in an optical microscope, then were replicated (cellulose acetate, gold coated), and scanned at 5000X in a scanning electron microscope (SEM). Parts of the top sheet of Lexan, after removal of the aluminum by a 296° K sodium hydroxide solution, were etched for 3 or 6 hr in 313° K 6.25N sodium hydroxide solution saturated with etch products (ref. 15-10). In one case, a preirradiation with UV was used to accelerate etching attack

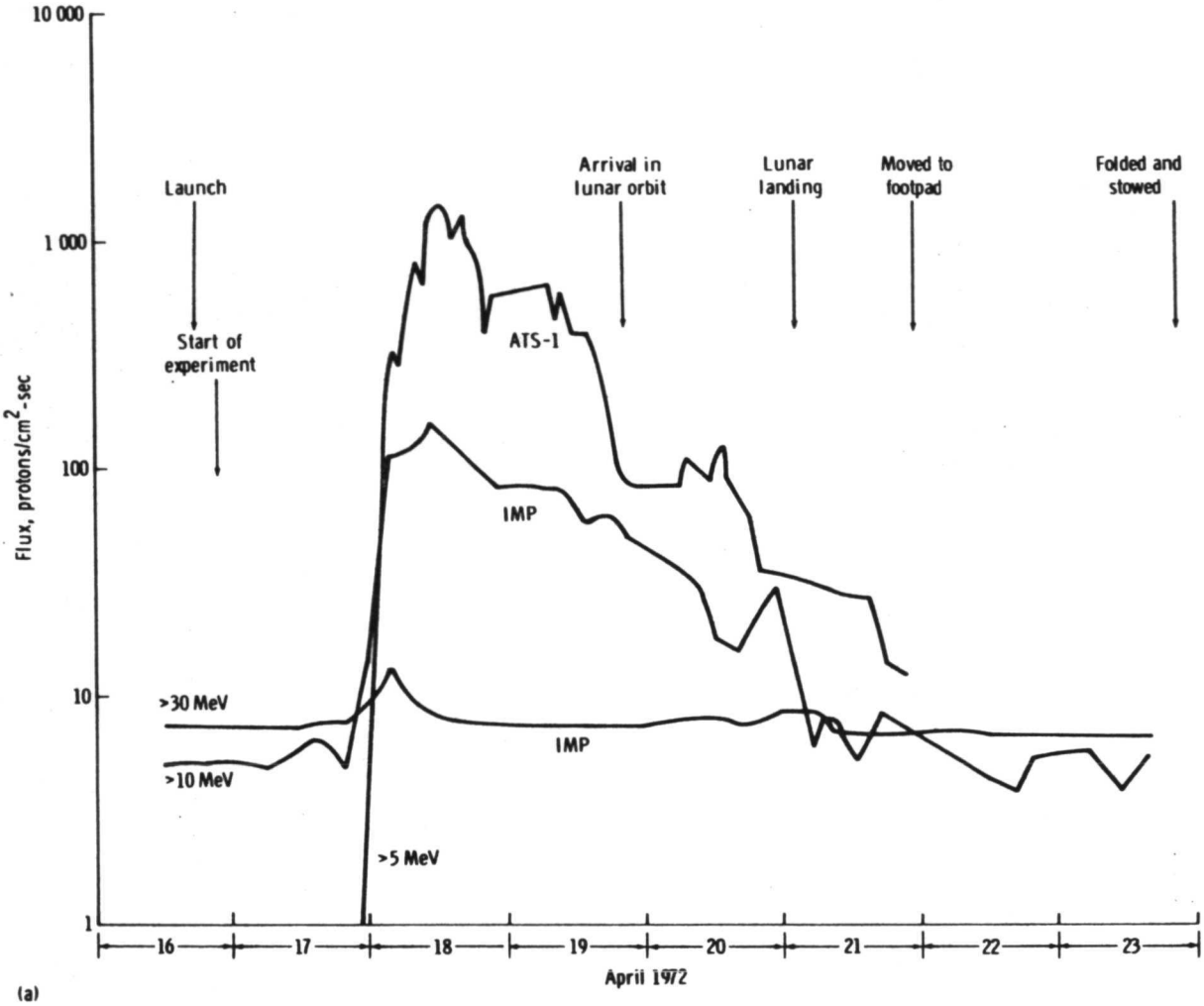

FIGURE 15-7.–Proton flux observed by various satellites during the first week of the Apollo 16 mission. The relevant operations affecting the cosmic ray experiment are noted at the top of each part of the figure. In all cases, the data are preliminary and subject to change. Data courtesy of C. Bostrom (IMP), G. Paulikas (ATS), and S. Singer (Vela). (a) Flux >5, >10, and >30 MeV.

along the tracks (refs. 15-8 and 15-9). Results are given in this subsection for a 6-hr etch of a sheet from the lower left part of panel 2 (hole 2) and a 6-hr etch of a UV-treated sheet from the upper right corner of panel 2 (hole 59). These parts are thought to correspond to the warmest and coolest parts of panel 2, respectively, as judged from the distribution of dust cover and temperature label readings. Sheets 2 to 11 below hole 2 were etched 40 hr under the etching conditions described previously. Solar flare tracks on the exposed surfaces of the phosphate glass and Lexan are shown in figure 15-9. From the optical scans in the central open regions of the different detectors, the track length distributions given in table 15-II were obtained. The differential energy spectrum is derived from these track lengths using range-energy relations (ref. 15-11) for iron nuclei, allowing for the thicknesses of the aluminum layer and the layer etched away and assuming that the aluminum is crossed at 45° incidence.

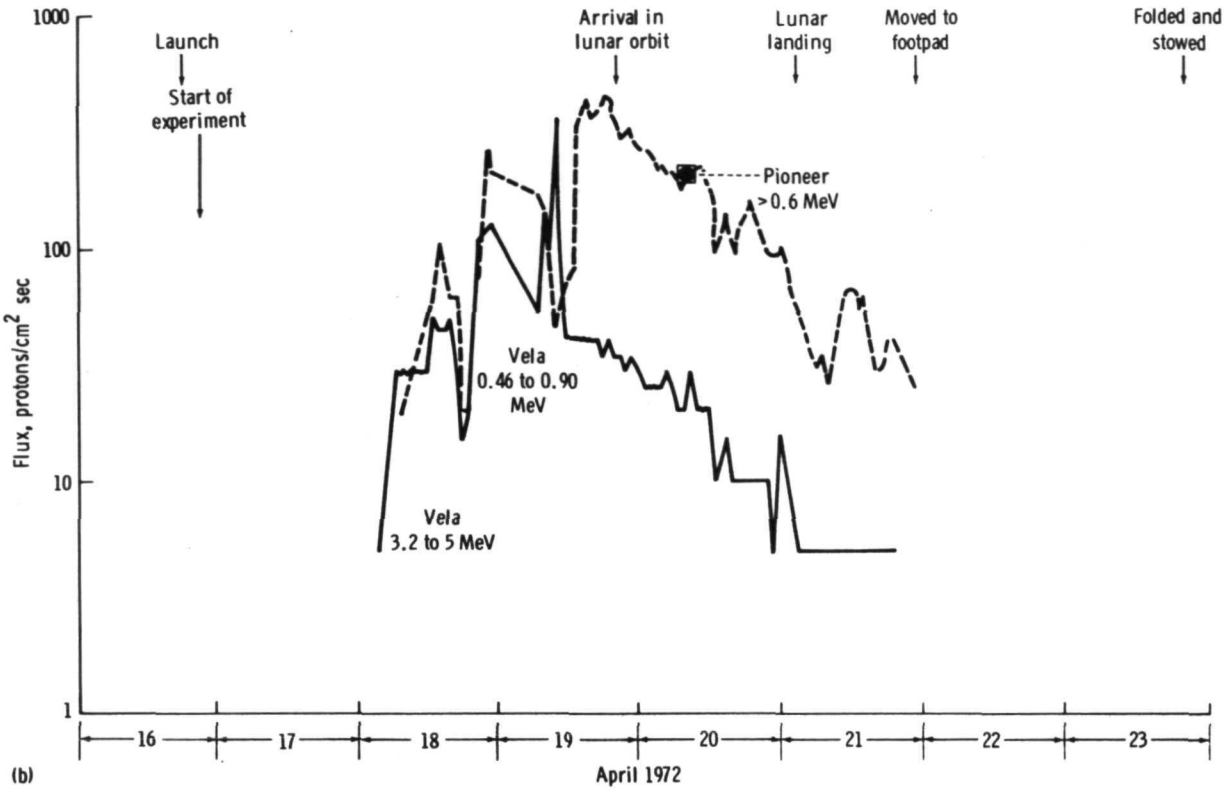

FIGURE 15-7.–Concluded. (b) Flux in the intervals 0.46 to 0.90 MeV and 3.2 to 5.0 MeV.

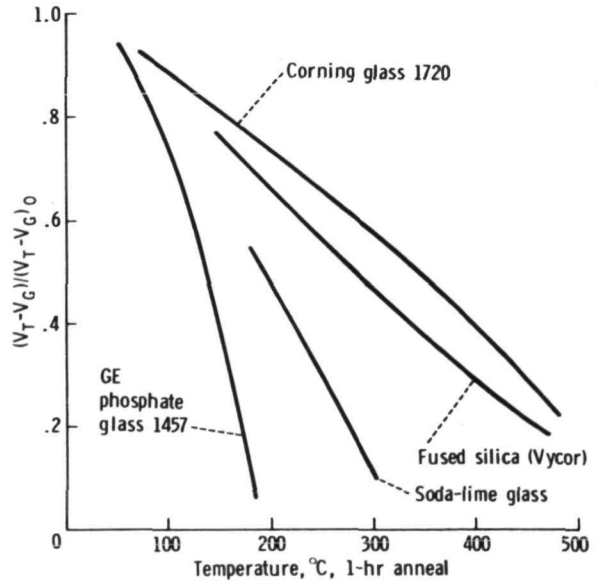

FIGURE 15-8.–Annealing of the track etching rate for californium-252 fission fragments in several glasses. The V_T is the average track etching rate, and V_G is the general etching rate for an unirradiated region. The reference V_T is that obtained after a long time at room temperature.

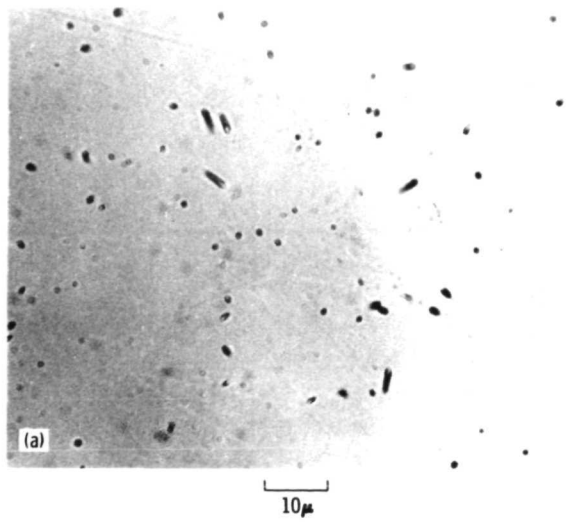

FIGURE 15-9.–Heavy solar cosmic ray tracks in plastic and glass detectors. The surface removal is 5 X 10^{-5} cm for the glass and 10^{-4} cm for the plastic. (a) Glass 1457 viewed optically.

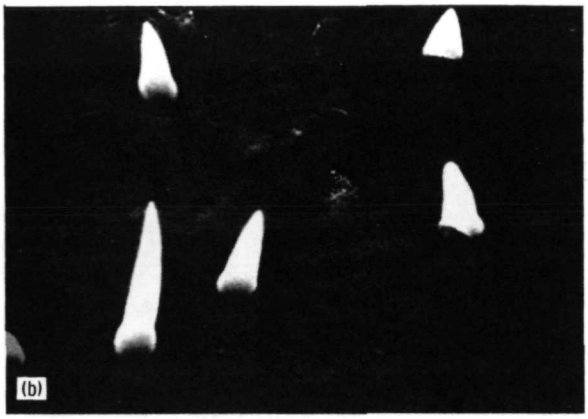

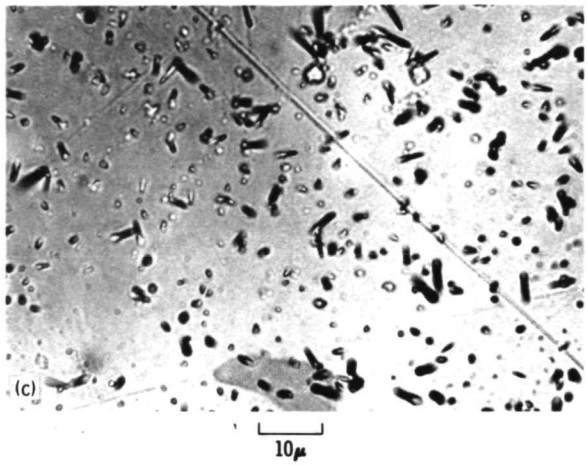

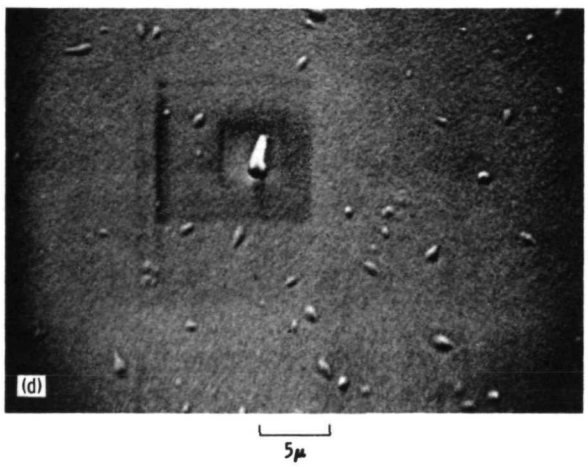

FIGURE 15-9.–Concluded. (b) Glass 1457 viewed in a scanning electron microscope. The SEM replica is cellulose acetate. (c) Lexan polycarbonate hole 4 viewed optically. (d) Lexan polycarbonate viewed in a scanning electron microscope. The SEM replica is silicone rubber.

TABLE 15-II.–Track Length Distributions at Detector Surfaces

(a) Track length

Length, cm	*Number*	*Tracks/cm²*
Phosphate glass 1457		
(0 to 0.5) × 10^{-4}	82	0.92 × 10^{6}
(.5 to 1.0)	26	.29
(1 to 2)	19	.21
(2 to 3)	10	.11
(3 to 6)	10	.11
Lexan (hole 2, 6-hr etch)		
(0.1 to 0.5) × 10^{-4}	108	1.1 × 10^{6}
(.3 to 1)	127	1.3
(.5 to 1)	65	.65
(1 to 2)	~50	1.5
(2 to 3)	51	.52
(3 to 4)	34	.35
(4 to 6)	25	.064
(6 to 8)	20	.034
(8 to 11)	9	.0066
(11 to 14)	9	.0042
(14 to 17)	6	.0028
(17 to 30)	3	.0014
Lexan (hole 59, UV + 6-hr etch)		
(0.5 to 1.5) × 10^{-4}	22	1.34 × 10^{6}
(.5 to 2.0)	79	2.07
(1.5 to 2.5)	8	.49
(2.4 to 4.5)	10	.61
(4.5 to 6.5)	5	.31
(6.5 to 10.5)	3	.18
(10.5 to 18.5)	3	.18

(b) Track density at exterior surface

Phosphate glass 1457	1.8 (±0.1)
Lexan (hole 2, 6-hr etch)	6.10 (±0.35) optical
Lexan (hole 59, UV + 6-hr etch) ..	7.5 (±0.3)

The justification for assuming that all particles are iron in computing the energies derives from the plot given in figure 15-10. For GE phosphate glass 1457, neon ions give tracks having an average cone angle of 30° to 35° over a distance of approximately 15 μm. The SEM photographs of cosmic ray tracks give the cone angle distribution for the >1-μm tracks shown in figure 15-10. This cone angle distribution indicates that the tracks are predominantly from particles much heavier than neon. Separate experiments by the

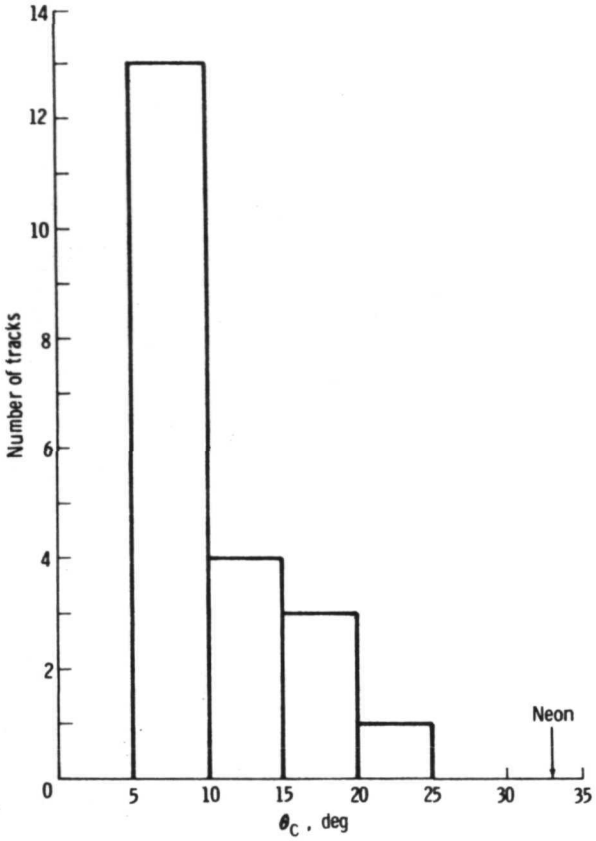

FIGURE 15-10.– Distribution of projected cone angles measured for solar flare tracks in phosphate glass 1457. The angles are obtained from SEM photographs of a cellulose acetate replica after a 12-min etch of the glass in 50 percent hydrofluoric acid.

authors with M. Saltmarsh and A. E. van der Woude of argon-40 and iron-56 beams indicate that the tracks were made by ions heavier than argon and close to iron in atomic number. From known solar abundances (ref. 15-12), it is expected that iron is dominant and that most of the nuclei observed have range-energy relations that are adequately approximated by that of iron. The justification in using iron for the 6-hr etch of hole 2 is that the results there agree with the phosphate glass. For hole 59 (UV treatment before a 6-hr etch), this assumption will be shown to be useful but quantitatively wrong.

Particles stopping at greater depths than were observed at the exposed Lexan surface could be counted on the same surface but beneath the silver-backed Teflon, at the back of the top sheet, and in sheets 2 to 11. These data lead to spectral information at ≈10 MeV/nucleon and above.

One interesting anomaly was the observation beneath the silver-backed Teflon of a high density (≈3000 tracks/cm^2 in the non-UV-irradiated Lexan and ≈10 000 tracks/cm^2 in the UV-irradiated Lexan) of short tracks ranging to ≈10^{-3} cm long with rapidly decreasing numbers of tracks with increasing length. Such tracks were fewer at the opposite side of the Lexan sheet (depth 0.035 to 0.050 cm rather than 0.010 to 0.014 cm). The falloff with depth is too rapid to be consistent with direct effects in the plastic of the appreciable proton irradiation from trapped particles encountered while leaving the vicinity of the Earth. A proton flux of ≈3 X 10^9 protons/cm^2, >3 MeV, and ≈8 X 10^6 protons/cm^2, >30 MeV, is inferred from reference 15-13, extrapolating to greater distances from the Earth on the basis of reference 15-14. The most likely source of the short tracks is the aluminum-Inconel-silver-Teflon composite adjacent to the surface where these short tracks were found. Whether these are reaction products, compound nuclei, or recoil nuclei has not been determined. The cosmic ray flux at 0.010- to 0.014-cm depth was inferred from the abundance of tracks >15 X 10^{-4}-cm length, which appear to form a distinctly separate population.

Energy Spectra

The energy spectra inferred for heavy particles and that derived for protons from the satellite data in figure 15-7 are shown in figure 15-11. The non-UV-irradiated Lexan gives results that are indistinguishable from those of the phosphate glass. Because those tracks have been identified as from iron nuclei or those close to iron in atomic number, the composite curve (the lowest of the three in figure 15-11) applies to the iron group nuclei.

The curve for the UV-irradiated Lexan lies generally above that for the non-UV-irradiated samples; examination of additional samples has shown that this difference is primarily caused by the effect of the UV in lowering the effective threshold for particle track registration (ref. 15-9). The approximate 10-to-1 ratio of differential fluence in the 20- to 60-MeV/nucleon range would be consistent with nuclei down to carbon-12 being revealed in the Lexan, as judged by neon-20 calibration tracks and as is consistent with the solar flare composition observed by Mogro-Campero and Simpson (ref. 15-15). Recalculation of the energy spectrum to include the carbon-nitrogen-oxygen (CNO) group for the UV-

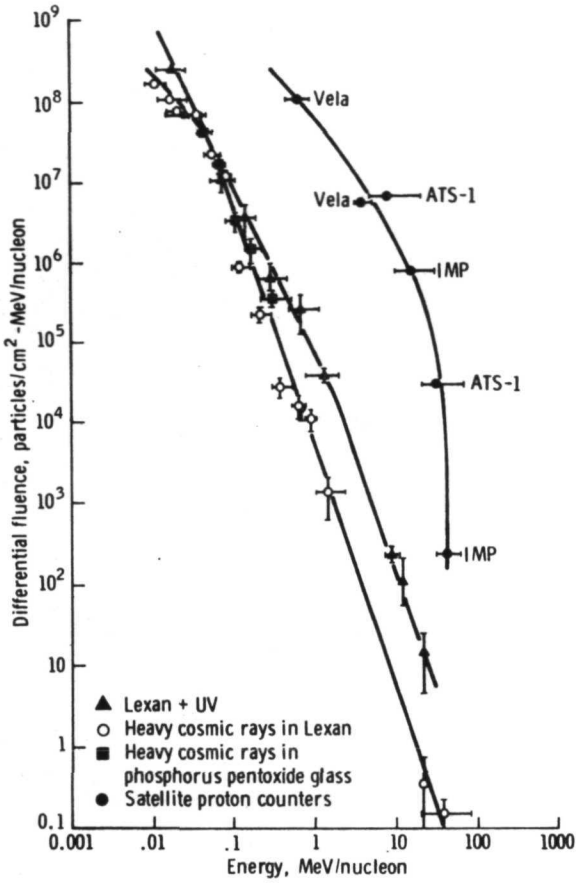

FIGURE 15-11.–Differential energy spectra for heavy cosmic rays during the period April 16 to 23, 1972, compared to the spectrum derived from various satellite proton counters. Fluence is given in protons/cm^2-MeV/nucleon integrated over a 2π solid angle. Proton data are derived from those given in figure 15-7.

irradiated sample would steepen the curve slightly but would not alter its qualitative character significantly.

Discussion

The spectrum for iron group cosmic ray is given by an energy$^{-\gamma}$ $E^{-\gamma}$ relation, where the spectral index γ is 3 (±0.3) from 30 MeV/nucleon down to 0.04 MeV/nucleon and flattens to $\gamma = 1$ (±0.5) from 0.04 to 0.01 MeV/nucleon. The $\gamma = 3$ result is identical to a previous conclusion (ref. 15-16) in the energy range 1 to 100 MeV/nucleon from examination of Surveyor III filter glass and with that of Mogro-Campero and Simpson from their counter telescope in the range 3 to 60 MeV/nucleon (ref. 15-15). The result is also similar to the results of two other studies of the Surveyor glass (refs. 15-17 and 15-18) although the spectrum was not expressed as E^{-3} in those papers.

The proton-to-iron ratios listed in table 15-III were derived from this result. With decreasing energy, the ratio decreases from 15 times the photospheric value at 10 MeV/nucleon to 0.05 times that value at 0.3 MeV/nucleon (ref. 15-19). Although proton data are lacking at the lower energy, the trends in the curves in figure 15-11 suggest that this enrichment in the heavy nuclei continues at least another order of magnitude in energy down to the break in the slope of the iron group curve. The existence of increasing enhancement of iron towards lower energies is in agreement with previous results by Price et al. (ref. 15-18) and Mogro-Campero and Simpson (ref. 15-15) but is quantitatively less at the same energies. The present results, however, extend to much lower energies.

TABLE 15-III.–Ratios[a] of Proton Flux to Iron Flux

Energy, MeV/nucleon	*Proton flux/iron flux*
10	4×10^5
3	6.5×10^4
1	1.2×10^4
.3	1.2×10^3

[a]Abundance ratio in photosphere = 2.5×10^4.

If the UV-irradiated data are recalculated on the assumption that oxygen-16 is the most abundant species present (approximating CNO plus all heavies by using oxygen range-energy curves), ⩾ carbon/⩾ iron ratios can be estimated: 25 (10 MeV/nucleon), 35 (3 MeV/nucleon), 40 (1 MeV/nucleon), 9 (0.3 MeV/nucleon), approximately 2 (0.1 MeV/nucleon), and approximately 1 (0.03 MeV/nucleon). A strong relative enrichment of iron relative to the lighter nuclei is apparent at low energies. These ratios are to be compared with values of 8 found by Mogro-Campero and Simpson (ref. 15-15) near 20 MeV/nucleon and 84 found by Bertsch et al. (ref. 15-20) near 60 MeV/nucleon, both these results being averages for groups of flares. The trend of relative enrichment of iron towards lower energies is again clear.

The relative heavy element enrichment at low energies is associated with the position of the decrease in the magnitude of slope of the energy

spectra, which occurs at progressively higher energies from iron (≈0.04 MeV/nucleon) to "≥ carbon" (≈1 MeV/nucleon) to hydrogen (≈10 MeV).

Total iron down to ≈0.01 MeV/nucleon is ≈4 X 10^6 particles/cm^2 per 2π solid angle as compared to ≈2.2 X 10^8 protons/cm^2 (as derived from fig. 15-11); these numbers give an enrichment by a factor ≈450 relative to the photospheric value. However, because the proton fluence below 0.3 MeV is unknown, the quantitative meaning of this value is not clear. It does, however, strongly suggest that the heavies in the solar flares are in fact appreciably more abundant than in the surface of the Sun. The preferential enhancement at low energies of the heavier nuclei because of their low charge-to-mass ratio was predicted in 1958 by Korchak and Syrovatskii (ref. 15-21).

Summary

Solid-state track detectors were exposed to the solar flare of April 18, 1972, during the Apollo 16 mission and etched to reveal tracks of cosmic ray nuclei. Iron group nuclei were observed in phosphate glass and desensitized Lexan polycarbonate detectors, and their spectrum was measured down to ≈0.02 MeV/nucleon, nearly two orders of magnitude lower in energy than had previously been observed in such nuclei. The relative enrichment of iron relative to lighter nuclei previously seen at higher energies continues to increase into the new low-energy region. The energy spectrum of particles equal to or greater than carbon is inferred from sensitized Lexan polycarbonate and allows the relative enrichment of iron relative to the medium and heavy nuclei to be estimated down to 0.03 MeV/nucleon.

Acknowledgments

The authors are indebted to C. Bostrum (Johns Hopkins U.), G. Paulikas (Aerospace Corp.), and S. Singer (Los Alamos) for permission to quote their satellite proton results; to W. R. Giard, M. McConnell, and G. E. Nichols (General Electric Research and Development Center) for experimental assistance; and to M. Saltmarsh and A. van der Woude (Oak Ridge National Laboratory) for permission to quote joint work prior to publication.

PART B

COMPOSITION OF INTERPLANETARY PARTICLES AT ENERGIES FROM 0.1 TO 150 MEV/NUCLEON

P. B. Price,[a] D. Braddy,[a] D. O'Sullivan,[ab] and J. D. Sullivan[a]

Introduction

The University of California cosmic ray experiment on Apollo 16 was designed to identify tracks of energetic nuclei with atomic numbers $Z \geq 2$ in the energy interval from ≈0.2 to ≈150 MeV/nucleon. Improved techniques allowed the energy interval to be extended to ≈0.1 MeV/nucleon. The goal of the experiment was to determine the composition and origin of interplanetary particles in the little-explored energy interval between solar wind energies (≈10^{-3} MeV/nucleon) and energies accessible to balloon-borne instruments (≈300 MeV/nucleon).

Energy spectra determined during solar quiet times by electronic detectors on satellites have been published (refs. 15-22 to 15-24) for iron group nuclei ($25 \leq Z \leq 28$) down to energies of ≈150 MeV/nucleon; for neon, magnesium, and silicon down to ≈50 MeV/nucleon; for boron and carbon, nitrogen, and oxygen (CNO) down to ≈40 MeV/nucleon; and for isotopes of hydrogen (H) and helium (He) down to ≈10 MeV/nucleon. The presence of boron, which is largely a spallation product of CNO, suggests that medium-charge galactic cosmic rays are present in interplanetary space down to energies of ≈40 MeV/nucleon. The presence of ^{2}H and ^{3}He, which are

[a]University of California at Berkeley.

[b]On leave from Dublin Institute for Advanced Studies, Dublin, Ireland.

largely spallation products of ^{1}H and ^{4}He, suggests that low-charge galactic cosmic rays are present down to even lower energies (≈10 MeV/nucleon). Nothing has been known before now about the origin (or even the existence) of nuclei at energies less than ≈10 MeV/nucleon present during solar quiet times. For heavy nuclei such as iron, knowledge is limited to greater than ≈150 MeV/nucleon. The limitation has been an experimental one. Electronic detectors on satellites detect only particles with range sufficient to penetrate various windows. Recent improvements in electronic detector design are reducing the minimum accessible energies, but experiment results for quiet times have not yet been published.

At very low energy (≈10^{-3} MeV/nucleon), the Sun continuously emits particles from hydrogen up to at least iron, the solar wind. Light ions of solar origin have occasionally been detected in interplanetary space with suprathermal energies (typically ≈0.01 MeV/nucleon) (ref. 15-25); and tracks of heavy ions ($Z \geqslant 20$) with energies above 0.01 MeV/nucleon have been observed in a glass filter from the Surveyor III camera (refs. 15-26 to 15-28), in an Apollo 12 spacecraft window (ref. 15-28), and in the lunar soils and rocks (refs. 15-29 and 15-30). In all these cases, it is most likely that the ions originated in solar flares.

The Solar Flare of April 18, 1972

A solar particle event occurred on April 18, 1972 (the second day of the Apollo 16 mission). It is not known what activity at the Sun was responsible, but the probable activity was just beyond the west limb, associated with a small X-ray burst and prominence activity about 1800 Greenwich mean time on April 17. The solar particle event had an extremely steep energy spectrum. The proton counting rates are given in figure 15-12. The energy spectrum was so steep that it was possible to study the composition of solar particles and, at the same time, to study preexisting interplanetary particles although not at as low an energy as originally hoped. Previously, the composition of solar particles emitted in only the most intense flares that occur occasionally during an 11-yr cycle had been studied. Rockets, which remain aloft for only approximately 4 min, are reserved for those rare flares of sufficient intensity to provide results of statistical significance. At energies of a few million electron volts per nucleon, flare particles have recently been found to be enriched in heavy nuclei such as iron (refs. 15-28, 15-31, and 15-32). The Apollo 16 experiment made it possible to test whether the composition depends on the strength of the flare as well as on energy.

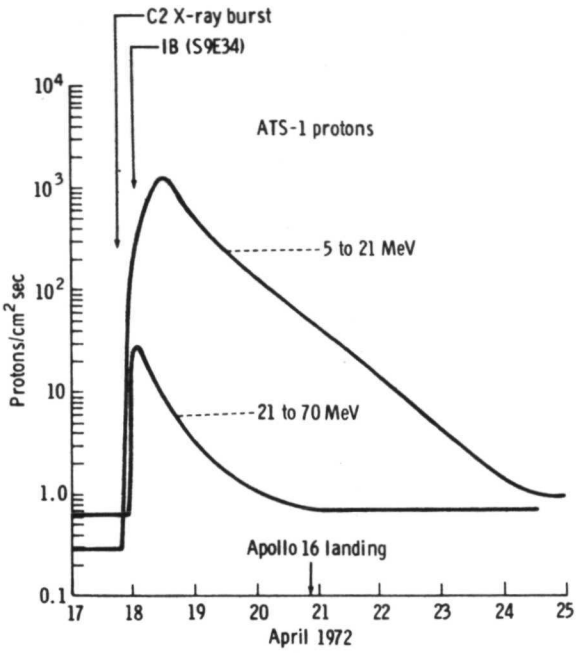

FIGURE 15-12.–Counting rates for protons in two different energy intervals determined on the Applied Technology Satellite (ATS).

Identification of Charged Particles

Dielectric track detectors have the following significant advantages over electronic detectors.

(1) Dielectric track detectors are not restricted in counting rate and can record solar flare particle tracks or galactic particle tracks with equal efficiency. Therefore, the problem of having the most abundant nuclei (hydrogen and helium) monopolize the data storage system does not arise.

(2) With ingenuity, dielectric track detectors can be used to energies much less than 1 MeV/nucleon. No inert window is needed, and the minimum range necessary for an acceptable signal may be as little as 1 μm in special cases.

(3) Dielectric track detectors can be made in virtually any size.

(4) A dielectric track detector can be used with a threshold that discriminates against unwanted particles below some minimum ionization rate.

The sensitivity of certain plastic detectors (Lexan, in particular) is increased by an ultraviolet (UV) irradiation. Coating the top sheet with 100 nm of aluminum is sufficient to eliminate that problem.

The chemical reactivity of tracks may decrease at elevated temperatures such as are reached in full sunlight on the lunar surface. The design of the heat shield is discussed in part A of this section.

The techniques for identifying charged particles by etching dielectric solids have been discussed in a comprehensive review (ref. 15-33), which includes chemical etching reagents for Lexan, cellulose triacetate (CTA), and silica glass. The following paragraphs contain a brief synopsis of the basic technique.

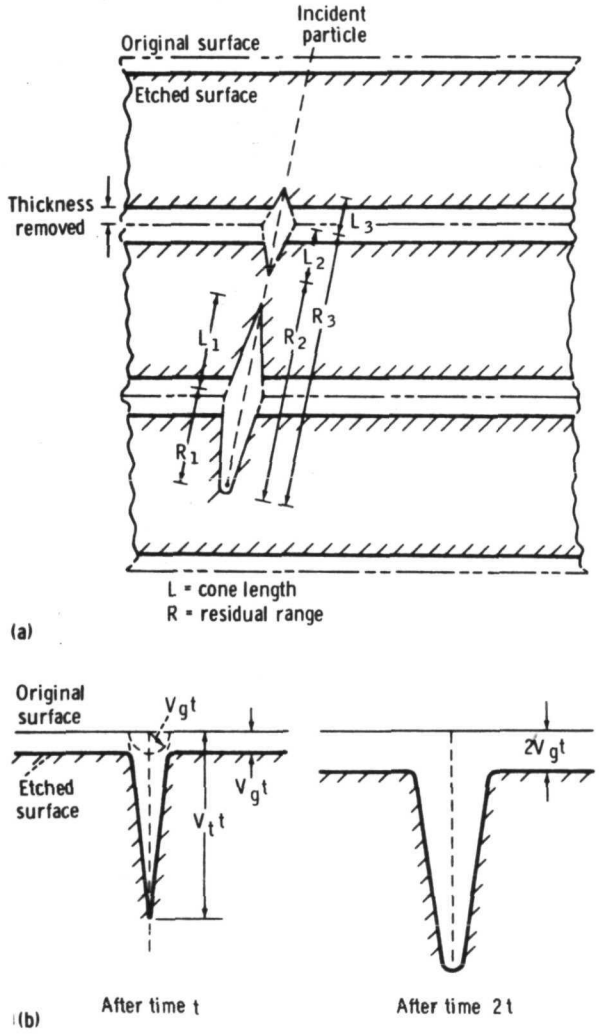

FIGURE 15-13.–Particle identification by etching rate method.

The basic idea (fig. 15-13) is that the rate of dissolution of a dielectric solid in a chemical etching solution is faster along the trajectory of a heavily ionizing particle than elsewhere. The shape of an etched track is roughly conical and is governed by the local ratio of the rate of etching along the track V_t to the general rate of etching V_g, which applies to all surfaces of the solid (including the exposed walls of the track). After the first etch, the length of an etched cone divided by the etching time gives an average value V_t along that part of the trajectory of the particle. If the particle passed completely through one or more sheets of dielectric solid, then several values of V_t will be obtained that fall on a smooth curve of V_t as a function of R, where R is the residual range of the particle at a point halfway along the cone. From appropriate calibrations with heavy ion accelerator beams, together with an ionization equation of the approximate form $J = AZ^{*2}/\beta^2$ and an empirical relationship between J and V_t, it is possible to generate a set of curves showing the response of a detector to slowing ions of differing Z. In this case, A is a constant, Z^* is the effective charge of the ion, and β is the velocity in units of the velocity of light. An example showing an ion that has passed through two plastic sheets and stopped in a third is shown in figure 15-13(a). Only one etching sequence was necessary. In figure 15-13(b), an ion penetrated only part of a detector. To study such low-energy ions, the etching time must be shortened so that the cone can be initially measured; then the detector is re-etched and the final length of the track is measured. The two measurements give V_t and R.

In the case of the etched cones in silica glass, diameter measurements provide additional information that aids in the determination of Z and R even at extremely small ranges.

The University of California experiment consisted of the following four components.

(1) Panel 1 contained 31 sheets of 250-μm Lexan, each 16.5 by 25.4 cm, fastened so that alternate sheets were translated by 2 mm when the astronauts folded the four hinged panels. This feature made possible the rejection of tracks of cosmic rays that passed through the spacecraft on the return trip. The 31 sheets were covered with a sheet of (50 μm) Teflon silvered on the back and with holes 2.5 cm

apart and 0.5 cm in diameter. The holes allowed a fraction of the stack to have a view of space with no covering material. The Teflon sheet was used to minimize absorption of visible sunlight, maximize emission of infrared, and keep the temperature of the underlying sheets below 343° K.

At some time during the mission, panel 1 became covered with a thin, dull, as yet unidentified film. The thermal properties of the film were so impaired that the final temperature exceeded 353° K. This seriously degraded the performance of panel 1, and, at present, an analysis of the panel has not been begun.

(2) One-half of panel 3 was used in the University of California experiment and contained the following detectors.

(a) A stack of sheets of 200-μm CTA, each 16.5 by 11.5 cm, was fastened so that alternate sheets could be translated 2 mm after the last EVA. Actually, the sheets shifted only ≈1 mm, which sometimes made difficult the determination of whether a track occurred before or after the stack was folded and brought into the spacecraft. The perforated Teflon sheet covering the CTA stack worked well; the temperature did not exceed 343° K, as judged by temperature indicating labels. Laboratory annealing experiments showed that tracks of argon and silicon ions in CTA sheets held at 343° K for 24 hr were decreased in V_t by only approximately 10 percent. The techniques illustrated in figure 15-13 were used to analyze tracks of particles with $Z \geqslant 3$ at energies from ≈0.2 to ≈100 MeV/nucleon.

(b) Tabs of Lexan previously irradiated with argon and krypton ions were inserted at three different depths in the CTA stack. After return, the tabs were etched to see if any fading of the tracks had occurred. The etching rate of the argon tracks proved to be the same, within experimental error, as the etching rate of argon tracks in a control piece kept in the laboratory. The krypton tracks etched three times faster than those in a control sample. At present, the only acceptable explanation is that some solar UV leaked into the panel through one of the holes and increased the reactivity of the krypton sample. Fortunately, CTA is extremely insensitive to UV.

(c) One slab of flame-polished silica glass 2.5 by 2.5 cm, aluminized on the bottom, was mounted on the CTA stack and covered with the Teflon heat shield. The center of the silica detector had a view of space through a 0.6-cm-diameter hole in the Teflon. Calibrations with heavy ion beams showed that, to a very good approximation, none of the ions of common elements in the Sun lighter than iron (e.g., silicon) will provide easily visible etched cones in the silica detector. The silica detector is thus extremely useful for determining the energy spectrum of the solar iron nuclei. It is also useful in searching for trans-iron nuclei among solar particles.

(d) A stack of 40 sheets of 6-μm Lexan, each 5 by 5 cm, was mounted on the CTA stack and covered with the Teflon heat shield. Its central portion viewed space through a 0.5-cm-diameter hole. The function of the stack was to determine the energy spectrum of particles of extremely low energy. Each sheet collects tracks of particles coming to rest in a narrow energy interval corresponding to a thickness of 6 μm of plastic. After irradiating each sheet with an intense dose of UV ($\lambda \approx 360$ nm), alpha particles leave visible etched cones in the last 1 to 5 μm of their range. The 6-μm stack thus serves as a differential alpha particle detector. Heavier ions leave tracks with nearly parallel walls that are distinctly different from the conical alpha particle tracks.

A more detailed general description of the overall design and deployment of the four panels, including the role of the astronauts, is given in part A of this section.

Results

Because of the passive nature of the detectors, it should be emphasized that the measurements and identification of tracks will extend over at least a 12-month period, in contrast to electronic experiments, which may be completed soon after a mission ends. At present, the results are still being analyzed, but the following conclusions have been reached.

Energy spectrum of particles with $Z \geqslant 6$.–The pair of photographs in figure 15-14(a) compares etch pits in a piece of silica glass irradiated with a beam of 3 MeV/nucleon iron ions in the University of California 224-cm cyclotron and etch pits in the uncovered portion of the silica glass irradiated in the solar flare. The density of tracks in the uncovered portion of the silica glass was 5×10^5 tracks/cm^2, which represents stopping iron nuclei alone. Some of the $\approx 3 \times 10^6$ tracks/cm^2 in the CTA (mainly $Z \geqslant 6$) are shown in figure 15-14(b), and some of the $\approx 2.5 \times 10^6$ tracks/cm^2 in the Lexan from panel 1 are shown in figure 15-14(c). At the top of the stack of 6-μm

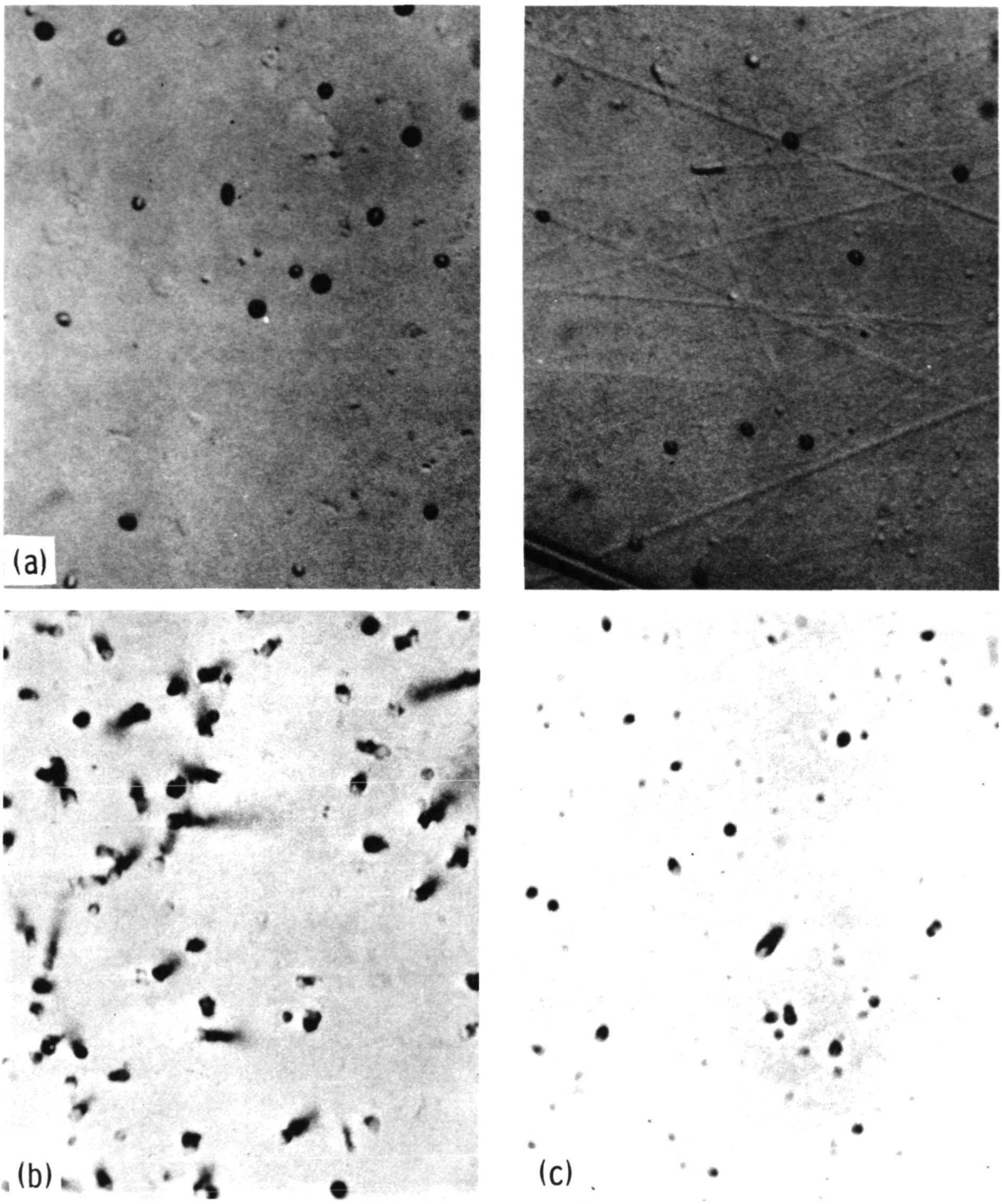

FIGURE 15-14.–Tracks of solar flare particles with $E \approx 0.1$ to ≈ 1 MeV/nucleon. (a) Etch pits of iron nuclei in the silica glass (left) compared with etch pits from iron nuclei produced in an accelerator (right). (b) Etched tracks of nuclei with $Z \geq 6$ in CTA from panel 3. (c) Etch pits of nuclei with $Z \geq 6$ in Lexan from panel 1, which was overheated. Each field of view is 70 by 53 μm.

Lexan sheets, the density of alpha particle tracks was difficult to determine quantitatively amid the background of heavy particle tracks and, at present, only a deeper sheet has been quantitatively studied.

Figure 15-15 shows portions of the energy spectra for four different charge groups: helium, $Z \geqslant 6$ (mainly CNO), $10 \leqslant Z \leqslant 15$, and iron. The helium point at ≈2 MeV/nucleon was determined from tracks of alpha particles that stopped in the part of sheet 3 of the thin Lexan stack that was covered with 50 μm of Teflon. The points for $Z \geqslant 6$ at energies of 0.1 to 1 MeV/nucleon were determined in CTA after a 1-hr etch; the point at 60 MeV/nucleon was obtained from a 30-hr etch. The data for $10 \leqslant Z \leqslant 15$ at low and high energies were obtained from CTA etched for 3 and 30 hr. The low-energy iron point was obtained from measurements in silica glass that was etched 1 hr.

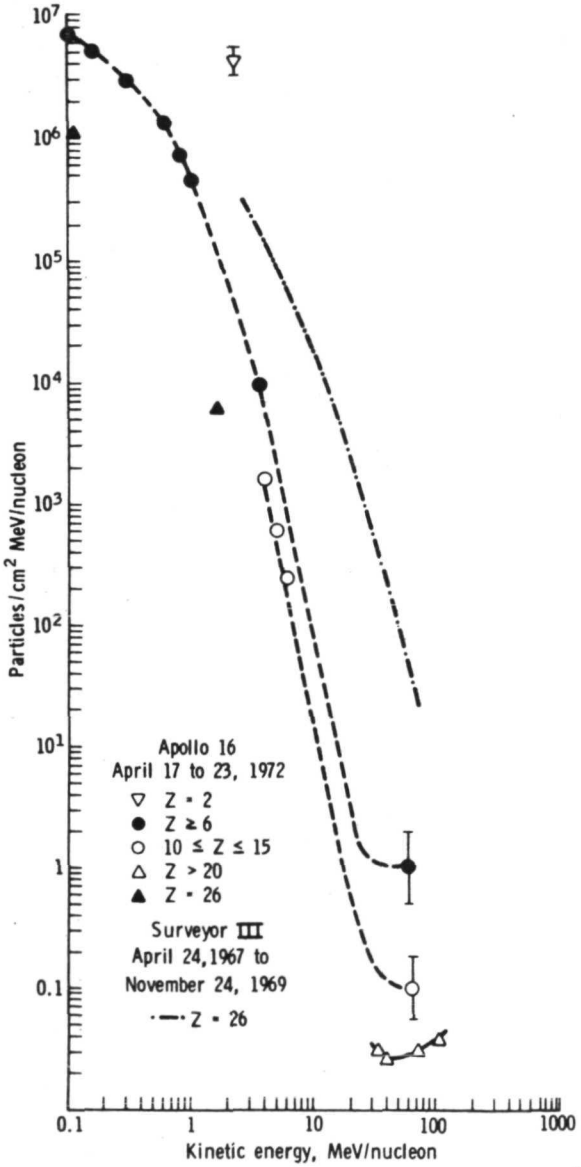

FIGURE 15-15.–Differential energy spectra for various charge groups during the period April 16 to 23, 1972.

One conclusion is that of a steep decrease of flux (by at least seven orders of magnitude) as the energy increases from ≈0.1 to ≈30 MeV/nucleon, followed by a flat portion at higher energies. At its steepest point, the spectrum falls off as $\approx E^{-5}$, where E is energy. With electronic detectors, solar flare energy spectra for protons and alpha particles have previously been observed that range from $\approx E^{-2.5}$ to $\approx E^{-4}$.

The steep portion could be ascribed to a solar contribution and the flatter portion to a galactic contribution that would not be significantly different in the absence of a flare. Compositional evidence supports this contention.

Composition of the solar flare particles.–At present, measurements of individual elements have been made in the CTA only at an energy of ≈4 MeV/nucleon. The limited data obtained from a part of the CTA etched for a time such that nuclei with $2 \leqslant Z \leqslant 14$ could be studied are summarized in table 15-IV. The absence of the secondary nuclei (lithium, beryllium, and boron) strongly supports the contention that the low-energy particles originated in the Sun.

The helium value in table 15-IV was obtained by comparing the helium flux at 2.1 MeV/nucleon in the

TABLE 15-IV.–Relative Abundances of Solar Particles ($E \approx 4$ MeV/nucleon)

Nuclei	*Observed*	*Solar (Cameron)*
Helium	[a]≈3000	2100
Lithium + beryllium + boron	0	≈0
Carbon	11	13.5
Nitrogen	3	2.4
Oxygen	20	24
Neon + magnesium + silicon	4.4	≈3 to ≈7
Iron	[b]6	.9

[a]Determined by comparing the helium flux at 2.1 MeV/nucleon in thin Lexan stack with the curve for $Z \geqslant 6$ in figure 15-15.

[b]Determined from the ratio of track densities in silica glass to track densities in CTA.

stack of the Lexan sheets with the flux of $Z \geq 6$ interpolated from the appropriate curve in figure 15-15.

The iron-to-($Z \geq 6$) ratio was estimated at an energy less than ≈0.5 MeV/nucleon by simply comparing the total track densities in the portions of silica glass and CTA directly under the holes in the Teflon heat shield. From comparisons with the rate of etching of iron tracks in silica bombarded with an iron beam in a cyclotron, it was established that the majority of the tracks in the glass were indeed iron. The result, iron/($Z \geq 6$) ≈ 6 for $E < 0.5$ MeV/nucleon, is uncertain by as much as a factor of 2 because of differences in stopping power of glass and plastic and because of uncertain recording efficiency of iron at large zenith angles in silica and of CNO at large zenith angles in CTA. The iron abundance is recorded in table15-IV.

Until another detector can be flown during a solar quiet time, the composition of the energy spectrum and interplanetary particles in the energy interval ≈0.1 to ≈30 MeV/nucleon cannot be determined.

Composition of the particles with $E > 30$ MeV/nucleon.–A portion of the CTA stack was etched 9 hr, and sheets at four different levels corresponding to mean energies of 34, 40, 75, and 105 MeV/nucleon were scanned for tracks of nuclei with $Z \geq 14$. Definite abundance peaks at silicon and iron, together with peaks at carbon and oxygen obtained in the solar particle identifications, established that the resolution was easily better than ±1 charge unit. Tracks of particles that entered the panel from the back constituted approximately one-third of the total. These tracks were not counted.

The presently available data are summarized in table 15-V. The number of events with $Z \geq 18$, although extremely limited, appears adequate to support the identification of the majority of these nuclei as galactic rather than solar, simply on the basis of the large fraction of secondary nuclei with $17 \leq Z \leq 25$.

Discussion

New capabilities. With the UV sensitization technique and a stack of 6-μm sheets of Lexan, it is possible for the first time to determine accurate differential energy spectra of alpha particles to energies as low as 0.1 MeV/nucleon and as high as ≈6 MeV/nucleon, the upper value being limited only by the stack depth. When the analysis is complete, it will be possible to determine definitively whether the spectrum rolls over at low energy or monotonically decreases with increasing energy. The identification of the alpha particles is reliable because protons are not recorded and because lithium and heavier nuclei leave tracks with markedly smaller cone angles than those of alpha particles.

Laboratory annealing and etching experiments on CTA have shown that alpha particle tracks are not observable after a 1-hr etch. Assuming no lithium, beryllium, and boron in the solar particles, it is then possible to attribute all observable tracks to nuclei with $Z \geq 6$. Because all nuclei have comparable range-energy relationships over the limited energy interval ≈0.1 to ≈2 MeV/nucleon, it is necessary only to measure range distributions to compute energy distributions for the charge group $Z \geq 6$ in this interval. At higher energies, the tracks are long enough that charges can be identified by the etch/re-etch scheme. One of the major new capabilities in this experiment is the ability to explore the newly accessible interval 0.1 to ≈10 MeV/nucleon.

In this laboratory, studies of the rate of growth of cones with etch time in silica glass have established the feasibility of identifying nuclei heavier than iron. Of the $\approx 10^5$ low-energy solar particles that entered the glass through the hole in the Teflon heat shield,

TABLE 15-V.–Relative Abundances of Heavy Galactic Cosmic Rays

Z	*At ≈40 MeV/nucleon*	*At ≈75 MeV/nucleon*	*At ≈140 MeV/nucleon*
Argon	1	0	2
Calcium	3	3	2
Titanium	1	0	1
Chromium	2	1	0
Iron	3	4	4
Nickel	0	0	1
>30	1	0	0

many are likely to be much heavier than iron. If they have the same composition as the Sun, it should be possible to detect charges to at least $Z = 40$. Several may have already been found that are heavier than iron, but the measurements are still in progress.

Enhancement of heavy nuclei in solar flares. - One of the unexpected results of recent solar flare studies is that at low energies the abundance of heavy elements like iron relative to that of light elements may be enriched by a factor of 10 or more (refs. 15-28, 15-31, and 15-32). At present, it is not clear whether the mechanism is associated with effective charge or ionization potential or some other aspect of atomic physics. It is therefore important to obtain systematic data at various energies and for various flare types. It is particularly important to be able, with the same system, to cover a large charge interval to test the idea of Price et al. (ref. 15-28) of an enhancement that increases with charge. The present system, with a capability of studying particles from helium on up, is ideal.

It is extremely interesting in the present work to find such a large abundance of iron relative to lighter elements at energies of ≈1 MeV/nucleon, as shown in table 15-IV. At energies of tens of million electron volts per nucleon where most of the particles are of galactic origin, no enhancement has been found in this work (fig. 15-15). The relatively high iron flux is thus exclusively associated with the flare particles. As data are accumulated, it will be possible to examine the energy dependence of the enhancement in detail.

Within present statistics, no evidence exists, at energies of ≈2 to 4 MeV/nucleon, for any deviation of the abundances of the elements with $2 \leqslant Z \leqslant 14$ from those expected in the Sun. However, the phosphate glass on Fleischer's panel (part A) shows 1.8×10^6 tracks/cm^2 (private communication) and should record mainly particles with $Z \geqslant 10$; the mica on Walker's panel (part C) shows $\approx 2 \times 10^6$ tracks/cm^2 (private communication) and certainly does not record CNO. These densities are within 50 percent of those in the CTA. All these data together indicate an enhancement of the neon-magnesium-silicon-to-CNO ratio at energies less than 1 MeV/nucleon, which disappears at higher energies.

Comparison of the April 18, 1972, flare spectrum with the Surveyor glass data. - In figure 15-15, the solid curve gives the differential energy spectrum of iron nuclei in interplanetary space integrated over a 2.6-yr interval beginning April 24, 1967 (ref. 15-28). The data were obtained by studying etched tracks as a function of depth in the glass filter within the Surveyor spacecraft camera. Because of the existence of an ≈1-μm coating on the surface and the fact that only those particles at a shallow angle could reach the glass, it was not possible to study energies less than ≈1 MeV/nucleon. If the energy spectrum during that 2.6-yr interval continues to increase steeply with decreasing energy, there would appear to be no inconsistency between it and the present data point at 0.1 MeV/nucleon for a single flare. It should be emphasized that the 1-week interval sampled by the Apollo 16 experiment was atypical in that solar particle events like that on April 18, 1972, are very infrequent.

Comparison of the April 18, 1972, flare spectrum with rocket data on flares. - Lexan detectors on rockets launched from Fort Churchill in Canada have recently been used (ref. 15-34) to study the composition of solar particles in the same energy interval accessible in the present experiment. The energy spectra in the rocket-borne detectors differ in an important way from those in figure 15-15. They go through a maximum at ≈1 to 2 MeV/nucleon and fall to zero at energies less than ≈0.2 MeV/nucleon. The present work shows that a well-defined maximum does not occur in all flares and raises several possible explanations for the maximum (ref. 15-34). Low-energy particles might have been excluded at Fort Churchill by a magnetospheric cutoff or because they had not reached the Earth from the Sun at the times of the rocket flights or even because of energy loss in the atmosphere of the Earth.

Origin of interplanetary charged particles with $E < 30$ MeV/nucleon. - The solar flare interference was an unprecedented opportunity to study a weak solar flare. However, studies of the origin of interplanetary charged particles will depend on future opportunities to use the same detectors to study the quiet-time spectra at energies of 0.1 to 30 MeV/nucleon.

Low-energy galactic cosmic rays. - At an energy of ≈60 MeV/nucleon, the flux of nuclei with $Z \geqslant 6$ shown in figure 15-15 is consistent with the flux at the same energy reported by Comstock et al. (ref. 15-22) during the previous period of minimum solar activity in 1964 and 1965. The level of quiet-time solar activity immediately before the flare of April 16 was only slightly above that in 1964 and 1965, as judged from neutron monitor levels. The flux of nuclei $10 \leqslant Z \leqslant 15$ at ≈65 MeV/nucleon during

Apollo 16 was similar to that reported in 1964 and 1965 at the same energy. No data exist for iron group nuclei at energies comparable to those measured in the present experiment.

The argument that these nuclei originated outside the solar system is based mainly on their composition as reported in table 15-V. At energies greater than 1 MeV/nucleon, the flux of nuclei with $17 \leqslant Z \leqslant 25$ is comparable to the iron flux (ref. 15-35), whereas the abundance of the same elements in the photosphere and in solar flares (ref. 15-34) is less than 15 percent that of iron. It seems inconceivable that these nuclei could actually have originated in the Sun but have passed through the amount of matter necessary to make the observed nuclei with $17 \leqslant Z \leqslant 25$ through nuclear reactions in interplanetary space.

The differential energy spectrum of nuclei with $Z \geqslant 6$ falls by seven orders of magnitude over the interval from 0.1 to 20 MeV/nucleon, then remains almost flat up to ≈100 MeV/nucleon. The two parts correspond to contributions from the Sun and from galactic cosmic rays. Any maximum in the spectrum occurs below the lowest energy studied.

At energies much below ≈4 MeV/nucleon, the abundance of heavy elements is enhanced by a large factor relative to lighter elements. At ≈4 MeV/nucleon, the abundances are similar to those in the Sun. At ≳40 MeV/nucleon, the abundances are similar to those in galactic cosmic rays, characterized by the presence of nuclei produced in spallation reactions in interstellar space.

Conclusions

During the Apollo 16 mission, a solar flare produced an enormous amount of low-energy nuclei, many orders of magnitude greater than the level inferred from studies of tracks in the window of the Apollo 12 spacecraft during a time when the Sun was quiet.

Acknowledgments

The authors thank Joan Steele of the University of California for help in making the measurements. We have had many useful discussions with E. K. Shirk, I. Hutcheon, and E. J. Kobetich of the University of California.

PART C

SOLAR COSMIC RAY, SOLAR WIND, SOLAR FLARE, AND NEUTRON ALBEDO MEASUREMENTS

D. Burnett,[a] *C. Hohenberg,*[b] *M. Maurette,*[c] *M. Monnin,*[d] *R. Walker,*[ab] *and D. Wollum*[a]

Introduction

Panel 4 of the cosmic ray experiment consisted of several detector systems designed to study various aspects of the radiation environment of the Moon. The detectors included mica, feldspar, three varieties of glass, two varieties of plastic, aluminum foil, and aluminum-coated platinum foil. The principal objectives were to study the heavy-element composition of the solar wind; the light-element composition of the solar wind in both interplanetary space and on the Moon; the thermal neutron albedo from the Moon; the radon atmosphere at the landing site; and, in general, all energetic heavy particles with $Z \geqslant 4$, either of solar or galactic origin, from energies from 1 keV/nucleon to tens of million electron volts per nucleon.

Several events occurred during the mission to modify or alter the information gained from panel 4. The most important of these events was an enhancement of particle fluxes, caused by a solar flare

[a]California Institute of Technology.

[b]Washington University, St. Louis, Missouri.

[c]Laboratoire de Spectrometrie Nucleaire et de Spectrometrie de Mass, (C.N.R.S.), Orsay, France.

[d]Laboratoire de Physique-Nucleaire, Universitc dc Clermont-Ferrand, France.

(described in part A of this section), during the trip to the Moon. The enhancement started approximately 36 hr after launch and diminished over a period of several days. The solar flare produced track densities of $\approx 10^6$ tracks/cm^2 at the surface of all the detectors and has given an unexpected and unprecedented opportunity to study heavy solar particles in the energy region from 10 keV/nucleon to >10 MeV/nucleon.

However, the high track density produced by the solar flare has made difficult the realization of some of the original goals of the experiment package. Measurement of the composition of quiet-Sun low-energy particles is clearly impossible, and measurement of the flux of heavy solar wind particles has been made difficult at best.

Panel 4 also contained a shifting mechanism that activated several experiments, most notably the neutron experiment, on the surface of the Moon. Because of a mistake in the final assembly, the shifting was only partially successful. This circumstance has degraded the information that can be obtained from the neutron experiment and also has made it very difficult to obtain information on the time variation of light solar wind nuclei.

Finally, the temperature rise in the package exceeded design specifications. Although this temperature rise has rendered the analysis of the experiment much more difficult and has limited the amount of hard results that can be presented in this preliminary report, it is felt that the effects of the temperature rise can be taken into account by future work.

General Description of Panel 4 Experiments

Panel 4 as it was returned from the Moon by the Apollo 16 astronauts is shown in figure 15-16. The lower part of the stack, labeled I, consisted of series of alternating layers of 60-μm-thick cellulose triacetate (triafol TN) and polycarbonate plastic (makrofol KG). This detector stack was covered with a 50-μm-thick coating of metallized Teflon to provide thermal protection and could thus be used only to study particles of $\geq$2 MeV/nucleon that were capable of penetrating this thermal shield. The last sheet in the stack consisted of a large TN foil designed to measure alpha particles from thermal neutron capture on an enriched boron-10 target plate found in the rear of part III.

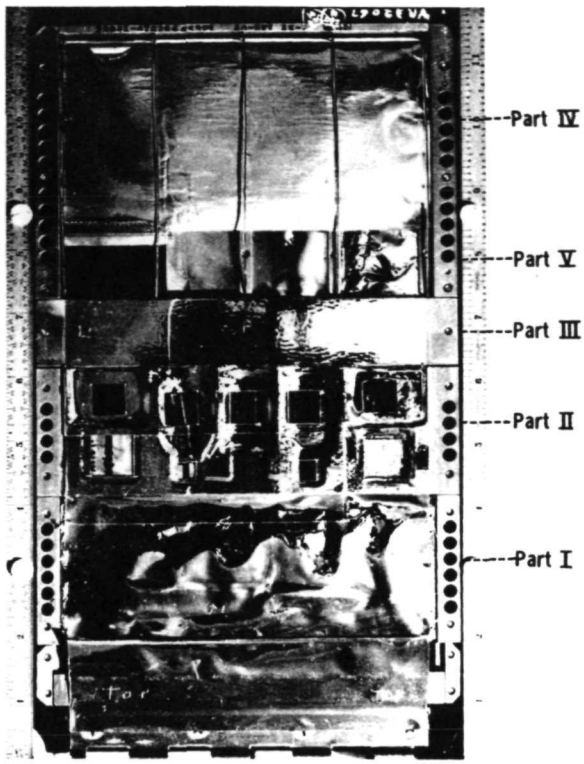

FIGURE 15-16.–Panel 4 as received on return from the Moon. Part labeled I is a stack of plastic detectors. Part II, the mineral assembly plate, contains mica, feldspar, and glass. Parts IV and V (partially visible) contain foils for trapping light solar wind.

Immediately adjacent to the plastic stack was a mineral assembly plate (part II) containing samples of mica, feldspar, soda-lime glass, tektite glass, and fused quartz. The mica detectors, which were included principally for the objective of measuring heavy solar wind ions with $Z \geq 26$, were also to be used to study any heavy particles with energy $\geq$1 keV/nucleon. The other mineral detectors were included to complement the mica and to provide samples that would be more directly comparable with lunar minerals.

Above the mineral assembly plate is an aluminum-coated platinum foil (part IV) that can be seen in figure 15-16 in partially retracted position. This foil was flush against part III during the outbound voyage and was retracted by the astronauts during the first EVA. The purpose of this foil was to measure the light solar wind in the interplanetary region to serve as a calibration for the heavy solar wind ions registered as tracks in the mica detector.

Seen under the partially retracted platinum foil (part IV) is another set of foils mounted in part V. Two of these consisted of aluminum-covered platinum, and one was anodized aluminum. The aluminum foil was provided by J. Geiss of the University of Bern and was the same material used in his more extensive light solar wind experiment (sec. 14 of this report). These part V foils were intended to measure differences in light solar wind flux and composition in time and space.

Two strips of mica (M10 and M11) are located on the left side of part V. During the flight to the Moon, the upper piece of mica (M10) was exposed to space through a 1.9-cm hole in the platinum foil. Half of this hole can be seen at the upper left corner of part IV. If the foil had been fully retracted, the second piece of mica would have been exposed to space starting with the time the astronaut shifted part IV. The purpose of this mica was to assess the importance of radon in producing shallow tracks (through the production of recoil atoms from alpha decay) that could be confused with extremely heavy solar wind ions.

Located in the rear of the panel is the neutron detector experiment. A schematic of this experiment is shown in figure 15-17. During the outbound voyage, a metal plate containing target strips of enriched boron-10 was located in the upper half of the panel behind parts III and IV. This target plate was connected to a wire lanyard, and pulling this lanyard (which moved the target plate down into the bottom part of the panel behind the plastic stack (part I)) activated the experiment. The photograph in figure 15-18, taken after removal of the mineral assembly plate, shows one target strip completely covered with plastic and another that has not moved into the plastic region. The target plate in turn was connected to the platinum foil (part IV), and pulling the lanyard also retracted part IV and exposed part V.

The proposed sequence of events was as follows. When the experiment was originally deployed, the minerals on part III, the plastic detectors (part I), and the aluminum-covered platinum foil (part IV) began registering solar and galactic particles. One piece of mica (M10) mounted on part V was also exposed during this time. Early in the first EVA, the astronaut was supposed to pull a lanyard that would retract part IV and expose part V. The mica (M10) on part V that had been irradiated up to this time would now

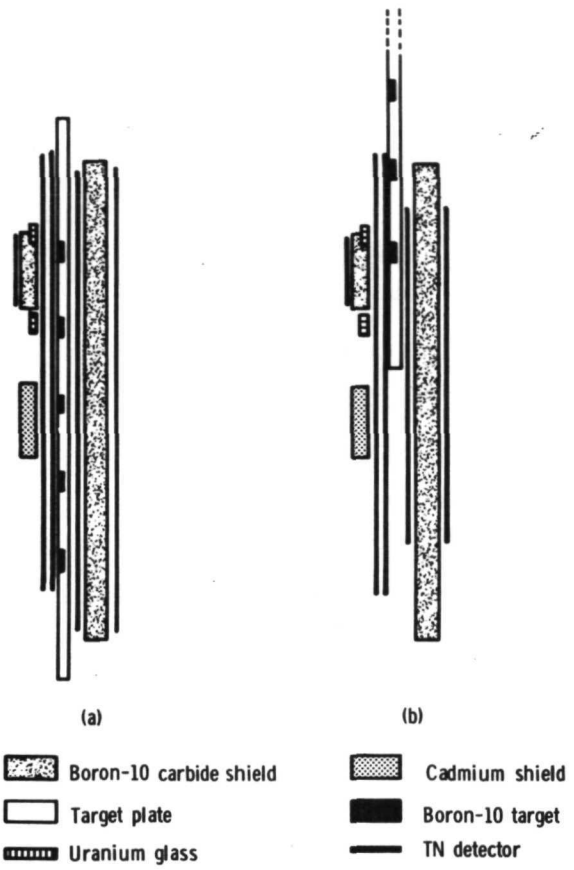

FIGURE 15-17.–Schematic diagrams of the neutron leakage flux experiment in panel 4. The scale in the horizontal direction has been grossly exaggerated to separate the components for easier viewing. (a) The experiment as it was designed. (b) The experiment as it was actually deployed because of the failure to achieve full activation.

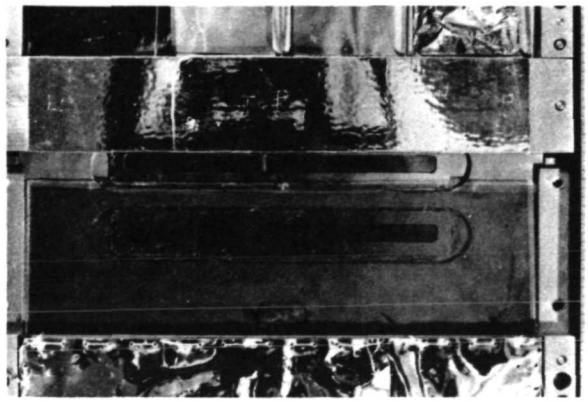

FIGURE 15-18.–Boron-10 target strip. The mineral assembly plate has been removed, and one target strip is visible through the covering sheet of triafol TN detector.

be shut off from low-energy particles by being covered with a tab of platinum foil attached to the lower left edge of part IV. Another piece of mica on part V (M11) would now be uncovered and start to register particle tracks. The lanyard shift would also move a boron-10 target plate into position to measure thermal neutrons. Both the neutron experiment and the plastic stack were deactivated by a final shift in the plastics that occurred automatically when the experiment was folded at the end of the final EVA.

The scheduled sequence of events did not occur completely as planned. When the commander attempted to pull the shifting lanyard that would have retracted part IV, he achieved only a partial shift of 2.5 cm, after which the lanyard broke. Several small screws mounted on the right side of part V were incorrectly installed and projected into the rear region of the panel. In effect, these screws clamped the target plate in position, making it extremely difficult to move. The failure to obtain a complete shift seriously degraded the neutron experiment and reduced the collection area for part V, making difficult the detection of differences in the solar wind at different times in the flight. Also, the mica (M11) on part V was never exposed to the space environment. This latter result was particularly unfortunate because the solar flare was almost over by that time and this mica would not have suffered from the enormous solar flare track background seen in the other micas.

The second unscheduled event was a relocation of the entire package at the end of the first EVA because of an increase in temperature as shown by several color indicators. The entire experiment was placed in the shade, further reducing the time of solar wind registration on the foils of part V. A summary of the exposure histories of the different samples is given in table 15-VI.

The temperature rise in panel 4 was monitored by several color indicators. Readings on the back of parts II and III and on the back of panel 4 indicated that the temperature was $>344^\circ$ K and $<355^\circ$ K.

The effects of temperature on the tracks themselves were monitored in several ways. First, the plastic stack included a set of preirradiated samples of TN and KG that had been exposed to oxygen ions of

TABLE 15-VI.–Exposure Conditions of Various Detectors

Detector	*Size, cm^2*	*Condition and time, hr:min*
Mica (M1 to M5) Quartz Tektite Soda-lime glass Feldspar Lower part of platinum foil Plastic stack	7.7 2.2 0.5 2.7 .58 112 75	LM deployed at 3:04 Experiment set in shade at 125:25 Experiment folded at 140:15 Total space exposure – 167:11 Exposure on Moon – 20:54 in Sun and 44:50 in shade Estimated total Sun exposure – 71:38
Mica (M10) Upper part of platinum foil	3.6 38	LM deployed at 3:04 Mica covered with platinum foil at 120:50 Total space exposure – 117:46 Exposure on Moon – 16:19 in Sun and 00:00 in shade Estimated total Sun exposure – 67:03
Lower part of part V Tab on part IV foil	28 10	Exposed at 120:50 Set in shade at 125:25 Folded at 170:15 Total space exposure – 49:25 Total Sun exposure – 4:35
Mica (M11) Upper part of part V foils		Always covered with 50-μm platinum foil
Neutron experiment		Activated at 120:50 Deactivated at 170:15 Total exposure – 49:25

different energies. This calibration set of plastics was located deep in the plastic stack, next to the TN foil used in the neutron experiment. No difference was observed in the etching of the oxygen tracks in control samples kept in the laboratory and in those returned from the Moon.

However, although no temperature effects were seen in the preirradiated foils, there are clear indications that temperature affected the registration of the tracks produced during flight. For example, in the neutron experiments, the alpha tracks are smaller and harder to recognize than normal alpha tracks registered in vacuum at room temperature.

Experimental Results on Mineral Detectors

The mineral detectors consisted of mica, feldspar (labradorite), soda-lime glass, tektite glass, and fused quartz. The areas and exposure conditions are listed in table 15-VI. The mica was taken from a large sheet of Indian muscovite and was preannealed at 923° K to remove fossil fission and alpha-recoil tracks. As a further step in eliminating stored tracks or potential spurious tracks, the mica was then pre-etched for 4 hr at 298° K in 40-percent hydrogen fluoride (HF). Following this step, it was verified that the surfaces were capable of registering tracks from 1-keV/nucleon heavy ions. The other detectors all consisted of polished surfaces obtained in a sequence of grinding and polishing steps culminating in the use of 0.05-μm aluminum oxide powder. The tektite and feldspar were also annealed, but no pre-etching was done. All samples except the fused quartz had a narrow, vapor-deposited strip of aluminum 100 nm thick across the center of the sample.

A summary of the track densities observed in the different materials is given in table 15-VII. The differences in track density arise from differences in the registration characteristics of the materials and do not represent inconsistencies in the track data. After photographic documentation, test pieces were removed from the detectors and etched to reveal particle tracks. The appearance of the tracks in mica and in two glass samples is shown in figure 15-19. The appearance of tracks in the feldspar after brief etching is similar to that in the mica and also to that in lunar feldspars etched for similar times.

The mica showed the highest track density and has been the most extensively studied in the work to date. A summary of the integral track length distribution measured by a combination of several techniques is given in table 15-VIII. It must be emphasized that this table does not include data on very shallow pits (or short tracks), the depth of which is in the range $\leqslant$100 nm. The length distribution for tracks in the range from 0.2 to 2 μm was obtained from SEM stereophotographs of a sample that had been etched for 2 hr to produce rather wide pits. A typical example is shown in figure 15-20. The length distribution from 2 to 12 μm was obtained by optical microscopy on a sample etched for 10 min. The length distribution for tracks $\geqslant$12 μm was obtained on a sample etched for 1 hr. Because the total track density did not vary during the etching times used, the data for different samples are directly comparable.

The major motivation for the inclusion of the mica detectors was the study of very shallow pits that should be produced by heavy solar wind ions. This idea was originally stimulated by the observation of alpha-recoil tracks in mica (ref. 15-36). These tracks,

TABLE 15-VII.–Surface Track Densities on Mineral Detectors

Sample	*Density, tracks/cm²*	*Etching conditions*	*Mode of observation*
Mica (M1 to M5)	$1.8 \pm 0.1 \times 10^6$	10 min to 2 hr, 30° C in 40 percent HF	Optical (OPT) (transmitted light) and scanning electron microscope (SEM)
Feldspar	$6.0 \pm 0.6 \times 10^5$	13 min to 1 hr, boiling sodium hydroxide (6 g sodium hydroxide, 8 g H_2O)	OPT
Soda-lime glass	$5.8 \pm 0.4 \times 10^5$	400 sec in dilute HF, 30° C, maximum pit diameter 3.0 μm	SEM
Tektite	$2.5 \pm 0.3 \times 10^5$	24 min in dilute HF, 30° C, maximum pit diameter 2.0 μm	SEM

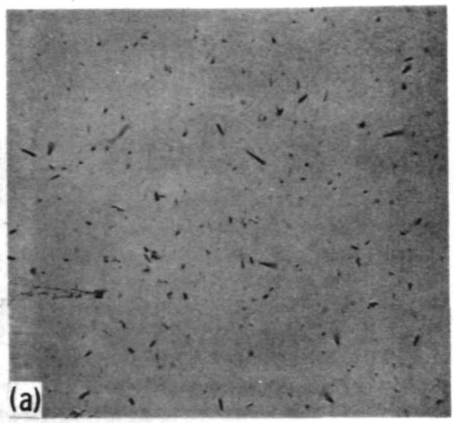

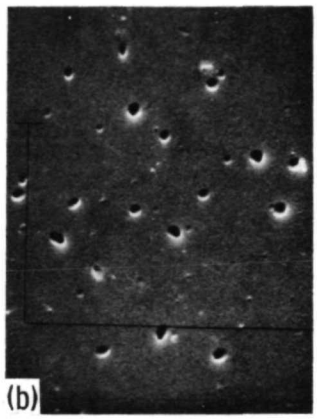

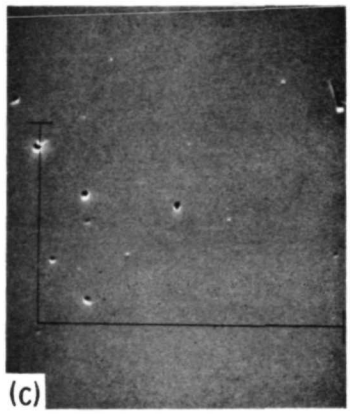

FIGURE 15-19.–Surface track densities in different detectors. Picture (a) was taken in an optical microscope at ≈1000X; (b) and (c) were taken in an SEM at 2000X. A feldspar crystal (not shown) has a similar appearance to picture (a) but has a track density more like picture (b). (a) Mica, 1.8 X 10^6 tracks/cm^2. (b) Soda-lime glass, 6 X 10^5 tracks/cm^2. (c) Tektite glass, 2 X 10^5 tracks/cm^2.

TABLE 15-VIII.–Integral Track Data in Mica

Track length, μm (a)	*Track density, tracks/cm^2*
>0.2	1.8 ± 0.1 X 10^6 (SEM)
>.5	1.8 ± 0.1 X 10^6 (SEM)
>1	1.1 ± 0.15 X 10^6 (SEM)
>2	7.4 ± 0.7 X 10^5 (OPT)
	4.4 ± 0.7 X 10^5 (SEM)
>4	2.6 ± 0.5 X 10^5 (OPT)
>6	5.5 ± 1.5 X 10^4 (OPT)
>8	2.2 ± 0.2 X 10^4 (OPT)
>12	6.3 ± 1 X 10^3 (OPT)
>20	1.4 ± 0.4 X 10^3 (OPT)
>34	2.8 ± 0.5 X 10^2 (OPT)
>50	8.5 ± 3 (OPT)

[a] ≲ 2 percent of total between 0.2 and 0.5 μm.

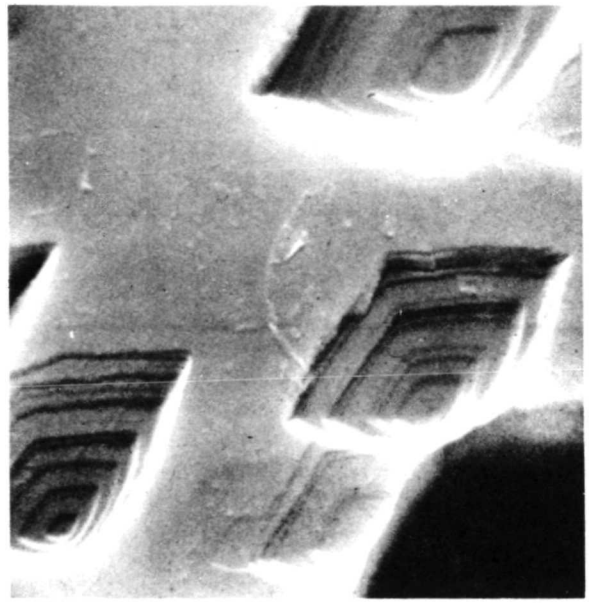

FIGURE 15-20.–An SEM photograph of short tracks in mica. The mica was etched for 2 hr at 30° C in concentrated HF to produce the enlarged pits.

which are produced by recoil nuclei from alpha particle decay of thorium and uranium, have energies similar to heavy solar wind ions. Subsequent, previously unpublished work has established that particles with energies in the range from 0.3 to 3 keV/nucleon produce observable pits in mica down to a charge of $Z = 26$.

It has been further shown that the diameters of the pits so produced vary in a systematic way with

the mass of the bombarding particles. This is illustrated in figures 15-21 and 15-22, which show pits produced by xenon atoms of 1 keV/nucleon and by the recoil atoms from a thorium-228 emanation source. Calibration irradiations with low-energy nickel, krypton, xenon, and lead ions on control pieces of muscovite have been used to establish a scale of mass as a function of diameter for particles with 1-keV/nucleon energy characteristic of the solar wind.

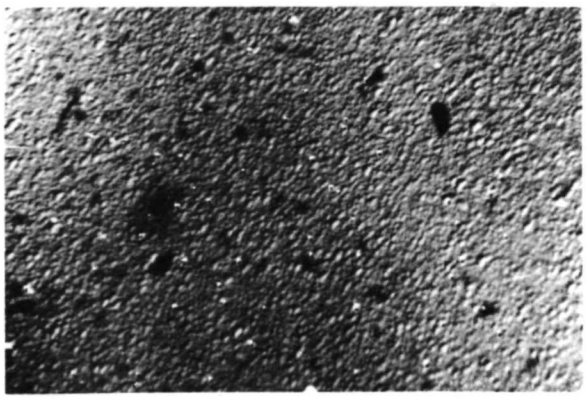

FIGURE 15-21.–Calibration irradiation of mica with 1-keV/nucleon zenon ions. The mica was etched for 2 hr, then silvered. The photograph was taken using a reflected light Nomarski phase contrast system.

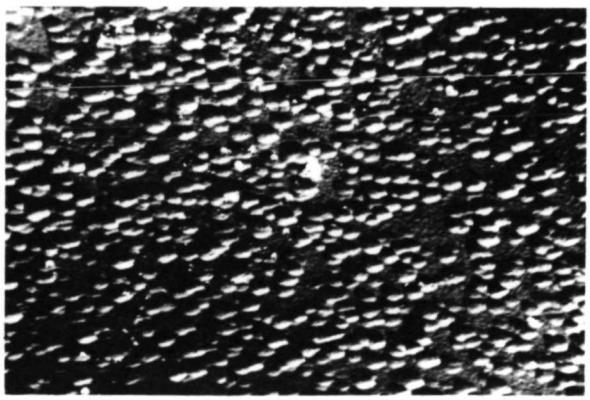

FIGURE 15-22.–Calibration irradiation similar to that in figure 15-21, using recoil atoms from a thorium-228 emanation source.

The best way of observing shallow pits in mica is to use a Nomarski phase contrast reflection system on samples that have surfaces that have been silvered by vacuum evaporation. Pit measurements are not made directly in the microscope but rather on 4- by 5-in. negatives made from high-contrast, high-resolution film. Although copy film has been found to give the best results, most of the measurements reported here were made on Polaroid 55PN film.

A sample of one of the micas, etched for 2 hr at 303° K in 40 percent hydrogen fluoride, using Nomarski phase contrast, is shown in figure 15-23. The principal difficulty in attempting to obtain heavy solar wind data from the Apollo 16 experiment is demonstrated by this figure. There is a large background of deep tracks (bright diamonds) that obscure much of the field of view. Also, there are pits of intermediate depth between the very shallow pits seen on the calibration photographs (figs. 15-21 and 15-22) and the deep pits. Most of the pits, including the very shallow ones, may have been produced in the solar flare and may not be associated with the heavy solar wind.

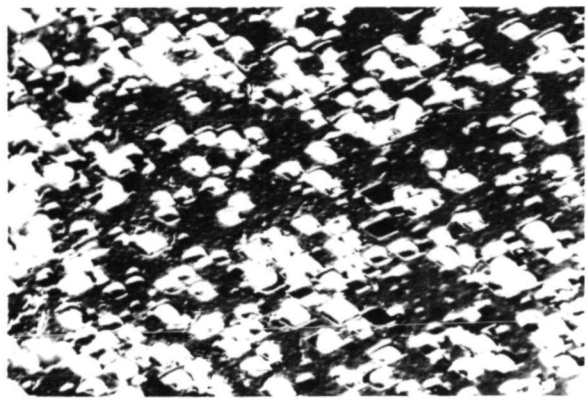

FIGURE 15-23.–Mica, taken under identical conditions to figures 15-21 and 15-22. The bright diamonds are deep tracks such as seen in figures 15-19(a) and 15-20.

Based on the previous calibration data, a scan was made of the photographs, dividing the shallow flat-bottomed pits into three categories: > xenon, > lead, > thorium. The corresponding densities were 2×10^5, 3.9×10^4, and 4.5×10^3 tracks/cm^2. The numbers are uncertain to at least 30 percent because of the difficulty in correcting for obscured regions. Similar numbers were found for both aluminum-covered and bare mica surfaces.

One sample of feldspar was given a prolonged etching to find the maximum etchable track length for slowing down iron nuclei. The maximum length was >25 μm.

Experimental Results on Plastic Detectors

The plastic stack consisted of a 75-cm^2 area containing 25 60-μm-thick sheets alternating between TN and KG, both manufactured by E. G. Bayer, Inc. One foil of cellulose acetate butyrate (BN) was also included. Adjacent sheets were shifted by 1 cm in the folding operation performed by the astronauts immediately before the storage of the package in the LM. Different batches of TN have been found to vary markedly in track registration properties, particularly when exposed to vacuum; all the sheets were therefore selected from a single roll of material. All calibration and temperature-control runs were made on material from this same roll adjacent to the material included in the flight package.

The first sheet of TN showed a density of $7.5 \pm 0.7 \times 10^4$ tracks/cm^2 of shallow pits less than ≈ 3 μm in length. These pits are similar to those seen in a calibration experiment in which a sample of TN was irradiated with alpha particles in vacuum at 353° K (slightly below the maximum possible temperature indicated by the temperature labels). The alpha particle identification is uncertain, and the short tracks could be recoil nuclei produced by proton and neutron interactions. The density of short pits in succeeding foils of TN are, respectively, $3.1 \pm 0.2 \times 10^4$, $2.2 \pm 0.5 \times 10^4$, and $1.5 \pm 0.4 \times 10^4$ tracks/cm^2.

The first TN sheet also contained a density of $3.9 \pm 0.4 \times 10^3$ tracks >6 μm in length, of which 10 percent penetrated the foil, producing a recognizable track on the back side. The corresponding density of long tracks in the second TN sheet was $3.1 \pm 0.5 \times 10^2$ tracks/cm^2.

Results of the Neutron Albedo Experiment

The neutron experiment was designed to estimate the leakage flux of low-energy (less than 10 eV) neutrons produced as a result of reactions of primary cosmic rays with lunar material. The experiment was based on the capture of neutrons by boron-10 targets producing alpha particles that were detected with a TN track detector. As shown in figure 15-17, a target plate consisting of a series of five boron-10 targets was mounted in the back of part III. Each strip was 5 mm wide and separated by 15 mm. Normally, the target plate should have slid in front of the TN detector (thereby activating the experiment) when the lanyard was pulled to retract the solar wind foil (part IV) in the initial deployment of the package on the lunar surface. The detector was deactivated by a 10-mm offset of the TN, when the panels were folded at the end of the final EVA.

Activation and deactivation were required to separate and eliminate the background from neutrons produced in the spacecraft before and after the lunar surface exposure. In particular, the activation and deactivation shifts were designed to eliminate background from neutrons produced by the radioisotope thermoelectric generator (RTG) on the trip to the Moon. To discriminate against neutrons produced in the LM during the period in which the detector was activated, an absorber made from boron carbide was placed between the neutron detector and the LM. (Control pieces of TN exposed to this boron-10 carbide plate showed track densities caused by the RTG that were 100 times that expected for the lunar neutron capture, showing the importance of the shifting operation.) A similar boron carbide absorber plate was placed between one target strip and the lunar surface to measure directly the contribution from LM-produced neutrons.

Small pieces of uranium glass were included as calibration sources to check possible thermal annealing of the alpha particle tracks. Comparisons of the uranium alpha particle tracks produced before and after the offset of the TN showed a decrease of 20 ± 10 percent in the rate of track production relative to the rate of track production during return of the package from the Moon to the laboratory. This amount of annealing may be important to the extent that it has degraded the appearance and length of the observed tracks, making them less easily identifiable.

The failure of the target plate to deploy completely (fig. 15-17) caused a loss of most of the data that would have been obtained from the neutron detector. It had been intended to have all five boron-10 target strips exposed to the TN detector, one with a cadmium shield between it and the lunar surface to supply spectral information on the neutron leakage flux and one with the small boron-10 carbide shield mentioned previously. However, the partial deployment lowered the bottom target strip (5) to a position beneath the small boron carbide plate and lowered target 4 to a position in line with the top of the TN sheet. The part of the TN that was finally

exposed to target 4 was not intended for data collection and contained glue on the rear side. Although the surface condition of the TN is less than ideal, it is possible to obtain some data from this area. Small uranium metal disks on the boron target plate provided fiducial marks to locate the positions of the boron targets precisely on the TN sheets, but the fiducial marks were lost because the uranium disks were not deployed properly. However, by means of the detailed documentary photography done at the disassembly of the package and a recent neutron exposure (radioautograph) of the reassembled panel, it is believed that the areas on the TN sheets that were exposed to the boron targets are accurately located. In addition, the positions of the uranium glass track distributions in the second large sheet of TN provide a rough check on the amount of shift achieved at the deactivation.

Based on a scan of ≈10 percent of the total area, the observed track density in the area exposed to target 4 is 870 ± 90 tracks/cm^2. However, only approximately one-third of these events are geometrically well-formed tracks. The remaining tracks are relatively short (less than 2 μm) and are more difficult to measure. Background measurements on regions between the target strips and under the shielded target (5) are consistent and give an average density of 700 ± 90 tracks/cm^2. The quoted errors are one standard deviation, but they may not be relevant in assessing the accuracy of the experiment. The ratio of well-formed tracks to total tracks is similar in the background and sample area. The density of long tracks (greater than 6 μm), ascribable to heavy ions, is roughly 10 tracks/cm^2 based on four events. This is consistent with the Apollo 15 measurements made on TN.

The high background is at least an order of magnitude higher than that measured on Apollo 15 TN control sheets and is of unknown origin. The soft spectrum found for the solar flare heavy particle tracks makes it unlikely that the background is of solar flare origin. Similarly, the density appears to be too high to be accounted for by galactic cosmic rays. Possibly, the background is caused by the proximity of the RTG with a subsequent production of alpha tracks by neutron interactions with oxygen-17 and carbon-16 or the production of heavy atom recoil tracks by elastic collisions. Another possibility is the production of tracks during passage through the radiation belts. It is also conceivable that the package was exposed to a high radon background at some time in its history.

Other Measurements

The scheduled measurements of the light solar wind have not been made at present because of difficulties with the appropriate mass spectrometer. However, two additional measurements, both with negative results, have been performed. Immediately after the demounting of the package, both the platinum foil (part IV) and the plastic stack (part I) were taken to the Battelle Memorial Institute, Richland, Washington, and counted in the special low-level counting facility developed by R. Perkins. No counts above background were observed in the counting system, which consisted of two 30-cm-diameter, 20-cm-thick scintillators. Therefore, a limit was set at the 95-percent confidence level of <1 disintegration/min for energetic single photon emitters and $<10^{-1}$ disintegration/min for two photon emitters such as cobalt-60.

A portion of the platinum foil (part IV) ≈1 cm^2 in area was also measured by T. Tombrello and D. Leach of the California Institute of Technology for implanted protons. Using a beam of fluorine ions of variable energy and measuring the gamma yield from the resonant fluorine-proton reaction, a limit was set of less than ≈10^{15} protons/cm^2 in the energy range 10 to 40 keV. However, a calibration irradiation showed that the platinum foil may not retain implanted protons; therefore, this experiment will be repeated on other materials.

Discussion

Origin of long (>0.5 μm) tracks in minerals: characteristics of the Apollo 16 solar flare event.–The largest tracks (>50 μm) in mica are produced by heavy particles of the heavy-particle group ($20 \leqslant Z \leqslant 28$). As the track length becomes smaller, lighter ions also begin to be included. From previous calibration work (refs. 15-37 and 15-38), it is estimated that the following even Z (i.e., abundant) nuclei would begin to register at different track lengths: argon, 34 μm; sulfur, 14 μm; silicon, 10 μm; and magnesium, 6 μm. Neon is somewhat ambiguous. Although previous work would suggest maximum track lengths of ≈2 μm, a new calibration irradiation with 100-keV/nucleon neon ions on a control mica heat treated in a similar fashion to the cosmic ray experiment mica failed to give any but the shallowest pits.

In figure 15-24, the integral track density as a function of energy has been plotted in two ways. In one set of points, it was assumed that all the tracks were produced by iron ions. In the other, the points have been corrected by taking into account the contribution of lighter elements using the universal abundances as given by Cameron (ref. 15-39). Because recent work (refs. 15-40 and 15-41) has shown that the iron tends to be more abundant in solar flares relative to silicon than given by the Cameron values, the real situation probably lies between these values.

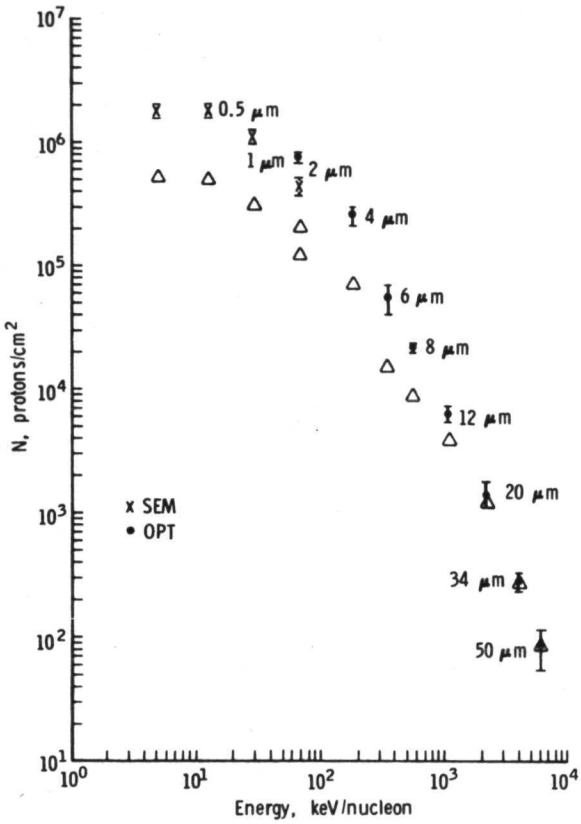

FIGURE 15-24.–Integral track densities as a function of energy in mica. The O and X points assume that all tracks are produced by iron. The Δ points have been corrected for an increasing contribution caused by lighter ions at shorter track lengths.

With either set of assumptions, the same general picture emerges. From ≈200 keV/nucleon to 6 MeV/nucleon, the differential spectrum can be represented by a power law in kinetic energy with

$$\frac{dN}{dE} = 4.2 \times 10^3 E^{-3.2} \text{ particles/cm}^2\text{-ster-MeV/nucleon}$$
(uncorrected)

and

$$\frac{dN}{dE} = 2 \times 10^3 E^{-2.8} \text{ particles/cm}^2\text{-ster-MeV/nucleon}$$
(corrected for light elements)

where E is expressed in million electron volts per nucleon. Below ≈200 keV/nucleon, the spectrum bends over. However, new particles continue to be registered down to an energy of ≈15 keV/nucleon. The bending over of the spectrum is consistent with the limit of $<10^{15}$ protons/cm^2 for 10- to 40-keV implanted protons. If the high-energy proton flare data were extrapolated to low energy with no bending over, then $>10^{16}$ protons/cm^2 would have been expected.

There seems to be a definite break at a track length of 0.5 μm with very few particles in the region of >1 to 15 keV/nucleon. Such a break could be an artifact if the etchable track lengths for low-energy iron ions are less than the actual ranges. However, calibration irradiations of other muscovite samples with 30 and 15 keV/nucleon nickel ions have given etchable ranges in good agreement with the theoretical ranges. A final decision on this point must await calibration irradiations of the mica actually used in flight.

Satellite observations during the mission showed a sudden enhancement in the flux of protons in interplanetary space. The enhancement, which occurred approximately 36 hr after launch and then decayed over a period of several days, was probably associated with a small X-ray burst and prominence activity just beyond the west limb at approximately 1800 Greenwich mean time on April 17, 1972. The flare was soft and rather small, having integrated fluxes of 1.04×10^8 tracks/cm^2 at 5 to 31 MeV/nucleon and 1.1×10^6 tracks/cm^2 at 21 to 70 MeV/nucleon. The very large track densities seen in the various detectors were probably predominantly caused by this flare. A similar, though somewhat harder, spectrum is observed in the minerals, and the number of iron tracks >5 MeV/nucleon is in reasonable accord with the proton data.

The possibility also exists that some of the tracks may have been produced during passage through the radiation belts where estimated proton fluxes of 3.3×10^8 protons/cm^2 > 4 MeV, 4.9×10^6 protons/cm^2 > 30 MeV, and 4.3×10^6 protons/cm^2 > 50 MeV were encountered. However, in view of the value of $\approx 10^{-7}$ given by several authors (refs. 15-42 and 15-43) for the ratio of the carbon-nitrogen-oxygen

group ($E \geq 0.3$ MeV/nucleon) to protons, this seems an unlikely source.

The limits on radioactivity measured by Perkins coupled with the measurement of heavy ion tracks in the minerals can be used to set limits on the abundance of specific radio elements in the flare. For example, sodium-22 and cobalt-56 must be present at levels $<10^{-3}$ and 10^{-4} of the total number of atoms from magnesium to iron.

Tracks in plastics.–The plastics in panel 4 were covered with a continuous sheet of 50-μm-thick Teflon instead of with the perforated sheets used in the other panels. Therefore, no low-energy data are available from this stack. However, the other panels in the package contained an abundant amount of plastic with which to study low-energy particles. It is evident also that no internal data on light elements at low energies are available to compare abundances in this part of the preliminary report.

The results on the alpha-sensitive TN are not understood at present. The densities of small pits, similar to those produced by low-energy alpha particles, are too high to be in accord with the heavy-particle data from the mica. Furthermore, the depth dependence is completely different from the behavior of the heavy-particle spectrum. Although previous work (refs. 15-40 and 15-41) has shown that the iron/helium ratio may be energy dependent, the differences are so extreme in this case as to suggest that the small track data refer to a completely different phenomenon.

It is considered possible that the small pits in the top three TN sheets are actually recoil nuclei produced by energetic protons from both the flare and the radiation belts. However, the number of tracks in the first TN sheet appears to be rather high for this explanation, and some helium particles from the radiation belts may be registering directly.

The difference in the density of long tracks (>6 μm) between the first and second TN sheets is compatible with the heavy-particle energy spectrum, and it is possible that these tracks are flare related. However, additional depth measurements are needed to test this point.

Heavy solar wind ions.–The cutoffs that have been used in counting shallow pits correspond roughly to element charge groupings of 50 to 70, 70 to 80, and ≥90. Taking a nominal solar wind proton flux of 3×10^8 protons/cm^2/sec and the estimated Sun exposure from table 15-VI, abundances relative to protons could be inferred for the charge groups of 2.6×10^{-9}, 5×10^{-10}, and 5.8×10^{-11}, respectively.

These values are similar to those given by the Cameron abundances of 10^{-9}, 3×10^{-10}, and 3×10^{-12} for the same elements. However, the track data on the aluminum-covered part of the mica is essentially identical to that on the bare mica surface. In principle, the aluminum is 100 nm thick and should have stopped all the heavy solar wind particles.

Until additional bombardment experiments on the aluminum-covered surfaces are made, the most likely source of the shallow pits is concluded to be the solar flare event. The solar flare itself could have contained very low-energy, very heavy ions; or, perhaps more likely, the shallow pits could have been produced by subtrack threshold energetic ions that produce occasional small regions of radiation damage capable of nucleating the shallow pits.

One firm conclusion that can be made is that there is no evidence for a large enrichment of very heavy ions in the solar wind.

Neutron albedo at the Apollo 16 site.–The neutron flux is given by the ratio ρ/ϵ where ρ is the measured track density in the TN detector and ϵ is the rate of track production per incident neutron. Coupling the previous values for ϵ, which were based on measurements up to 343° K in vacuum, with recent theoretical calculations of the lunar leakage neutron flux by Lingenfelter, Canfield, and Hampel (submitted to Earth and Planetary Science Letters, June 1972), a density of 400 to 600 tracks/cm^2 is predicted. The chemical composition of Apollo 16 material has been taken into account in this estimate. In contrast, the experimental value is 870 ± 90 minus a large background of 700 ± 90.

The low value of the measured track density relative to the predicted value cannot be taken at this time as indicating disagreement with the theory. The altered nature of the tracks, coupled with the preliminary results of a vacuum heating experiment at 353° K, indicates that the value of ϵ appropriate to the experiment is probably substantially lower than previous estimates.

Additional work is in progress to define ϵ for the actual flight conditions. It is hoped that this determination, coupled with a better understanding of the background problem, will provide a more critical test of the theory of lunar neutron albedo.

Implications for lunar sample studies.–The most significant result of this experiment to date is the

demonstration that heavy ions, capable of registering tracks in lunar-like minerals, continue to increase with decreasing energy down to ≈15 keV/nucleon. One of the intriguing results of lunar sample analysis has been the demonstration by Maurette et al. (ref. 15-44) and subsequently by Price et al. (ref. 15-45) that tiny lunar dust grains less than ≈1 μm size have extremely high track densities in the range 10^{10} to 10^{11} tracks/cm^2. Maurette et al. previously postulated the existence of a large flux of low-energy particles to explain these very high densities. Radiochemical measurements give a value of ≈80 protons/cm^2/sec >10 MeV from solar flares averaged over many solar cycles. If this is taken as the basis of comparison, the present flare represents ≈0.4 percent of a normal yearly dose. To accumulate 10^{10} to 10^{11} tracks would therefore require approximately 10^2 to 10^3 yr exposure. This is compatible with the known solar wind data on the lunar soil and on the estimated depth of the lunar regolith.

However, these calculations should be taken cautiously. Only one flare has been dealt with for this report, and it has a somewhat softer spectrum than solar flares measured over the longer period of time of the nearly 3-yr exposure of the Surveyor III glass filter previously studied (refs. 15-40, 15-46, and 15-47). In particular, in comparing surface track densities with those taken at a depth of ≈5 μm, no evidence was found previously for a large abundance of heavy particles with energies less than ≈0.5 MeV/nucleon in the Surveyor III glass. One major task for the future is to reexamine the Surveyor material to understand the differences with the present results.

The observation of very long iron tracks in feldspar confirms earlier accelerator experiments by Price (private communication). These tracks are much longer than those normally observed in lunar samples that are partially annealed under normal lunar environmental conditions.

At the Apollo 12 conference, Bhandari et al. (ref. 15-48) reported evidence for tracks from extinct superheavy elements. The analysis was based on the separation of fission tracks from cosmic ray tracks on the basis of length. Significantly, it was found that only crystals removed from the soil showed an excess of long tracks that were attributed to the fission of superheavy elements. The lunar soil is an extremely good insulator, and crystals imbedded even a few centimeters into the surface will have only modest temperature fluctuations around a mean of 250° K (refs. 15-49 and 15-50). Thus, cosmic ray tracks will be less annealed than in the case of exposed lunar rocks that reach temperatures of ≈423° K. The long tracks attributed to fission by Bhandari et al. may thus be simply less-annealed, long cosmic ray tracks.

Summary

(1) All mineral detectors exposed on Apollo 16 had high surface track densities (≈10^6 tracks/cm^2) probably produced by a solar flare that occurred during the mission.

(2) The heavy ions followed a power law spectrum with exponent ≈3 down to ≈200 keV/nucleon. Although the spectrum bent over below this energy, a considerable number of particles were present to 15 keV/nucleon. Few particles were evident between 1 and 15 keV.

(3) The abundance of low-energy particle tracks observed in this flare may explain the high track densities observed in lunar dust grains.

(4) Pristine heavy-particle tracks in feldspar give long (>25 μm) tracks. All tracks in lunar feldspars thus appear to be partially annealed. This result also casts doubt on previous claims for fossil tracks from extinct superheavy elements in lunar samples.

(5) Shallow pits similar to those expected from extremely heavy solar wind ions were observed in about the expected number. However, these may be caused by solar flares and not by solar wind. No evidence is found for the enhancement of ions with $Z > 50$ in the solar wind.

(6) Initial results give a low apparent value of neutron albedo relative to theory. However, the results are affected by thermal annealing during flight, and much additional work has to be done to give a critical test of the theory.

(7) The ratio of radioactive atoms to stable atoms in the Apollo 16 flare was such as to give <1 disintegration/min (single-gamma process) and <0.1 disintegration/min (two-gamma process) for 10^8 stopped heavy particles (magnesium-iron).

Acknowledgments

The authors acknowledge the experimental support of P. Swan and S. Sutton of Washington University for the SEM work and of R. Mourior and P. Petor of Laboratoire de Spectrometrie Nucleaire et

de Spectrometrie de Mass for several calibration irradiations. The final package design was arrived at in concert with E. Stockhoff of GE, who was also responsible for its construction and testing. The authors also thank R. Perkins of Battelle Memorial Institute and D. Leach and T. Tombrello of California Institute of Technology for the permission to quote the results given herein. The California Institute of Technology is also gratefully acknowledged.

REFERENCES

15-1. Fleischer, R. L.; Price, P. B.; and Walker, R. M.: Tracks of Charged Particles in Solids. Science, vol. 149, no. 3682, July 23, 1965, pp. 383-393.

15-2. Fleischer, R. L.; Price, P. B.; and Walker, R. M.: Solid-State Track Detectors: Applications to Nuclear Science and Geophysics. Annu. Rev. Nucl. Sci., vol. 15, 1965, pp. 1-28.

15-3. Fleischer, R. L.; Price, P. B.; and Walker, R. M.: Nuclear Tracks in Solids. Sci. Amer., vol. 220, no. 6, June 1969, pp. 30-39.

15-4. Price, P. B.; and Fleischer, R. L.: Identification of Energetic Heavy Nuclei with Solid Dielectric Track Detectors: Applications to Astrophysical and Planetary Studies. Annu. Rev. Nucl. Sci., vol. 21, 1971, pp. 295-334.

15-5. Fleischer, R. L.; Hart, H. R., Jr.; and Giard, W. R.: Particle Track Identification: Application of a New Technique to Apollo Helmets. Science, vol. 170, no. 3963, Dec. 11, 1970, pp. 1189-1191.

15-6. Fleischer, R. L.; Price, P. B.; and Walker, R. M.: Ion Explosion Spike Mechanism for Formation of Charged-Particle Tracks in Solids. J. Appl. Phys., vol. 36, no. 11, Nov. 1965, pp. 3645-3652.

15-7. Fleischer, R. L.; Price, P. B.; and Woods, R. T.: Nuclear-Particle-Track Identification in Inorganic Solids. Phys. Rev., vol. 188, no. 2, Dec. 10, 1969, pp. 563-567.

15-8. Crawford, W. T.; DeSorbo, W.; and Humphrey, J. S., Jr.: Enhancement of Track Etching Rates in Charged Particle-Irradiated Plastics by a Photo-Oxidation Effect. Nature, vol. 220, Dec. 28, 1968, pp. 1313-1314.

15-9. Price, P. B.; and Fleischer, R. L.: Particle Identification by Dielectric Track Detectors. Radiation Effects, vol. 2, 1970, pp. 291-298. Proceedings of the International Topical Conference on Nuclear Track Registration in Insulating Solids and Applications. May 1969, vol. I, D. Isabelle, ed., pp. IV 2-34.

15-10. Peterson, D. D.: Improvement in Particle Track Etching in Lexan Polycarbonate Film. Rev. Sci. Instr., vol. 41, no. 8, Aug. 1970, pp. 1252-1253.

15-11. Northcliffe, L. C.; and Schilling, R. F.: Range and Stopping Power Tables for Heavy Ions, Texas A&M (College Station), 1970; Nuclear Data Tables, vol. 7, 1970, p. 233ff.

15-12. Allen, L. H.: Abundance of the Elements. J. Wiley & Sons (New York), 1961.

15-13. Fillius, R. Walker; and McIlwain, Carl E.: Anomalous Energy Spectrum of Protons in the Earth's Radiation Belt. Phys. Rev. Letters, vol. 12, no. 22, June 1, 1964, pp. 609-612.

15-14. Katz, Ludwig: Electron and Proton Observations. Radiation Trapped in the Earth's Magnetic Field, vol. 5, Billy M. McCormac, ed., Gordon & Breach (New York), 1966, pp. 129-153.

15-15. Mogro-Campero, Antonio; and Simpson, J. A.: Enrichment of Very Heavy Nuclei in the Composition of Solar Accelerated Particles. Astrophys. J. (Letters), vol. 171, no. 1, part 2, Jan. 1, 1972, pp. L5-L9.

15-16. Fleischer, R. L.; Hart, H. R., Jr.; and Comstock, G. M.: Very Heavy Solar Cosmic Rays: Energy Spectrum and Implications for Lunar Erosion. Science, vol. 171, no. 3977, Mar. 26, 1971, pp. 1240-1242.

15-17. Crozaz, G.; and Walker, R. M.: Solar Particle Tracks in Glass from the Surveyor 3 Spacecraft. Science, vol. 171, no. 3977, Mar. 26, 1971, pp. 1237-1239.

15-18. Price, P. B.; Hutcheon, I.; Cowsik, R.; and Barber, D. J.: Enhanced Emission of Iron Nuclei in Solar Flares. Phys. Rev. Letters, vol. 26, no. 15, Apr. 12, 1971, pp. 916-919.

15-19. Unsöld, A.: Abundance of Iron in the Photosphere. Phil. Trans. Roy. Soc. London, vol. A270, no. 1202, July 16, 1971, pp. 23-28.

15-20. Bertsch, D. L.; Fichtel, C. E.; and Reames, D. V.: Nuclear Composition and Energy Spectra in the 1969 April 12 Solar-Particle Event. Astrophys. J., vol. 171, no. 1, part 1, Jan. 1, 1972, pp. 169-177.

15-21. Korchak, A. A.; and Syrovatskii, S. I.: On the Possibility of a Preferential Acceleration of Heavy Elements in Cosmic-Ray Sources. Soviet Phys. Dokl, vol. 3, no. 5, Sept.-Oct. 1958, pp. 983-985.

15-22. Comstock, G. M.; Fan, C. Y.; and Simpson, J. A.: Energy Spectra and Abundances of the Cosmic-Ray Nuclei Helium to Iron from the OGO-I Satellite Experiment. Astrophys. J., vol. 155, no. 2, Feb. 1969, pp. 609-617.

15-23. Hsieh, K. C.; and Simpson, J. A.: The Isotopic Abundances and Energy Spectra of ^{2}H, ^{3}He, and ^{4}He of Cosmic-Ray Origin in the Energy Region ~10-100 MeV Nucleon^{-1}. Astrophys. J. (Letters), vol. 158, no. 1, Oct. 1969, pp. L37-L41.

15-24. Baity, W. H.; Teegarden, B.; Lezniak, J. A.; and Webber, W. R.: Intensities of Low-Energy Cosmic-Ray ^{2}H and ^{3}He Nuclei Measured in 1967-68. Astrophys. J., vol. 164, no. 3, Mar. 15, 1971, pp. 521-527.

15-25. Frank, L. A.: On the Presence of Low-Energy Protons ($5 < E < 50$ kev) in the Interplanetary Medium. J. Geophys. Res., vol. 75, no. 4, Feb. 1, 1970, pp. 707-716.

15-26. Crozaz, G.; and Walker, R. M.: Solar Particle Tracks in Glass from the Surveyor 3 Spacecraft. Science, vol. 171, no. 3977, Mar. 26, 1971, pp. 1237-1239.

15-27. Fleischer, R. L.; Hart, H. R.; and Comstock, G. M.: Very Heavy Solar Cosmic Rays: Energy Spectrum and Implications for Lunar Erosion. Science, vol. 171, no. 3977, Mar. 26, 1971, pp. 1240-1242.

15-28. Price, P. B.; Hutcheon, I.; Cowsik, R.; and Barber, D. J.: Enhanced Emission of Iron Nuclei in Solar Flares. Phys. Rev. Letters, vol. 26, no. 15, Apr. 12, 1971, pp. 916-919.

15-29. Borg, J.; Dran, J. C.; Durrieu, L.; Jouret, C.; and Maurette, M.: High Voltage Electron Microscopic Studies of Fossil Nuclear Particle Tracks in Extraterrestrial Matter. Earth Planet. Sci. Lett., vol. 8, 1970, pp. 379-386.

15-30. Barber, D. J.; Hutcheon, I.; and Price, P. B.: Extralunar Dust in Apollo Cores? Science, vol. 171, no. 3969, Jan. 29, 1971, pp. 372-374.

15-31. Mogro-Campero, Antonio; and Simpson, J. A.: Enrichment of Very Heavy Nuclei in the Composition of Solar Accelerated Particles. Astrophys. J. (Letters), vol. 171, no. 1, part 2, Jan. 1, 1972, pp. L5-L9.

15-32. Lanzerotti, L. J.; MacLennan, C. G.; and Graedel, T. E.: Enhanced Abundances of Low-Energy Heavy Elements in Solar Cosmic Rays. Astrophys. J. (Letters), vol. 173, no. 1, part 2, Apr. 1, 1972, pp. L39-L43.

15-33. Price, P. B.; and Fleischer, R. L.: Identification of Energetic Heavy Nuclei with Solid Dielectric Track Detectors: Applications to Astrophysical and Planetary Studies. Annu. Rev. Nucl. Sci., vol. 21, 1971, pp. 295-334.

15-34. Shapiro, Maurice M.; and Silberberg, Rein: Heavy Cosmic Ray Nuclei. Annu. Rev. Nucl. Sci., vol. 20, 1970, pp. 323-392.

15-35. Crawford, H. J.; Price, P. B.; and Sullivan, James D.: Composition and Energy Spectra of Heavy Nuclei with $0.5 < E < 40$ MeV per Nucleon in the 1971 January 24 and September 1 Solar Flares. Astrophys. J. (Letters), vol. 175, no. 3, part 2, Aug. 1, 1972, pp. L149-L154.

15-36. Huang, W. H.; and Walker, R. M.: Fossil Alpha-Particle Recoil Tracks: A New Method of Age Determination. Science, vol. 155, no. 3765, Mar. 3, 1967, pp. 1103-1106.

15-37. Fleischer, R. L.; Price, P. B.; Walker, R. M.; and Hubbard, E. L.: Track Registration in Various Solid-State Nuclear Track Detectors. Phys. Rev., vol. 133, no. 5A, Mar. 2, 1964, pp. A1443-A1449.

15-38. Fleischer, R. L.; Price, P. B.; Walker, R. M.; and Hubbard, E. L.: Criterion for Registration in Dielectric Track Detectors. Phys. Rev., vol. 156, no. 2, Apr. 10, 1967, pp. 353-355.

15-39. Cameron, A. G. W.: A Revised Table of Elemental Abundances. Origin and Distribution of the Elements, L. H. Ahrens, ed., Pergamon Press (Oxford), 1968.

15-40. Price, P. B.; Hutcheon, I.; Cowsik, R.; and Barber, D. J.: Enhanced Emission of Iron Nuclei in Solar Flares. Phys. Rev. Letters, vol. 26, no. 15, Apr. 12, 1971, pp. 916-919.

15-41. Mogro-Campero, Antonio; and Simpson, J. A.: Enrichment of Very Heavy Nuclei in the Composition of Solar Accelerated Particles, Astrophys. J., vol. 171, no. 1, part 2, Jan. 1, 1972, pp. L5-L9.

15-42. Krimigis, S. M.; Verzariu, P.; Van Allen, J. A.; Armstrong, T. P.; et al.: Trapped Energetic Nuclei with $Z \geq 3$ in the Earth's Outer Radiation Zone. J. Geophys. Res., vol. 75, no. 22, Aug. 1, 1970, pp. 4210-4215.

15-43. Van Allen, James A.; Randall, Bruce A.; and Krimigis, Stomatias M.: Energetic Carbon, Nitrogen and Oxygen Nuclei in the Earth's Outer Radiation Zone. J. Geophys. Res., vol. 75, no. 31, Nov. 1, 1970, pp. 6085-6091.

15-44. Borg, J.; Dran, J. C.; Durrieu, L.; Jouret, C.; and Maurette, M.: High Voltage Electron Microscopic Studies of Fossil Nuclear Particle Tracks in Extraterrestrial Matter. Earth Planet. Sci. Lett., vol. 8, 1970, pp. 379-386.

15-45. Barber, D. J.; Hutcheon, I.; and Price, P. B.: Extralunar Dust in Apollo Cores? Science, vol. 171, no. 3969, Jan. 29, 1971, pp. 372-374.

15-46. Crozaz, G.; and Walker, R. M.: Solar Particle Tracks in Glass from the Surveyor 3 Spacecraft. Science, vol. 171, no. 3977, Mar. 26, 1971, pp. 1237-1239.

15-47. Fleischer, R. L.; Hart, H. R., Jr.; and Comstock, G. M.: Very Heavy Solar Cosmic Rays: Energy Spectrum and Implications for Lunar Erosion. Science, vol. 171, no. 3977, Mar. 26, 1971, pp. 1240-1242.

15-48. Bhandari, N.; Bhat, S.; Lal, D.; Rajagopalan, G.; et al.: Spontaneous Fission Record of Uranium and Extinct Transuranic Elements in Apollo Samples. Proceedings of the Second Lunar Science Conference, vol. 3, A. A. Levinson, ed., MIT Press (Cambridge, Mass.), 1971, pp. 2599-2609.

15-49. Langseth, Marcus G., Jr.; Clark, Sydney P., Jr.; Chute, John L., Jr.; Keihm, Stephen J.; and Wechsler, Alfred E.: Heat Flow Experiment, Sec. 11 of Apollo 15 Preliminary Science Report. NASA SP-289, 1972.

15-50. Hoyt, H. P., Jr.; Miyajima, M.; Walker, R. M.; Zimmerman, D. W.; et al.: Radiation Dose Rates and Thermal Gradients in the Lunar Regolith: Thermoluminescence and DTA of Apollo 12 Samples. Proceedings of the Second Lunar Science Conference, A. A. Levinson, ed., MIT Press (Cambridge, Mass.), 1971, pp. 2245-2263.

APPENDIX II

Enrichment of Heavy Nuclei in the 17 April 1972 Solar Flare*

R. L. Fleischer and H. R. Hart, Jr.
General Electric Research and Development Center, Schenectady, New York 12301
(Received 31 July 1972)

Polycarbonate and glass detectors exposed on Apollo 16 to the 17 April 1972 solar flare were used to measure the spectrum of iron-group cosmic-ray nuclei down to ~ 0.02 MeV/nucleon. The enrichment of iron relative to lighter nuclei previously seen at higher energies increases markedly in this new, very-low-energy region. The energy spectrum of carbon and heavier nuclei inferred from sensitized Lexan polycarbonate reveals the enrichment of iron relative to carbon and heavier nuclei down to ~ 0.03 MeV/nucleon.

The relative abundances and energy spectra of heavy solar and cosmic-ray particles contain a wealth of information about the sun and other galactic particle sources, and about the acceleration and propagation of the particles. In particular, the lowest-energy range from a few million electron volts per nuclear mass unit (MeV/nucleon) down to a keV/nucleon (a solar wind energy) has been largely unexplored. On Apollo 16 there were three cosmic-ray experiments which contained track detectors designed to examine this energy range.[1] We report here energy spectra and relative abundances for heavy solar cosmic rays from the flare of 17 April 1972.

A four-panel detector array was mounted on the lunar module at launch and first exposed to space just after translunar injection when the lunar module was withdrawn from the adapter panels which enclosed it during launch. Exposure ended just before the termination of the third extravehicular activity on the moon, at which time the array was pulled out of its frame and folded into a compact package for return to Earth. The portion of the experiment considered here consisted of two types of detectors: In panel 2 the entire exposed detector area of 14.7 by 22.6 cm was composed of sheets of 0.010-in. Lexan polycarbonate type 9070-112 plastic; panel 3 included a 1-in. × 1-in. × 1-mm plate of General Electric phosphate glass 1457.[2] Portions of each of these detectors were exposed to space protected only by 2100-Å evaporated aluminum films. Other portions were covered by 0.002-in. silver- and Inconel-backed Teflon thermal control material.

Particle tracks in solids are affected by elevated temperature[3] and, in particular, both the polycarbonate films and the glass plate used in this experiment are affected by temperatures above 55°C. Since the temperature labels present in the experiment showed temperatures ~ 70°C, some desensitization did occur through track annealing. Consequently, it was found helpful in some cases to use uv irradiation of the polycarbonate to enhance sensitivity.[4,5] We refer to the as-received and uv-irradiated samples as *densensitized* and *sensitized*, respectively.

Satellite measurements by C. Bostrum, G. Paulikas, and S. Singer (unpublished) showed that late on 17 April during the translunar portion of the mission, a medium-sized solar flare occurred that contained ~ 10^8 protons/cm^2 of energies > 5 MeV, but included no extra particles beyond the general steady background above 60 MeV. It will be noted that the major portion of the flare particles arrived prior to lunar landing; at > 5 MeV only a few percent arrived after landing, and even for the slowest particles for which data are available (0.46–0.90 MeV) less than 10% arrived after that time. Since the period of most intense heating of the experiment occurred 20 h after landing, the significant heat effects for all of the solar tracks were identical. For the uppermost detector sheets, which we consider here, the flood of solar-flare particles gives an abundance that is many times the expected galactic fluence. Consequently, the results we report here are essentially solely for the 17 April flare.

Samples were treated in room-temperature NaOH for 1 to 2 min to remove the aluminum coating. The glass was then etched in HF in order to remove roughly $\frac{1}{2}$ μm of glass from each surface and reveal cosmic-ray tracks. The etched glass was scanned at 1000× in an optical microscope, then replicated (cellulose acetate, gold coated) and scanned at 5000× in a scanning electron microscope. Portions of the top sheet of Lexan polycarbonate, after removal of the aluminum, were etched for 6 h in 40°C 6.25 *N* NaOH solution saturated with etch products.[6] The preirradiation with uv used conditions described earlier.[4] Results are given here for a sheet from

the lower-left portion of panel 2 and a uv-treated sheet from the upper-right corner of panel 2. Examination of duplicate samples has shown that the presence or absence of the uv treatment is the significant difference between these two samples. From optical scans of the different detectors we obtained the track-length distributions given in Ref. 1. From these track lengths the differential energy spectrum is derived using range-energy relations[7] for iron nuclei, allowing for the thicknesses of the aluminum layer and the layer etched away, and assuming for simplicity that the aluminum is crossed at 45° incidence.

The justification for assuming that all particles are iron in computing the energies derives from comparing the observed cone angles in the glass with those from accelerator irradiations with ^{20}Ne, ^{40}Ar, and ^{56}Fe. For the range 0 to 2 MeV/nucleon, in General Electric 1457 phosphate glass, neon ions give tracks having an average cone angle of 30–35° and argon ions give a value of ~10°.[8] The scanning electron-microscope photographs of cosmic-ray tracks give a cone-angle distribution for >1-μm tracks that are mostly below 10°, with decreasing abundance at larger angles. This cone-angle distribution indicates that the tracks are predominantly from particles appreciably heavier than neon. From known solar abundances[9] we expect iron to be dominant and that most of the nuclei observed have range-energy relations that are adequately approximated by that of iron. The justification in using iron for the desensitized Lexan is that the results there agree with the phosphate glass. For the sensitized Lexan the ^{20}Ne calibrations reveal that nuclei down through ^{12}C should be readily detectible. This result is in contrast to that in the desensitized Lexan, where Ne is undetectible for the etching time that was used. Particles at depths greater than were observed at the exposed Lexan surface could be counted on the same surface but beneath the silver-backed Teflon, and also at the back of the top sheet.

One interesting anomaly was the observation, just beneath the silver-backed Teflon, of a high density (~3000/cm^2 in the desensitized and ~10 000/cm^2 in the sensitized Lexan) of short tracks ranging up to ~10^{-3} cm long with rapidly decreasing numbers toward greater lengths. Since we infer that these short tracks are reaction products, as yet unidentified, from the metallic coating, we ignore them in deriving the cosmic-ray flux at 12- to 17-mg/cm^2 depth. This cosmic-ray flux was inferred from the abundance of tracks of length $>15\times10^{-4}$ cm, which appear to form a distinctly separate population.

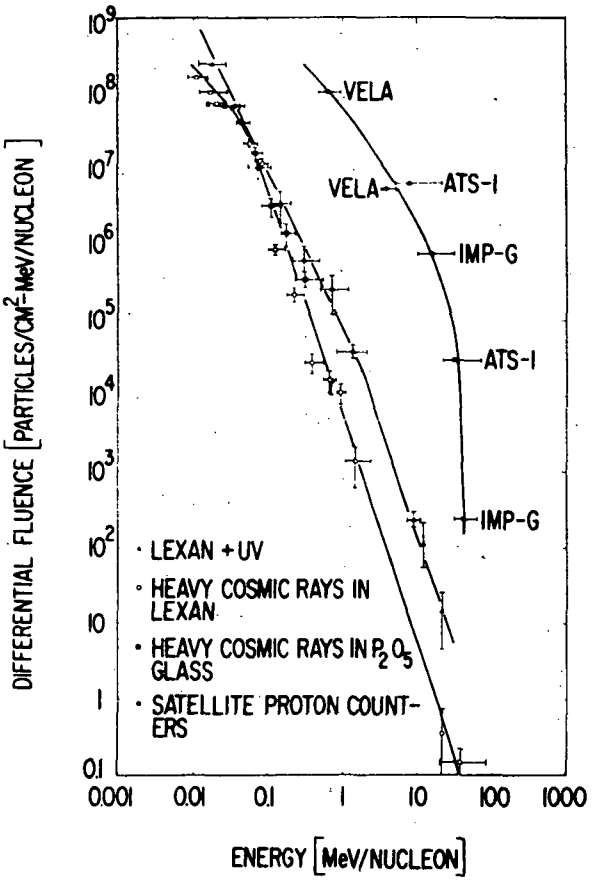

FIG. 1. Differential energy spectra for heavy cosmic rays during the period 16–23 April 1972 compared to the spectrum derived from various satellite proton counters. Fluence is given in particles/cm^2 MeV per nucleon integrated over a 2π solid angle. The "Lexan + uv" is referred to as "sensitized" Lexan in the text. The proton results are from preliminary data from satellite proton counters operated by C. Bostrom (IMP), G. Paulikas (ATS), and S. Singer (Vela).

Figure 1 gives the energy spectra inferred for heavy particles and that derived for protons from preliminary satellite data from several groups. As is obvious in Fig. 1, the desensitized Lexan gives results that are indistinguishable from those of the phosphate glass; since we have identified those tracks as being from iron nuclei or nuclei close to iron in atomic number, the composite curve (the lowest of the three in Fig. 1) applies to the iron-group nuclei.

The curve for the sensitized Lexan, which we noted records carbon and heavier nuclei, lies generally above that for the non-uv-irradiated Lexan because of the effect of uv radiation in low-

ering the effective threshold for particle track registration.[5] Recalculation of the energy spectrum using the range-energy relations of the CNO group for the sensitized Lexan would steepen the curve very slightly, but would not alter its qualitative character significantly. In using these curves to derive ratios of CNO and greater to the iron group, we recalculated the higher of our two spectra using the ^{16}O range energy curve as an approximation of the range energy curves of CNO plus all heavy nuclei.

The spectrum for iron-group cosmic rays in Fig. 1 is given by a relation (energy)$^{-\gamma}$, where the spectral index γ is 3 (± 0.3) from 30 MeV/nucleon down to 0.04 MeV/nucleon and flattens to $\gamma = 1$ (± 0.5) from 0.04 to 0.01 MeV/nucleon. The $\gamma = 3$ result is identical to our previous conclusion[10] in the energy range 1 to 100 MeV/nucleon from examination of Surveyor-III filter glass and with that of Mogro-Campero and Simpson from their counter telescope in the range 3–60 MeV/nucleon[11]; it is also roughly consistent with the results of two other studies of the Surveyor glass,[12,13] although the spectrum was not expressed as E^{-3} in those papers.

From the spectra just given a striking result can be inferred, namely, the sequence of ratios of iron nuclei to carbon and heavier nuclei listed in Table I. With decreasing energy the ratio increases from roughly $\frac{2}{3}$ of the photospheric value of 0.04 in the range 1–10 MeV per nucleon to ~25 times that value of 0.03 MeV/nucleon. The statistics allow a factor-of-2 error in the cosmic-ray ratios. The values are to be compared with ratios of iron-group nuclei to carbon and heavier nuclei of 0.08 and 0.13 above 10 MeV/nucleon by Teegarden, van Rosenvinge, and McDonald[14] for two flares, of 0.3 found by Mogro-Campero and Simpson[11] near 20 MeV/nucleon (average of several flares with spectral index 3), and of 0.015 to 0.03 above 20 MeV/nucleon by Bertsch *et al.*[15,16] near 60 MeV/nucleon averaged for several flares. None of these results included the 17 April event. There appears to be a rough trend of relative enrichment of iron towards lower energies in this higher-energy region also.

TABLE I. Abundance ratio of iron group to carbon and heavier nuclei.

Energy MeV/nucleon	Relative abundance
10	0.04
3	0.03
1	0.025
0.3	0.11
0.1	~0.5
0.03	~1

The relative heavy-element enrichment at low energies is associated with the change of slope of the energy spectra, which occurs at progressively higher energies in Fig. 1 as one goes from iron (~0.04 MeV/nucleon) to carbon and heavier nuclei (~1 MeV/nucleon) to hydrogen (~10 MeV). The observed increasing enhancement of iron towards lower energies is in agreement with previous results by Price *et al.*[13] and Mogro-Campero and Simpson,[11] but is quantitatively less at the same energies. The present results, however, extend to much lower energies.

α-particle spectra are not available through enough of the energy region of interest to give iron-to-α ratios. Dietrich and Simpson (personal communication) obtain an $E^{-5.5\ (\pm 1.3)}$ spectrum in the region 8.5 to ~15 MeV/nucleon where we have E^{-3}. If taken literally, these results too imply an ascending Fe/He ratio with decreasing energy. However the spectral index 5.5 is subject to a slight downward correction because the counting procedure used gave diminished weight to the early portion of the flare, when the proton spectral index was lower (4.5 as compared to 5.5 later). Consequently, any inference on Fe/He should await more complete data. Although proton data are lacking at the lower energies, proton-to-iron ratios can be quoted. They range downward from 4×10^5 at 10 MeV/nucleon (15 times the photospheric value[17]) to 6.5×10^4, 1.2×10^4, and 1.2×10^3 at 3, 1, and 0.3 MeV/nucleon. Similar variations in proton-to-α ratios have often been observed.[18]

The integrated fluence of iron down to ~0.01 MeV/nucleon is $\sim 4\times10^6$ particles/cm^2 per 2π solid angle as compared to $\sim 2.2\times10^8$ protons/cm^2 down to 0.3 MeV; these numbers could give an enrichment of at most a factor of 450 relative to the photospheric value. Since the proton fluence below 0.3 MeV is unknown, the quantitative meaning of this value is by no means clear. It does, however, strongly suggest that the heavy nuclei in the solar flare are in fact appreciably more abundant than in the surface of the sun. The preferential enhancement at low energies of the heavier nuclei because of their low charge-to-mass ratio was predicted in 1958 by Korchak and Syrovatskii.[9]

We are indebted to C. Bostrum, W. F. Dietrich,

G. Paulikas, J. A. Simpson, and S. Singer for permission to quote their preliminary satellite proton and α results, to W. R. Giard, M. McConnell, and G. E. Nichols for experimental assistance, and to M. Saltmarsh and A. van der Woude for permission to quote joint work prior to publication.

---

*Work supported by The National Aeronautics and Space Administration under Contract No. NAS 9-11468.

[1]More detailed descriptions of the experiments are given by R. L. Fleischer and H. R. Hart, Jr., in National Aeronautics and Space Administration Apollo-16 Preliminary Science Report, 1972 (unpublished); P. B. Price *et al.*, *ibid.*; R. M. Walker *et al.*, *ibid.*

[2]R. L. Fleischer, P. B. Price, and R. T. Woods, Phys. Rev. 88, 563 (1969).

[3]R. L. Fleischer, P. B. Price, and R. M. Walker, J. Geophys. Res. 70, 1497 (1965).

[4]W. T. Crawford, W. DeSorbo, and J. S. Humphrey, Nature (London) 220, 1313 (1968).

[5]P. B. Price and R. L. Fleischer, Radiat. Eff. 2, 29 (1970).

[6]D. D. Peterson, Rev. Sci. Instrum. 41, 1254 (1970).

[7]L. C. Northcliffe and R. F. Schilling, *Range and Stopping Power Tables for Heavy Ions* (Texas A & M, College Station, Texas, 1970), and Nucl. Data, Sect. B 7, 233 (1970).

[8]H. R. Hart, Jr., M. Saltmarsh, A. van der Woude, and R. L. Fleischer, to be published.

[9]L. H. Aller, *Abundance of the Elements* (Wiley, New York, 1961).

[10]R. L. Fleischer, H. R. Hart, Jr., and G. M. Comstock, Science 171, 1240 (1971).

[11]A. Mogro-Campero and J. A. Simpson, Astrophys. J. 171, L5 (1972).

[12]G. Crozaz and R. M. Walker, Science 171, 1237 (1971).

[13]P. B. Price, I. Hutcheon, R. Cowsik, and D. J. Barber, Phys. Rev. Lett. 26, 916 (1971).

[14]B. Teegarden, T. T. van Rosenvinge, and F. B. McDonald, Goddard Space Flight Center Report No. X-661-72-222 (to be published).

[15]D. L. Bertsch, C. E. Fichtel, C. J. Pellerin, and D. V. Reames, Goddard Space Flight Center Report No. X-662-72-197 (to be published).

[16]D. L. Bertsch, C. E. Fichtel, and D. V. Reames, Astrophys. J. 171, 169 (1972).

[17]A. Unsöld, Phil. Trans. Roy. Soc. London, Ser. A 270, 23 (1971).

[18]S. Biswas and C. E. Fichtel, Space Sci. Rev. 4, 709 (1965).

[19]A. A. Korchak and S. I. Syrovatskii, Dokl. Akad. Nauk. SSSR 122, 792 (1958) [Sov. Phys. Dokl. 3, 983 (1958)].

APPENDIX III

ENRICHMENT OF HEAVY NUCLEI IN THE APRIL 17, 1972 SOLAR FLARE

R. L. Fleischer, H. R. Hart, Jr., A. Renshaw, and R. T. Woods*

General Electric Research and Development Center

P.O. Box 8, Schenectady, New York (USA) 12301

Cosmic ray nuclei from the April 17, 1972 solar flare were recorded in polycarbonate plastic and phosphate glass track detectors exposed on the Apollo 16 flight. The energy spectra of iron group nuclei and of carbon and heavier nuclei were measured down to ~0.02 MeV/nucleon, revealing that the enrichment of iron relative to carbon and heavier nuclei increases markedly in this very low energy region.

1. Introduction. The relative abundances and energy spectra of heavy solar cosmic ray particles contain a wealth of information about the sun as a source body and about the acceleration and propagation of the particles. It is only recently that the very low energy range from a few MeV/nucleon to a few keV/nucleon has been studied. We report here very low energy spectra and relative abundances for heavy solar cosmic rays from the flare of April 17, 1972, as determined from track detectors flown on Apollo 16. There are in print two detailed descriptions of our experiment (1,2).

2. Experimental. A multi-institutional detector array was mounted on the Apollo 16 lunar module and first exposed to space just after translunar injection; the exposure was ended just before the end of the third extravehicular activity on the moon, for a total exposure of 167 hours. The portions of our experiment considered here consisted of two types of detectors: sheets of Lexan polycarbonate plastic, and a small plate of GE phosphate glass 1457 (3). Portions of these detectors were protected only by 2100Å aluminum deposited films; other portions were covered by 50 μm silver-and-Inconel-backed Teflon thermal control material.

A dust coating on the thermal control material led to some overheating of the detectors on the moon's surface, changing the calibration of the plastic detector. This calibration change was measured using preirradiated plastic tabs which had been mounted in the array.

During the translunar portion of the mission, a small solar flare (~10^8 protons/cm^2, E>5 MeV) was recorded by several satellites (Figure 1). In Figure 1 we see that the major portion of the flare

*Also at State University of New York at Albany, Albany, New York.

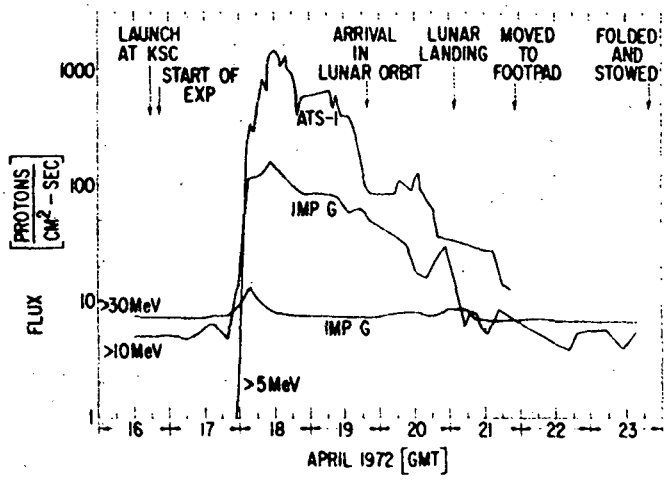

Figure 1. Proton fluxes (preliminary), at energies greater than 5 MeV, observed during the exposure period. The data are courtesy of C. Bostrom (IMP) and G. Paulikas (ATS). Lower energy fluxes (VELA, S. Singer) are displayed in reference 1.

particles arrived before the lunar landing; thus the heating episode on the lunar surface affected virtually all flare particle tracks in the same way.

The glass was etched in HF to remove ½ μm. The Lexan plastic was divided into two groups; one was irradiated with UV to enhance its sensitivity, and the other was studied as received. Both Lexans were etched for 6 hours in 40°C 6.25N NaOH solution saturated with etch products (4).

Optical scans at 1000X yielded track length distributions which could be converted into differential energy spectra. On the basis of calibration data (2) and track counting criteria we made the following elemental assignments for the various detectors: The phosphate glass and as-received Lexan yield the fluence of iron group nuclei; the UV-sensitized Lexan yields the fluence for carbon-nitrogen-oxygen and heavier nuclei. Work in progress should help us identify with more precision the elemental assignments, especially at the lower energies.

3. Results. The resulting differential energy spectra for heavy cosmic rays, calculated using range-energy relations for iron (5), and that derived for protons from preliminary satellite data, are shown in Figure 2. Work in progress will extend the data to 150 MeV/nucleon.

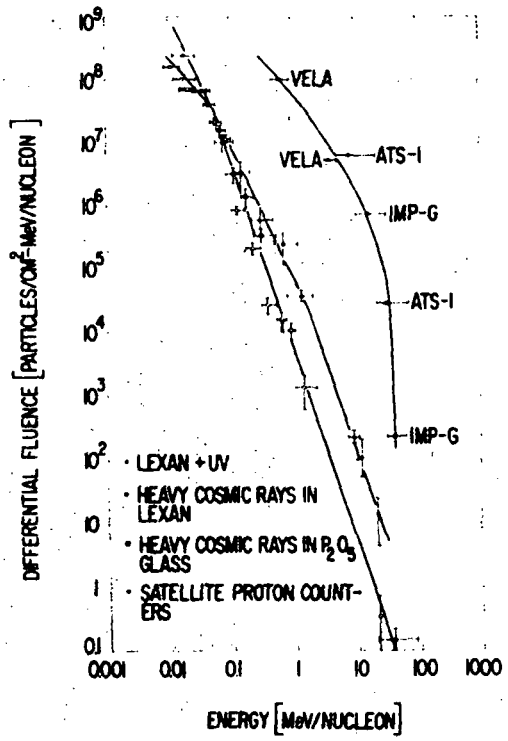

Figure 2. Differential energy spectra for heavy cosmic rays during the period 16-23 April 1972, compared to proton spectra from satellite counters. Fluence is given in particles/cm^2 MeV per nucleon integrated over a 2π solid angle.

A recalculation of the UV-sensitized Lexan data using ^{16}O range-energy relations would steepen the curve very slightly but would not alter its character significantly. Such a recalculation was used in calculating the abundance ratios presented below. The spectrum for iron group cosmic rays is steep, flattening out at lower energies: E^{-3} ($\pm$ 0.3) for 0.04 < E < 30 MeV/nucleon, flattening to E^{-1} ($\pm$ 0.5) in the energy range 0.04 to 0.01 MeV/nucleon.

The spectra of Figure 1 yield the elemental abundance ratios shown in Table I. For iron nuclei to carbon-plus-heavier the ratio increases with decreasing energy from the photospheric value of 0.04 at 10 MeV/nucleon to roughly 25 times that value at 0.03 MeV/nucleon. The statistics allow a factor of two error in the ratios.

Table I. Abundance Ratio of Iron Group to Carbon and Heavier Nuclei

Energy (MeV/nucleon)	Relative Abundance
10	0.04
3	0.03
1	0.025
0.3	0.11
0.1	~0.5
0.03	~1

Likewise, the data of Figure 1 yield an enhancement of iron group nuclei relative to protons, and of carbon and heavier nuclei relative to protons (2).

4. Discussion and Conclusions. As described above, the differential energy spectrum for iron group cosmic rays shows the now familiar roughly E^{-3} energy dependence (6,7,8,9). The present results show that this behavior extends to energies as low as 0.03 MeV/nucleon.

The ratios of iron relative to carbon and heavier elements indicated in Table I are to be compared with ratios of 0.08 and 0.13 above 10 MeV/nucleon found by Teegarden, et al (10) for two flares, of 0.3 found by Mogro-Campero and Simpson (7) near 20 MeV/nucleon for the average of several flares, and of 0.015 to 0.03 at higher energies found by Bertsch et al (11). None of these results include the 17 April flare. Mogro-Campero and Simpson (7) have emphasized the variations in elemental ratios from flare to flare.

The relative heavy-element enrichment at low energies is associated with the changes of slope of the energy spectra which occur at progressively higher energies (in Figure 2) as one goes from iron to carbon plus heavier nuclei to hydrogen. This increasing enhancement of iron towards lower energies is in agreement with previous results of Price et al (12) and Mogro-Campero and Simpson (7), but is quantitatively less at the same energies; the present results extend to lower energies. Energy-dependent abundance ratios for individual elements, rather than for groups of elements, have been reported by Braddy, et al (8) and Price, et al (9) for several flares, including the 17 April flare.

The data presented in Figure 2 imply that the heavy nuclei in the solar flare are appreciably more abundant than in the solar photosphere (2). As early as 1958 Korchak and Syrovatskii

predicted preferential enhancement at low energies of heavier nuclei during the acceleration process because of their lower effective charge-to-mass ratios (13). More recent explanations involve not only acceleration processes but also possible variations in the composition of the solar atmosphere in the vicinity of solar flares (9).

Acknowledgments. We are indebted to C. Bostrom, W. F. Dietrich, G. Paulikas, J. A. Simpson, and S. Singer for permission to quote their preliminary satellite data, to W. R. Giard, M. McConnell, and G. E. Nichols for experimental assistance. The work has been supported by The National Aeronautics and Space Administration under Contract No. NAS 9-11468.

1. Fleischer, R. L., and H. R. Hart, Jr., Cosmic Ray Experiment, Apollo 16 Preliminary Science Report. NASA SP-315, 15-1--15-11, 1972.

2. Fleischer, R. L., and H. R. Hart, Jr., Enrichment of Heavy Nuclei in the 17 April 1972 Solar Flare, Phys. Rev. Lett., 30, 31-34, 1973.

3. Fleischer, R. L., P. B. Price, and R. T. Woods, Nuclear-Particle-Track Identification in Organic Solids, Phys. Rev., 188, 563-567, 1969.

4. Peterson, D. D., Improvement in Particle Track Etching in Lexan Polycarbonate Film, Rev. Sci. Instr., 41, 1252-1253, 1970.

5. Northcliffe, L. C., and R. F. Schilling, Range and Stopping Power Tables for Heavy Ions, (Texas A&M, College Station, Texas, 1970), and Nucl. Data, Sect. B, 7, 233ff, 1970.

6. Fleischer, R. L., H. R. Hart, Jr., and G. M. Comstock, Very Heavy Solar Cosmic Rays: Energy Spectrum and Implications for Lunar Erosion, Science, 171, 1240-1242, 1971.

7. Mogro-Campero, A., and J. A. Simpson, Enrichment of Very Heavy Nuclei in the Composition of Solar Accelerated Particles, Astrophys. J. (Lett.), 171, L5-L9, 1972; The Abundances of Solar Accelerated Nuclei from Carbon to Iron, ibid., 177, L37-L41, 1972.

8. Braddy, D., J. Chan, and P. B. Price, Charge States and Energy-Dependent Composition of Solar-Flare Particles, Phys. Rev. Lett., 30, 669-671, 1973.

9. Price, P. B., J. H. Chan, I. D. Hutcheon, D. Macdougall, R. S. Rajan, E. K. Shirk, and J. D. Sullivan, Low-Energy Heavy Ions in the Solar System, Proc. of the Fourth Lunar Sci. Conf., Geochim. Cosmochim. Acta, Suppl. 4 (to be published, 1973).

10. Teegarden, B., T. T. van Rosenvinge, and F. B. McDonald, Goddard Space Flight Center Report No. X-661-72-222 (to be published).

11. Bertsch, D. L., C. E. Fichtel, and D. V. Reames, Nuclear Composition and Energy Spectra in the 1969 April 12 Solar-Particle Event, Astrophys. J., 171, 169-177, 1972; Bertsch, D. L., C. E. Fichtel, C. J. Pellerin, and D. V. Reames, Goddard Space Flight Center Report No. X-662-72-197 (to be published).

12. Price, P. B., I. Hutcheon, R. Cowsik, and D. J. Barber, Enhanced Emission of Iron Nuclei in Solar Flares, Phys. Rev. Lett., 26, 916-919, 1971.

13. Korchak, A. A., and S. I. Syrovatskii, On the Possibility of a Preferrential Acceleration of Heavy Elements in Cosmic-Ray Sources, Soviet Phys. Dokl., 3, 983-985, 1958.

APPENDIX IV

Reports

Apollo 14 and Apollo 16 Heavy-Particle Dosimetry Experiments

Abstract. *Doses of heavy particles at positions inside the command modules of Apollo missions 8, 12, 14, and 16 correlate well with the calculated effects of solar modulation of the primary cosmic radiation. Differences in doses at different stowage positions indicate that the redistribution of mass within the spacecraft could enhance safety from the biological damage that would otherwise be expected on manned, deep-space missions.*

Densely ionizing, heavy atomic nuclei are the most individually damaging form of cosmic radiation encountered by space personnel on missions outside the earth's atmosphere. For example, an iron nucleus leaves a cytologically lethal swath of damage as it crosses cell nuclei through its last ~3 mm of range. Earlier measurements in which Apollo helmets were used as dosimeters have indicated that a significant fraction (~1 percent) of certain nonregenerative motor-control cells would be killed in a Mars-length mission with the present Apollo spacecraft shielding (*1*). As an extension of the dosimetry work for Apollo 8 and Apollo 12 (*1*), we have used a number of the parts from the Apollo 14 electrophoresis experiment (*2*) and tracks formed after stowage of the Apollo 16 cosmic-ray experiment (*3*) to measure the doses of heavy nuclei that penetrated the interiors of the command modules during these two missions. During most of the Apollo 14 mission the equipment for the electrophoresis experiment was located in a compartment just beneath astronaut Edgar D. Mitchell.

First, we discuss the Apollo 14 experiment. In this experiment we etched and examined the tracks produced by the heavy particles that entered the Lexan polycarbonate parts forming the main body of the electrophoresis experimental device. The ionization threshold for particle registration of this material [if untreated by ultraviolet (UV) radiation] is that for single-hit inactivation of human kidney cells (*4*) and hence is appropriate for assessing the biological effects of heavily ionizing particles. The experimental procedures were essentially identical to those used in our earlier work, except that the largest piece of Lexan was re-etched for an extra 31.4 days after its original 8-day treatment in order to enlarge the tracks for photography and ready viewing with the naked eye. Figure 1 shows a track at low magnification, illustrating the geometrical variation that allows individual particles to be identified (*5*). As noted earlier (*1*), most of the nuclei observed are either iron, or its near neighbors in the periodic chart, or spallation products of iron, and all are of atomic number ≥ 10. The particle shown here has been identified according to the analytical technique described earlier (*6*) as argon. Because the nucleus was not observed as it stopped, with lower probability it could be potassium or calcium. More extensive calibration data than now exist for the etchant used could readily resolve such an uncertainty.

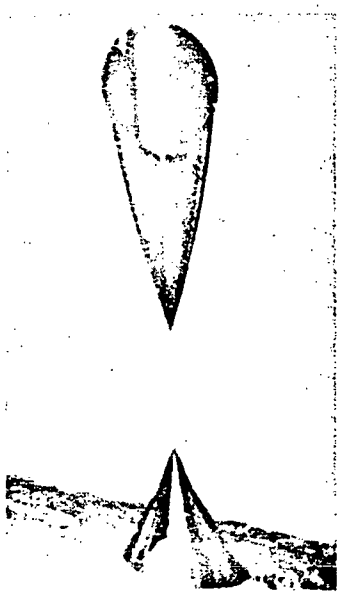

Fig. 1. Etched cosmic-ray track that penetrated the Apollo 14 electrophoresis experimental device. From the variation of the taper along it, this 2-mm-long track is identified by the method given in (*6*) as caused by an argon ion. The track intersected two etched surfaces, giving rise to two separate cones.

The equipment for the Apollo 16 cosmic-ray experiment was exposed on the lunar surface and later folded and stowed just prior to lift-off. The Lexan detectors that made up a major portion of the experimental device were held in such a manner that each sheet was displaced relative to its neighbor as the device was folded (*3*). By counting particle tracks that line up in the shifted position, we have a measure of particles that registered after the shift and therefore penetrated the spacecraft walls before entering the detectors. This fluence describes a particular position in the command module, since for most of the time after the shift the experimental device was stored in the same location. These samples were etched with 6.25*N* NaOH saturated with etch products (*7*). Since with this etchant the detector is less sensitive than with the NaOH-ethanol etchant that was used previously (*1*), track counts for the cosmic-ray experiment must be increased (by an estimated 80 percent) to make them comparable with the track counts of the helmet (*1*) and electrophoresis experiments. The numbers we will quote here are so corrected.

We observed 0.608 ($\pm$ 0.041) track cm^{-2} in the Apollo 14 command module and 0.334 ($\pm$ 0.041), corrected to 0.594, in the Apollo 16 command module, as compared to 0.56 ($\pm$ 0.053) and 1.41 ($\pm$ 0.146) in the Apollo 8 and Apollo 12 command modules, respectively. If we allow for the different lengths of the four missions and the time when the experimental devices were partially shielded by the moon, the four flux values for Apollo missions 8, 12, 14, and 16 are 1.53×10^{-7}, 3.12×10^{-7}, 1.92×10^{-7}, and 3.42×10^{-7} particle cm^{-2} sec^{-1} ster^{-1}, respectively (*8*). These values may be compared with those expected from solar modulation of the primary cosmic radiation and with the results of Benton and Henke (*9*), who used somewhat different procedures. As the entries in column 5 of Table 1 indicate, the sun became decreasingly active in the sequence of Apollo missions 8, 12, 14, and 16; fewer of the penetrating galactic cosmic rays were deflected away from the inner solar system in the Apollo 16 mission as compared with the

Apollo 8 mission, and the calculated (*1*) relative track density therefore rises from 0.66 for Apollo 8 to 1.00 for Apollo 12, 1.43 for Apollo 14, and 2.50 for Apollo 16. For Apollo 8 both our measurements ("≧ neon") and those of Henke and Benton ("≧ carbon") are consistent with the effects of solar modulation; for Apollo 14 and Apollo 16 Benton and Henke's measurements are roughly consistent with the calculations carried out by the method described in (*1*) giving the results summarized in Table 1, but the results presented here appear to be lower for both the Apollo 14 and the Apollo 16 missions.

The discrepancies between the two sets of observations could, in principle, be related to three possibilities: (i) differences in the fluxes of the different nuclei observed by the two groups of experimenters ("≧ carbon" by Henke and Benton and "≧ neon" by ourselves), (ii) differences in the Lexan detectors used in the helmet (type 111 or 112) and in the Lexan detectors used in the electrophoresis experiment (type 100), or (iii) different thicknesses of shielding at different positions in the spacecraft. As noted by the column headings in Table 1, the two groups measured particles of different mass. Benton and Henke used an intense UV irradiation (producing more etchable tracks, presumably to enhance statistics) to give very different registration properties (*10*), allowing nuclei as light as helium to register (*11*) although only nuclei at least as heavy as carbon were counted. Depending on the extent of the UV irradiation, track densities for the Apollo 8 mission ranged from 0.56 track cm^{-2} [no UV (*1*)] to 0.62 track cm^{-2} [some UV (*12*)] to 2.64 track cm^{-2} [intense UV (*9*)]. In our experiments UV was excluded to produce, as noted earlier, a biologically meaningful registration threshold as well as to allow valid intercomparison of the four missions. The first possibility—that the (≧ carbon/≧ neon) ratio was higher by a factor of ~ 3 during the Apollo 14 and Apollo 16 missions—is highly unlikely, since fluctuations in this ratio of greater than 30 percent would be inconsistent with measurements of galactic cosmic rays (*13*). The second possibility—that the two detectors we intercompare on the Apollo 12 mission and on the Apollo 14 mission were different—we ruled out on the basis of calibration measurements of etching rates for full-energy and low-energy fission fragments. For helmet Lexan, electrophoresis Lexan, and the usual 112 Lexan used for particle identification (*5*) the etching rates were identical within the experimental uncertainty (± 1.5 percent for full-energy particles and ± 7 percent for low-energy particles). The final possibility is the preferred one—that the storage positions of the Apollo 14 and Apollo 16 experimental devices were close to some thicker-than-average shielding in the command module, so that the effective solid angle through which cosmic rays could approach was reduced. Figure 2 shows the fractions of the solid angle occupied by shielding of different thickness intervals, as seen by the detectors in the helmet, electrophoresis, and cosmic-ray experiments we are considering. These calculations, which were carried out for the positions in the spacecraft for which the period of exposure of the apparatus for each experiment was the greatest, show clearly that the Apollo 8 and Apollo 12 helmets had some shielding thinner than 4 g cm^{-2} (1.5 cm of aluminum) and that the Lexan for the other experiments had, on the average, thicker shielding.

Since the calculated relative fluxes given in Table 1 were derived for the position of the helmets used on the Apollo 8 and Apollo 12 missions, we calculated corrections for the Apollo 14 and Apollo 16 experiments, using the distributions of matter given in Fig. 2 and calculations of flux versus depth as observed in meteorites (*14*) corrected for the average difference in density

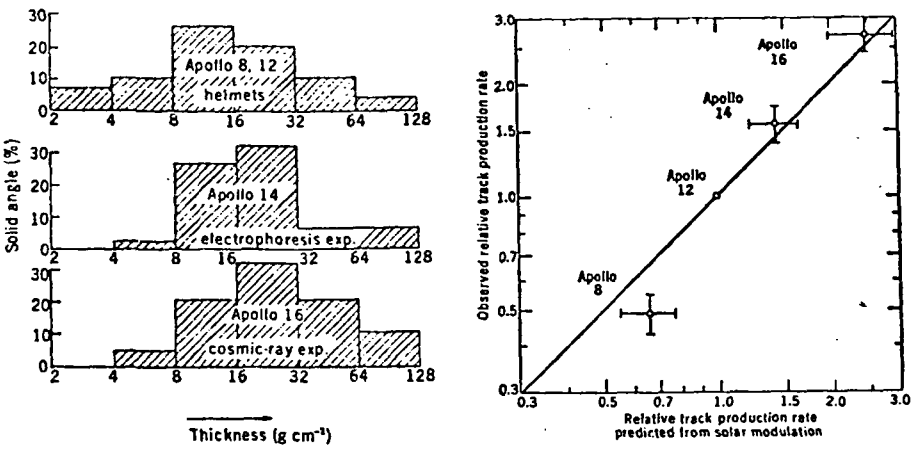

Fig. 2 (left). Distribution of mass around the three experiments considered in this report: Apollo helmets on Apollo 8 and Apollo 12 missions, the electrophoresis demonstration on Apollo 14 mission, and the cosmic-ray detector on Apollo 16 mission. We calculated these distributions from the known positions of storage of mass in the spacecraft, using a computerized description of the mass distribution of the command module. The distributions are used as described in (*1*) to derive track production rates for the three missions. For each experiment 10 percent of the solid angle was obscured by thicknesses greater than 128 g cm^{-2}, which allow negligible contributions to the observed track density. Fig. 3 (right). Observed track production rates, corrected for shielding thicknesses, plotted against the production rates calculated from solar modulation, corrected for shielding thicknesses. In all cases the rates are given relative to those for the Apollo 12 mission.

Table 1. Heavy-particle fluxes relative to the Apollo 12 mission.

Mission	Observed in command modules			Calculated from solar modulation*
	≧ Neon		≧ Carbon [Benton and Henke (*9*)]	
	Directly observed	Corrected for position in spacecraft		
Apollo 8	0.49 ± 0.06 (*1*)	0.49 ± 0.06	0.54 ± 0.14	0.66 ± 0.11 (*1*)
Apollo 12	1.00† (*1*)	1.00†	1.00†	1.00†
Apollo 14	0.60 ± 0.07	1.57 ± 0.18	2.00 ± 0.39 1.47 ± .28‡	1.43 ± 0.21
Apollo 16	1.10 ± .12	2.68 ± .29	3.25 ± .14	2.5 ± .5

* We calculated the fluxes listed in this column as described in (*1*), using the counting rates of the neutron monitor at Climax, Colorado, as a measure of solar activity; these fluxes include the effects of ionization and spallation loss of nuclei in passing through the spacecraft walls. † The directly observed track densities of each experiment were normalized to those of the Apollo 12 experiments. ‡ Film badge on E. D. Mitchell, crew member closest to the electrophoresis experiment.

between meteorites and aluminum. Column 3 of Table 1 gives the results of these corrections (factors of ~ 2.5 for each), and Fig. 3 presents a comparison of theory and experiment. We see from Table 1 that solar modulation has been responsible for variations from the Apollo 8 mission to the Apollo 16 mission by a factor of 5; shielding differences at different positions caused differences of a factor of ~ 2.5. These two factors thus explain the apparent discrepancy between our results and those of Benton and Henke (*9*).

The total doses of particles in the Apollo 14 and Apollo 16 command modules are higher but comparable to that in the Apollo 8 command module and presumably would cause the killing of a number of cells comparable to our calculation (*1*) for that mission. Even for the giant cells, the fraction killed is probably trivial, less than 500 cells per 10^6. However, relevant to a Mars-like mission (of ~ 2 years in duration), cellular damage would be extensive—as great as ~ 3 percent for the Apollo 16 flux level. The inadvertent reductions by a factor of ~ 2.5 in flux as a result of differences in shielding presumably could be enhanced by judicious planning and rearrangement of needed mass to provide optimum shielding at particular positions which the crew would occupy during most of a long voyage.

R. L. FLEISCHER, H. R. HART, JR.
G. M. COMSTOCK*, M. CARTER†
A. RENSHAW
General Electric Research and Development Center, Schenectady, New York 12301
A. HARDY
NASA Manned Spacecraft Center, Houston, Texas 77058

References and Notes

1. G. M. Comstock, R. L. Fleischer, W. R. Giard, H. R. Hart, Jr., G. E. Nichols, P. B. Price, *Science* **172**, 154 (1971).
2. E. C. McKannan, A. C. Krupnick, R. N. Griffin, L. R. McCreight, *NASA Tech. Memo X-64611* (July 1971); see also *Chem. Eng. News* (25 January 1971), p. 25.
3. R. L. Fleischer and H. R. Hart, Jr., in *Apollo 16 Preliminary Science Report* (National Aeronautics and Space Administration, Washington, D.C., 1973); *Phys. Rev. Lett.* **30**, 31 (1973).
4. P. Todd, *Radiat. Res.* **7** (Suppl.), 196 (1967).
5. P. B. Price and R. L. Fleischer, *Annu. Rev. Nucl. Sci.* **21**, 295 (1971).
6. R. L. Fleischer, H. R. Hart, Jr., W. R. Giard, *Science* **170**, 1189 (1970).
7. D. D. Peterson, *Rev. Sci. Instrum.* **41**, 1254 — (1970).
8. The Apollo 8 and Apollo 12 values are higher by a factor of 2 than the values quoted previously (*1*) because of a corrected computation of the solid angle factor.
9. E. V. Benton and R. P. Henke, *U.S. Air Force Weapons Lab. Rep. AFWL-TR-72-5* (June 1972); *Univ. San Francisco Tech. Rep. 20* (Aug. 1972).
10. W. T. Crawford, W. DeSorbo, J. S. Humphrey, *Nature* **220**, 1313 (1968); D. D. Peterson, thesis, Rensselaer Polytechnic Insitute (1969) [summaried in P. B. Price and R. L. Fleischer, *Radiat. Eff.* **2**, 291 (1970)]; E. V. Benton, R. P. Henke, H. H. Heckman, *Radiat. Eff.* **2**, 269 (1970).
11. H. J. Schaefer, E. V. Benton, R. P. Henke, J. J. Sullivan, *Radiat. Res.* **49**, 245 (1972).
12. E. V. Benton and R. P. Henke, paper presented at the 7th International Colloquium on Corpuscular Photography and Visual Solid Detectors, Barcelona, Spain, July 1970.
13. G. M. Comstock, C. Y. Fan, J. A. Simpson, *Astrophys. J.* **146**, 51 (1966); T. Saito, *J. Phys. Soc. Jap.* **30**, 1535 (1971); W. R. Webber, S. V. Damle, J. Kish, *Astrophys. Space Sci.* **15**, 245 (1972); E. Julinsson, P. Meyer, D. Müller, *Phys. Rev. Lett.* **29**, 445 (1972).
14. R. L. Fleischer, P. B. Price, R. M. Walker, M. Maurette, *J. Geophys. Res.* **72**, 333 (1967).
15. We thank M. V. Doyle for calling our attention to the electrophoresis experiment, R. Griffin and L. R. McCreight for loan of the electrophoresis experiments, W. Eichelman for necessary information, and G. E. Nichols and E. Stella for experimental assistance. This work was supported in part under NASA contract NAS 9-11486.

* Present address: Centre National pour la Recherche Scientifique, Orsay, France.
† Present address: Central State College, Wilberforce, Ohio.

23 March 1973; revised 4 May 1973

APPENDIX V

ABSTRACT FORM

FOURTH ANNUAL LUNAR SCIENCE CONFERENCE

INSTRUCTIONS FOR PREPARATION OF ABSTRACT TO BE REDUCED AND REPRODUCED BY PHOTO-OFFSET PROCESS: Type Single Line Title in caps, underscore in copy only. Insert 10 spaces on first line and type in the TITLE IN CAPS; follow with Author(s) and Affiliation, e.g., D. J. Jones, Geophysics Corp. of America, Bedford, Mass., 01730 (abbreviate where appropriate). Start Abstract on next line, indent 5 spaces. Mail Abstract to: ABSTRACTS, The Lunar Science Institute, 3303 NASA Road 1, Houston, Texas 77058.

APOLLO 16 COSMIC RAY EXPERIMENT--SOLAR FLARE ENERGY SPECTRUM AND HEAVY ELEMENT ENRICHMENT AT LOW ENERGY,
Howard R. Hart, Jr. and Robert L. Fleischer, General Electric Research and Development Center, Schenectady, New York.

The relative abundances and energy spectra of solar flare particles contain detailed information about the sun as a cosmic ray source and about the acceleration and propagation of solar particles. The low energy range from a few MeV per nucleon down to a keV per nucleon (a solar wind energy) has been largely unexplored. On Apollo 16 there were three cosmic ray experiments which contained track detectors designed to examine this energy range [1]. We report here energy spectra and relative abundances for heavy solar cosmic rays from the flare of April 17, 1972.

A detector array was mounted on the lunar module at launch and exposed to space from translunar injection until the end of the third EVA on the moon. As indicated by the satellite proton fluxes recorded in Fig. 1, a medium sized solar flare occurred during the translunar portion of the mission [2]; more than 90% of the flare particles recorded arrived before the lunar landing. The portion of the experiment considered here consisted of two types of detectors: sheets of .010 inch Lexan polycarbonate plastic and a 1 mm thick plate of GE phosphate glass 1457. Portions of each of these detectors were exposed to space protected only by a 2100Å film of aluminum; other portions were covered by .002 inch silver-and-Inconel backed Teflon thermal control material. For the uppermost portions of the detectors the flood of solar particles gave an abundance many times the expected galactic fluence; the results we report are essentially therefore only those for the April 17 flare. While on the lunar surface the detectors, particularly the Lexan, were heated by an amount sufficient to cause some desensitization through track annealing. Since this heating occurred after the end of the solar flare particle flux, the heat effects for all of the solar particles were identical.

Portions of the glass were etched in HF to reveal cosmic ray tracks. Segments of the Lexan sheets were etched in NaOH, some in the as-received, thermally desensitized condition and some after UV-sensitization. From measured track length distributions we derive differential energy spectra using range-energy relations for iron nuclei. The use of the iron range-energy

relations is justified for the glass and the desensitized Lexan, which record predominately iron group cosmic rays; it is slightly in error for the UV-sensitized Lexan which records particles as light as ^{12}C[1]. In Fig. 2 we plot three energy spectra (integrated over a 2π solid angle): The upper-most curve gives preliminary satellite data for protons [2]; the lowest curve is a composite of the data from the glass and the desensitized Lexan, i.e. the iron group nuclei; the intermediate curve, the data from the sensitized Lexan, represents carbon and heavier nuclei. If the data are represented by a relation $(\text{energy})^{-m}$, the spectral index m is 3 (± 0.3) at higher energies and flattens to m=1(± 0.5) at lower energies. The energy at which the flattening occurs differs for the different curves, going from ~.04 MeV/nucleon for iron to ~1 MeV/nucleon for carbon and heavier nuclei to ~10 MeV/nucleon for hydrogen. The resulting striking increases in relative heavy element enrichment are summarized in Table I. Here the "carbon and heavier nuclei" values have been recalculated using range energy curves for ^{16}O. The observed increasing enhancement of iron towards lower energies is in agreement with previous results by Price, et al [3], and Mogro-Campero and Simpson [4], but is qualitatively less at the same energies; the present results, however, extend to much lower energies. Though it would be desirable to compare our results to proton and helium fluxes in the lower energy region, these data do not exist. Subject to this limitation our results strongly suggest that the heavy nuclei in the solar flare particle flux are appreciably more abundant than in the surface of the sun. The preferential enhancement at low energies of the heavier nuclei because of their low charge-to-mass ratio was predicted in 1958 by Korchak and Syrovatskii [5].

REFERENCES

(1) More detailed descriptions are given in: FLEISCHER R.L. and HART H.R. JR. (1973) NASA Apollo 16 Preliminary Science Report (to be published); PRICE P.B., BRADDY D., O'SULLIVAN D., and SULLIVAN J.D., ibid.; BURNETT D., HOHENBERG C., MAURETTE M., MONNIN M., WALKER R. and WOLLUM D., ibid. More detailed references and discussion are in: FLEISCHER R.L. and HART H.R. JR. (1973) Phys. Rev. Lett. 30, 31-34.

(2) Preliminary satellite proton fluxes are from: BOSTROM C. (IMP-G), PAULIKAS G. (ATS-1), and SINGER S. (Vela).

BRIEF TITLE APOLLO 16 COSMIC RAY
(Abbreviated Title – All Capital Letters)

INITIAL AUTHOR Hart, H. R., Jr. et al.
(Initial author: e.g., Smith, A. B. et al.)

Type within margins only

(3) PRICE P.B., HUTCHEON I., COWSIK, R. AND BARBER D.J. (1971) Phys. Rev. Lett. 26, 916-919.
(4) MOGRO-CAMPERO A. and SIMPSON J.A. (1972) Astrophys. J. 171, L5-L9.
(5) KORCHAK A.A. and SYROVATSKII S.I. (1958) Dokl. Akad. Nauk. SSSR 122, 792-794 [Sov. Phys. Dokl. 3, 983-985].

TABLE I Abundance Ratios

Energy MeV/Nucleon	Iron/Carbon + Heavier	Iron/Proton
10	0.04	2.5×10^{-6}
3	0.03	1.5×10^{-5}
1	0.025	0.8×10^{-4}
0.3	0.11	0.8×10^{-3}
0.1	~0.5	-
0.03	~1	-
Photospheric	.04	4×10^{-5}

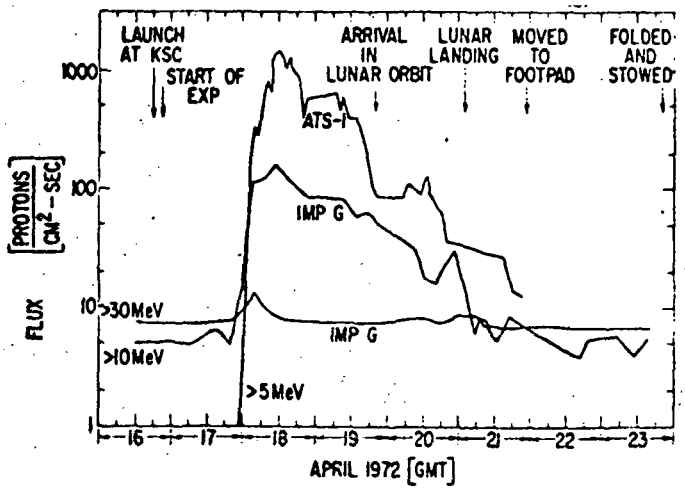

Fig. 1

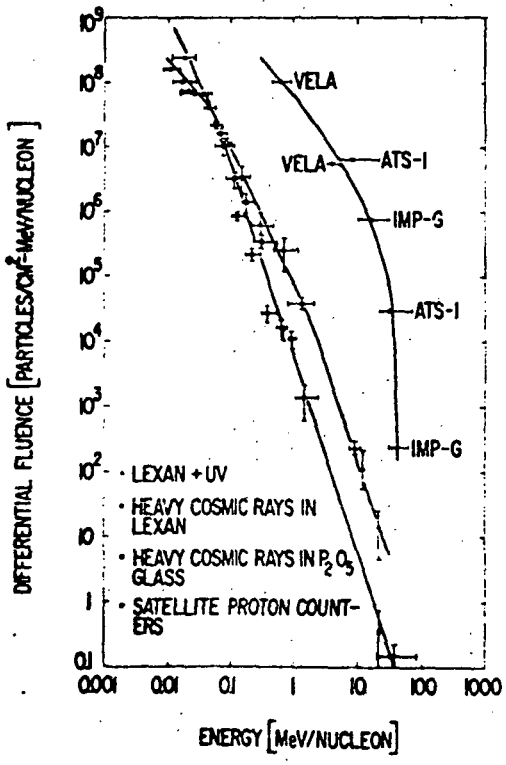

Fig. 2